Quantitative analysis of α-Gal trisaccharide content and its contribution to degeneration of bioprosthetic heart valves

Konstantina Kyriakopoulou

Institute of Cardiovascular Science

University College London

A thesis submitted for the degree of Doctor of Philosophy in Cardiovascular Science

2016

Dedication

To my parents,

Panayiota and Spyros

Declaration

I, Konstantina Kyriakopoulou confirm that the text and the work presented in this document are original and are my own. No sources other than those mentioned in the text and its references have been used in creating this thesis. All technical assistance received during this work has been acknowledged in the Materials and Methods section.

Abstract

Background: Commercial bioprosthetic heart valves (BHVs) are generally produced from porcine aortic heart valves or sewn from bovine pericardium. BHVs are durable in older patients, but in younger patients they are subject to age-dependent structural valve degeneration (SVD). SVD involves tissue calcification, which our research suggests is due in part to an immune mediated BHV injury caused by high levels of xenogeneic antigen galactose-alpha-1,3-galactose (α-Gal) on commercial valves and anti-Gal antibody universally present in patients. This suggests that α-Gal-free BHVs, unaffected by anti-Gal antibody could resist calcification and show improved durability in younger patients.

Aim: This research was to develop quantitative methods to measure α-Gal antigen on animal tissue and further characterize the role of α-Gal-specific immune injury in tissue calcification.

Methodology: I tested an α-galactosidase based colorimetric enzymatic assay for detecting galactose liberated from tissue and an α-Gal-specific inhibition ELISA (GIE) to measure α-Gal on fixed porcine pericardium. The α-Gal levels on wild type (WT), and α-Gal-free (GTKO) porcine tissue after glutaraldehyde fixation and after treating with various anticalcification processes were measured. The effects of anti-Gal antibody on WT and GTKO tissue calcification were measured using subcutaneous implants in anti-Gal antibody producing GTKO mice.

Results: The α-galactosidase based colorimetric assay showed low sensitivity and was not pursued. The GIE, using two different anti-Gal reagents, was sensitive and reliable. A-Gal antigen levels, measured by GIE were not reduced by anticalcification processing. Minimal tissue calcification was observed in GTKO mice for both WT and GTKO tissue. There was no clear anti-Gal immune response to WT implants.

Conclusion: This research shows that the current BHVs remain susceptible to immune injury as α-Gal antigen is not eliminated by the current anticalcification treatments. In addition caution is required when choosing the appropriate animal model to address the immune response factor in tissue calcification studies.

Acknowledgements

I would first like to thank my supervisors Dr Gerry Byrne and Professor Christopher McGregor for their support and guidance. I would like to thank Dr Byrne for training me and helping me with the mice surgeries and for his invaluable suggestions during the writing of this thesis.

I would like to thank the MRC CASE Studentship for funding my PhD.

I would especially like to thank Professor Philippa Talmud for all her support and encouragement during this PhD. Her role as a graduate tutor was pivotal.

I would like to thank our lab technician Miss Elisa Chisari for kindly doing the staining and helping to complete the ELISA analysis of the mice samples. I would also like to thank Dr Heide Kogelberg for preparing the samples for calcium analysis.

I would like to thank the technologists at the UCL Cruciform Animal Unit for offering training and help.

I would like to thank all my colleagues and tutors, past and present at UCL who have offered valued encouragement and support; with particular mention to Charis, Vera and Dia for putting up with me during periods of stress and sharing knowledge and experience and of course for the fun.

Finally, I would like to thank my family and friends for their constant love and support. In particular my parents, whom without their financial support it would have been impossible to remain in London and do the mice experiments during my writing up year.

Contents

List of figures

List of tables

Abbreviations

Ab	antibody
ADH	alcohol dehydrogenase
α-Gal	galactose-α1,3-galactose-β1,4-N-acetylglucosamine
AOA	2-α-amino-oleic-acid
ASPA	Animals (Scientific Procedures) Act
AVR	acute vascular rejection
bp	base pair
BHV	bioprosthetic heart valve
BSA	bovine serum albumin
DAB	3,3'diaminobenzidine
dH_2O	distilled water
DPBS	Dulbecco's phosphate-buffered saline
EBM-2	endothelial cell basal medium-2
EC	endothelial cells
ECM	extracellular matrix
EDC	[1-ethyl-3-(3-dimethylaminopropyl) carbodiimide hydrochloride]
EDTA	ethylenediaminetetraacetic acid
ELISA	enzyme linked immunosorbent assay
EtOH	ethanol
FACS	fluorescence-activated cell sorting
FBS	fetal bovine serum
FET	formaldehyde, ethanol and Tween 80
FITC	fluorescein isothiocyanate
GAGs	glycosaminoglycans
GH	galactose dehydrogenase
GIE	Gal inhibition ELISA
GIE_{GSIB-4}	Gal Inhibition ELISA using lectin GSIB-4
GIE_{M86}	Gal Inhibition ELISA using antibody M86
GGTA-1	alpha-1,3-galactosyltransferase gene
GLUT	glutaraldehyde
GSIB-4	*Griffonia simplicifolia* lectin I isolectin B4
GTKO	α-galactosytransferase gene GGTA-1 knock-out
HAR	hyperacute rejection
H&E	haematoxylin and eosin
HET	heterozygous

HRP	horseradish peroxidase
IC50	half maximal inhibitory concentration
IgG	immunoglobulin class G
IgM	immunoglobulin class M
KLH	keyhole limpet hemocyanin
KLH-Gal	α-Gal conjugated with keyhole limpet hemocyanin (KLH)
LVADs	left ventricular assist devices
MES	2-[N-morpholino]- ethanesulfonic acid
MFI	mean fluorescence intensity
MHV	mechanical heart valve
min	minute
NAD	nicotinamide adenine dinucleotide
NADH	reduced nicotinamide adenine dinucleotide
Neu5Gc	N-Glycolylneuraminic acid
OCT	optimal cutting temperature
ON	overnight
PAECs	porcine aortic endothelial cells
PBS	phosphate-buffered saline
PCR	polymerase chain reaction
PE	phycoerythrin
PIL	Personal licence
PPL	project licence
RBC	red blood cell
RIA	radioimmune assay
rRBC	rabbit red blood cell
r	Pearson correlation coefficient
rhEGF	recombinant human epidermal growth factor
rhFGF-B	recombinant human fibroblast growth factor
R^3-IGF-1	recombinant long R insulin-like growth factor 1
rpm	revolutions per minute
r_s	Spearman's rank correlation coefficient
RT	room temperature
SDS	sodium dodecyl sulfate
SDS-PAGE	sodium dodecyl sulfate polyacrylamide gel electrophoresis
SEM	standard error of the mean
SNPs	single nucleotide polymorphisms
SVD	structural valve deterioration

TBE	Tris - Boric acid – EDTA buffer
tri-α-Gal	α-Gal trisaccharide
Tris	trisaminomethane
VEGF	vascular endothelial growth factor
WST-1	water soluble formazan tetrazolium salt
WT	wild type

1 Introduction

1.1 Prosthetic heart valves

Heart valve disease constitutes a significant part of cardiovascular diseases which are the number one cause of death in the developed world (Simionescu 2004). Treatment of valvular heart disease comprises approximately 20% of all cardiac surgery. Surgery options include repairing the valve or replacing the valve. Annually more than 250,000 heart valves are implanted worldwide (Siddiqui et al. 2009). There are four valves in the human heart - the mitral, tricuspid, aortic and pulmonary valves. Aortic and mitral valves are the most frequently damaged in part due to the higher pressure they experience. The main causes for heart valve dysfunction are senile degeneration, genetic abnormalities and infective endocarditis. In the developing world there is high incidence of rheumatic heart disease which can lead to heart valve dysfunction in children and young adults (Zilla et al. 2008). The need for heart valve replacement is increasing in proportion to the demographics of an aging global population. In addition the growing emergence of wealth in developing nations with its concomitant improvement in healthcare further increases the demand for cardiovascular healthcare (Zilla et al 2008).

The most common treatment for heart valve dysfunction is heart valve replacement. Currently there are two types of clinical prosthetic heart valves - biological heart valves (BHVs) and mechanical heart valves (MHVs) (**Figure 1.1**). Clinical heart valve replacements using BHVs started in the early 1960s,

when unfixed aortic valves from human cadavers were implanted into patients and functioned normally for up to six years prompting their use by more cardiothoracic surgeons (BARRATT-BOYES 1964;KERWIN et al. 1962). Due to the shortage of human valves heart valve replacement was subsequently attempted using porcine heart valves. Marian Ionescu was the first who used aortic valves from pigs to construct valve replacements for use in humans at the General Infirmary at Leeds and Leeds University. Porcine valves were initially treated with formalin for sterilisation, preservation of tissue and prevention of autolysis (Ionescu et al. 1968;Rose 1972). Formalin fixed valves had a high failure rate, which was associated with mononuclear and multinuclear cell infiltration (Albert et al. 1977;Ionescu et al. 1972). In failed valves valvular incompetence was caused by stretching and deformation of the cusps resulting from denaturation of collagen within 2-32 months implantation (Rose 1972). The use of animal heart valves to treat patients became effective only after the introduction of glutaraldehyde fixation (Albert et al. 1977). Glutaraldehyde is a crosslinking reagent which reacts with the ε-amino groups of amino acids of collagen and other proteins through a Schiff-base reaction to produce intra- and inter- molecular crosslinks (Bezuidenhout et al. 2009). Crosslinking reduces immunogenicity of proteins, preserves structural integrity of the valve and serves as a sterilizer. The Hancock valve fixed in 0.2% glutaraldehyde (Medtronic Heart Valves, Santa Ana, CA) was the first glutaraldehyde fixed clinical BHV to be introduced in the market. This was followed by the Carpentier-Edwards porcine valve (Baxter Cardiovascular, Santa Ana, CA) fixed in 0.6% glutaraldehyde (Schoen and Levy 1999). Since that time heart valve

replacement has become common practice, however, manufacture of animal based BHVs remains largely based on glutaraldehyde fixation (Zilla et al. 2008).

Currently BHVs are made from either human heart valves (homografts) that are usually cryopreserved, or glutaraldehyde fixed porcine aortic heart valves or assembled from glutaraldehyde fixed bovine pericardium (heterografts). BHVs are generally three-leaflet valves, mounted on a synthetic stent and surrounded by a sewing ring at their base (stented valves) (Schoen & Levy 1999). Examples of stented BHVs include Hancock, Epic Supra (St Jude Medical, Minnesota, USA), Mosaic (Carpentier–Edwards). In other instances stentless valves are produced. Stentless valves were developed for aortic valve replacement, where their larger orifice area offers better hemodynamic performance and reduced mechanical stress (Butany et al. 2006;David et al. 1988). Examples of stentless valves include the Toronto porcine stentless valve and Medtronic Freestyle. Stented or stentless, the main advantage of BHVs is their low level of thrombogenicity, such that they generally do not require chronic anticoagulation (Schoen & Levy 1999). Largely because of their low thrombogenic potential BHVs constitute nearly 60% of the implanted valves and the percentage is growing.

Mechanical valves are made from non-biological materials (metal, plastic, carbon). The use of these non-biological materials causes the MHV to be prothrombotic, as circulating platelets are spontaneously activated on contact with non-biological surfaces. Exposure of the synthetic surfaces to blood circulation leads to activation of the coagulation and complement systems

(Nilsson et al. 2010). As a consequence MHVs require lifelong anticoagulation treatment. Anticoagulation is often achieved using Coumadin and is associated with a high risk of spontaneous bleeding if the dosage is too high and thrombotic occlusion if the dose is too low (Cannegieter et al. 1994). Thus mechanical valves impose lifestyle restrictions leading to reduced participation in activities (work and leisure), which makes their application less desirable especially for young patients and patients with physically demanding professions. Moreover, young patients in the developing world where the frequency of infection related valve disease may be high, may have no effective treatment if the infrastructure for monitoring anticoagulation is not in place (Manji et al. 2012).

Figure 1.1 Commercial BHVs. Medtronics Hancock II is a biological and St.Jude Regent a mechanical heart valve.

Stented BHVs and mechanical heart valves are surgical valves which require intensive open heart surgery. Not all patients, especially older and high-risk patients can withstand this surgery. Recently a new valve design and delivery

method was developed to permit the percutaneous implantation of a replacement heart valve, the transcatheter valves. Their use has gradually been introduced in intermediate and low risk patients but their performance and durability remains to be determined (Hamm et al. 2015). While the collapsible design of these valves is unique, the tissue used to construct the valve remains glutaraldehyde fixed porcine pericardium.

1.2 BHV degeneration

Although BHVs do not require chronic anticoagulation and thereby offer an attractive alternative to mechanical prostheses, they degenerate. The single, greatest predictor of BHV degeneration is patient age. BHVs in patients older than 65 years of age are durable with approximately 10% structural valve degeneration (SVD) in 10 years. In contrast, BHVs in patients younger than 35 years of age show a high frequency of structural defects with up to 100% failure, requiring re-operation in 5 years (Schoen & Levy 1999). SVD takes the form of calcium nodules, leaflet tears, fractures or perforations which result in stenosis, leaflet immobilization and tearing (**Figure 1.2**). This damage causes clinical pathologies due to excessive pressures (stenosis) or valvular regurgitation (Schoen and Levy 2005). The mechanism(s) which contribute to valvular calcification and degeneration are multifactorial and include mechanical strain, biochemical, immunological and surgical (patient - size mismatch) factors.

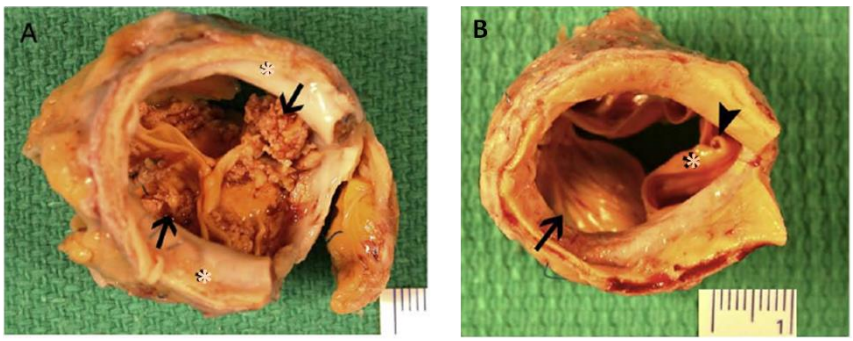

Figure 1.2 Degenerated BHVs. **A)** Excessive nodular calcification (arrows) on porcine cusps resulted in stenosis of the valve. **B)** One cusp prolapsed (arrow) and a tear (arrowhead) resulted in valve regurgitation [as published in (Nair, Law, Li, Phillips, David, & Butany 2012)].

Evidence of mechanical factors that contribute to SVD: Tissue fixation strengthens and stabilizes the overall structure of the valve, however, the dynamic microstructural rearrangements and normal reparative processes typical of native heart valves are not present in BHVs and render the valve susceptible to progressive mechanical fatigue (Schoen & Levy 1999). Consistent with this, explanted failed valves exhibit leaflet tears mostly in regions that receive high mechanical stress, such as points of maximal flexion and valvular commissures. Calcium deposition also occurs frequently at these points where it may further weaken the structural integrity to promote leaflet tearing. Interestingly inflammatory infiltrates are also more concentrated at sites of high stress suggesting that mechanical injury may expose the tissue to cellular infiltration and further degeneration (Zilla et al. 2008).

Evidence of biochemical processes that contribute to SVD: Unreacted glutaraldehyde used during fixation can provide free aldehyde groups that may

entrap calcium ions (Simionescu 2004). Fixation can also expose cellular phospholipids, the polar heads of which can provide nucleation sites for mineralisation. In addition accumulation of infiltrating cells can contribute to proteolytic degradation of collagen fibres by increasing matrix metalloproteinases activity (Bracher et al. 2001). Although collagen is effectively crosslinked by glutaraldehyde, other extracellular matrix (ECM) components, elastin and glycosaminoglycans (GAGs), are not as effectively stabilized and may be subjected to enzymatic degradation. As noted before, fixed BHVs lack live cells that would normally mediate remodelling and replenishment of extracellular matrix proteins. This absence of regenerating potential is the eventual source of BHV degradation (Schoen & Levy 1999).

Evidence that immunological processes contribute to SVD: Immune responses to implanted heart valves have long been recognized, even for homograft valves. Homograft recipients may develop sensitisation to human leucocyte antigens after heart valve replacement (Hogan et al. 1996). Explanted failed commercial animal derived BHVs show consistent evidence of innate and induced inflammatory reactions. The histopathology and immune staining of explanted degenerated BHVs includes inflammatory infiltrates consisting mostly of macrophages (Manji et al. 2015) but also including platelet aggregates, microthrombi, surface deposition of complement components, antibodies and adherence of neutrophils, T cells and B cells (Manji et al. 2012;Nair et al. 2012). In some cases macrophages infiltration into the valvular tissue has been reported and correlated with phagocytosis of collagen

supporting the view that macrophage derived lytic enzymes and matrix metalloproteinases contribute to BHV collagen degradation (Stein et al. 1988).

The histopathology of explanted BHVs represents the terminal stage of BHV degeneration associated with clinical SVD. Since SVD develops over time it is difficult to distinguish if this immune inflammation is a primary cause of SVD or a secondary reaction to a degenerating valve. The histologpathology of BHVs such that detected in BHVs retrieved from left ventricular assist devices (LVADs), in the absence of calcification, infection or structural deterioration, after only a few months of implantation, exhibit similar inflammatory processes (Khan et al. 2008;Moczar et al. 2000) and may be more informative of the early degenerative process. An immune response to BHVs is consistent with their age dependent degeneration, as young adults and children have a more robust immune system than older people (Manji et al. 2012).

1.3 LVAD devices- early post-implantation changes

Insight into the early events of BHV degeneration can be gained by studying the histopathology of BHVs prior to clinical dysfunction. Valves retrieved from LVADs, originally used for a limited time span (months) as a bridge to transplant, represent such an opportunity. Early LVADS produced by Novacor (WorldHeart, USA) contained two porcine prosthetic heart valves to regulate flow from the left ventricle to the pump (inflow valve) and to regulate the flow from the pump to the aorta (outflow valve) (Khan et al. 2008). BHVs were recovered from Novacor devices implanted for 37 to 1,293 days. Most BHVs were macroscopically normal without tears, perforations or calcification,

however, immunohistochemical analysis showed in the inflow valves deposit of fibrin, adherence of macrophages and neutrophil granulocytes on the outflow surface of the cusps. This histopathology grew progressively more intense over time. Further analysis showed the ECM stained positive for IgG and complement proteins C1q and C3c. The outflow valves exhibited similar findings but their structural deterioration was less rapid than the inflow valves, which received increased mechanical stress (Moczar et al. 2000). A second study of BHVs from explanted LVADs (Novacor and HeartrMate) (7 to 567 days implantation) indicated that a similar inflammatory response was evident in all cases (Khan et al. 2008). Macrophages were found in all inflow and outflow valves and the inflammatory response was more severe the longer the implant duration. There was no endocarditis or calcification in any of the valves. These findings suggest that an early host immune response to BHVs is present soon after implantation. The inflammatory reaction precedes calcification and tissue failure and may be a primary injury to the BHV that eventually leads to SVD. The histology of this process is consistent with an antibody mediated inflammatory reaction where antibody bound to BHV can fix complement attracting neutrophils, monocytes and mast cells. Activated macrophages may release proteolytic enzymes, reactive oxygen and nitrogen intermediates (oxidative burst) resulting in damage of the surrounding tissue. Progression of this antibody mediated inflammatory process can eventually lead to collagen degradation and calcification and thus to premature SVD.

1.4 Alternative processing for improving durability of BHVs

Changes in valve design and processing have been made to improve BHV durability. These changes have taken two predominant forms, engineering changes to improve valve flow and ease of implantation and altered chemical processing to reduce calcification. The Ionescu-Shiley bovine pericardial BHVs were re-engineered to align the stitches at the commissures of cusps a design flaw in the original version (Walley and Keon 1987). Another redesign was the introduction of low profile valves. This design reduced the protrusion of the stent into the left ventricular cavity for improved function of mitral valve prosthesis. Early versions of low profile valves had a high frequency of commissural tears in the right coronary cusp resulting in excess regurgitation. The redesign increased mechanical stress in this area leading to accelerated calcification and tears (Ius et al. 1996). As a consequence of these design failures computational simulations of valve function and stress and bench top flow devices for accelerated wear testing are routinely used for such biomechanical studies (Vesely 2003).

A significant research effort has been made to improve BHV tissue processing with the goal to reduce calcification and improve BHV durability. Typically these processing methods are tested in a rodent subcutaneous implant model to examine overall toxicity and the rate of calcification of BHV material and by hemodynamic testing of valve function in juvenile sheep (Schoen & Levy 1999).

1.4.1 Animal models used for the development of improved BHVs

The juvenile rat subcutaneous implant model is used in industry to test new anti-calcification treatments. Disks of fixed bioprosthetic material that have undergone various processing are implanted subcutaneously in rats or intramuscularly in rabbits. Tissue calcification levels are determined on the explants after a certain period of time using spectrophotometry or other chemical methods. The rate of calcification varies depending on the intrinsic calcification properties of the tissue, the recipient age, with younger animals calcifying faster than older animals, on the recipient species and site of implantation (Mako et al. 1999). In juvenile rats calcification levels reach a range of (80-120) μg/mg after 3-weeks, with maximal calcification (200-250 μg/mg) after 8 weeks [reviewed by (Schoen & Levy 1999)]. This subcutaneous implant model offers relative ease of use and its cost is low. However, it has its limitations mainly in the absence of blood contact and lack of haemodynamic stress. Nevertheless this model has been a valuable tool for developing anticalcification methods (Simionescu 2004).

A corollary to the subcutaneous implant model is valve replacement in juvenile sheep. This is a functional model where valves are implanted into sheep for 90 days or longer to test haemodynamic function and calcification. The sheep implant model simulates heart valve implantation in humans and consequently is expensive and technically demanding. BHV calcification may develop more slowly in this model compared with the subcutaneous model often requiring 3-5 months to accumulate similar levels of calcification (Schoen & Levy 1999).

1.4.2 Alternative crosslinking methods

Glutaraldehyde fixation has been the golden standard for BHVs manufacture since the 1960s and remains the only commercial fixative in clinical use today. Glutaraldehyde fixation is not without drawbacks as it shows a propensity towards calcification. Glutaraldehyde is also not an effective stabilizer of major components of ECM, such as elastin and GAGs which may affect tissue strength (Tam et al. 2015). Several alternative fixation agents have been tested including dye-mediated photo fixation (Photofix), alternative crosslinking agents such as carbodiimide, Epoxy, Genipin, and others. Many of these preservation methods have shown positive results in animal models but none have not been adopted for clinical use (Simionescu 2004).

1.4.3 Anticalcification treatments

Commercial post fixation strategies have been developed to mitigate calcification by blocking unreacted glutaraldehyde and extracting cellular phospholipids (Lentz et al. 1982;Shen et al. 2001). Unreacted glutaraldehyde is quenched by reacting the free aldehyde group with primary amines (Zilla et al. 2001). Commonly used primary amines tested to neutralize glutaraldehyde include L-glutamic acid, glycine, L-lysine and diamine (Zilla et al. 2001). Other quenching compounds include sodium borohydride, urazole and biphosphonates. Apart from neutralizing aldehydes biphosphonates bind to hydroxyapatite preventing further growth of calcium crystals (Zilla et al. 2004). Another anti-calcification compound, 2-α-amino-oleic acid (AOA®), is a detergent which reacts with aldehyde groups via a Schiff base reaction. AOA is

considered to covalently bind to glutaraldehyde and inhibit Ca^{2+} circulation in the tissue (Chen et al. 1994). From these glutaraldehyde quenching treatments only AOA processing has been adopted for clinical BHV and is used by Medtronic for the manufacture of the Mosaic and Freestyle valves (Girardot et al. 1994).

Cellular damage during fixation exposes phospholipids which are a major component of the cell membrane composed of a lipid tail and negatively charged polar head. Exposure of the negatively charges head is thought to serve to attach free plasma calcium and thereby serve as a site for calcium crystal growth. Post glutaraldehyde fixation treatment with ethanol extracts phospholipids and cholesterol (Vyavahare et al. 1997) and has been used in commercial BHVs, such as the Epic valves (St.Jude Medical, Minneapolis, MN, USA). Other clinical BHVs (Medtronic, Minneapolis, MN, USA) use sodium dodecyl sulphate (T6), to extract lipids (Simionescu 2004). Multiple variations of post fixation processing have been developed by Edwards Lifesciences Corporation. XenoLogix® uses a combination of ethanol, formalin and Tween-80 to reduce phospholipid content and calcification of tissues. Tissues treated by this method show reduced calcification in the rat subcutaneous implant model (Shen et al. 2001). This process is used commercially in the Carpentier-Edwards PERIMOUNT aortic and PERIMOUNT Plus mitral valves (Edwards Lifesciences Corporation, Santa Ana, CA, USA). Edwards Lifesciences have developed ThermaFix Tissue™ which involves heat treatment of glutaraldehyde fixed tissue, followed by alcohol to kill bacteria and surfactant for phospholipids

removal. These treatments have been used in commercial valves (e.g. Magna). Edwards Lifesciences is also developing additional post fixation processing to cap free aldehydes, extract phospholipids and infuse glycerol into the tissue to allow dry storage of the valves. This Resilia^{TM} treatment has been reported to significantly reduce calcification compared to glutaraldehyde fixed tissue in the intramuscular rabbit model (Tod and Dove 2016), but has not yet been used in commercial valves.

These anti-calcification treatments reduced calcification in the subcutaneous implant and juvenile sheep models (Weber et al. 2006), and have been in commercial use for many years but have not substantially altered BHV durability, nor permitted their routine use in younger patients. This suggests that the calcification mechanisms addressed by these methods (free aldehydes and phospholipid nucleation sites), while significant have not addressed a key mechanism which affects age dependent SVD of BHVs in younger patients.

1.5 Decellularized valves

Another strategy to reduce cell related antigenicity from bioprosthetic materials is decellularization. A decellularization protocol generally includes the use of ionic solutions or physical treatments to lyse the cell membrane, followed by enzymatic treatment to separate cellular components from ECM and detergents to remove the cellular debris (Gilbert et al. 2006). Although decellularized materials are used in several clinical applications, decellularized valves had detrimental effects when used in children and were removed from the market (Simon et al. 2003). These decellularization protocols do not seem

to eliminate xenoantigens from bioprosthetic tissue. The only decellularized heart valve commercially available is a cryo-preserved human heart valve, CryoValve aortic valve (CryoLife, USA).

1.6 Further evidence of immune injury and SVD

The failure of anticalcification treatments to provide a BHV durable in young adults and children supports the notion that immunologic injury contributes to degeneration of BHVs. The antibody mediated inflammatory response is consistent with results in subcutaneous implant models. Vincentelli and associates used the juvenile sheep subcutaneous implant model to compare calcification of fixed pericardium (0.65% glutaraldehyde) of xenogeneic (human) and autologous (sheep) origin. They showed that fixed human pericardium had 35-fold more calcium accumulation than autologous (sheep) fixed tissue (Vincentelli A et al. 1998). The above findings supported the notion that more immunogenic tissue (xenogeneic as opposed to autologous), despite fixation induces an immune response which is accompanied by proportionate calcification, much higher than the intrinsic calcification of autologous, less immunogenic tissue. Further evidence that immune rejection is involved in BHVs calcification was demonstrated by Manji and colleagues using young rats transplanted with glutaraldehyde fixed or fresh right outflow tracts (containing both aortas and valve) from rats (syngeneic), or fixed right outflow tracts from guinea pigs (xenogeneic). Xenogeneic implants showed three times more inflammation. Graft infiltration by T cells and macrophages was ten times more intense compared to syngeneic implants, either glutaraldehyde fixed or fresh,

and there was a three-fold induction of antibody in the xenogeneic recipients not seen in the syngeneic groups. Xenogeneic groups that had received steroids demonstrated decreased inflammation and lower antibody rise supporting the thesis that this is an immune mediated process. This study revealed that xenogeneic fixed valves underwent cellular/ humoral rejection and calcified secondarily (Manji et al. 2006).

Human and Zilla (Human and Zilla 2001) directly tested the impact of antibody on tissue calcification using a subcutaneous implant model. They created a specific immune response by immunizing New Zealand White rabbits with glutaraldehyde fixed porcine aortic wall tissue. Glutaraldehyde fixed porcine aortic wall buttons incubated in either immunized serum or in pre-immunization serum were then subcutaneously implanted and the level of tissue calcification determined three weeks later. Calcification of the tissue that had been incubated with specific antibody was significantly higher than that of the tissue that had been incubated in the control pre-immune serum. These results showed that specific antibody binding to fixed bioprosthetic material can enhance calcification (Human & Zilla 2001) and moved the authors to propose a model of graft-specific antibody induced tissue calcification.

These experimental results show that there is a greater immune response to xenogeneic tissue, compared to autologous tissue, and that antibody bound to fixed bioprosthetic tissue induces increased calcification. Since younger patients typically have more reactive immune systems, this immune mediated mechanism of BHV injury may have an important role in age-dependent SVD.

The major difficulty with this mechanism however is that glutaraldehyde fixation, through inter and intramolecular crosslinking drastically reduces the immunogenicity of the protein component of BHV tissue making it difficult to envision how such an immune response might develop in patients.

1.7 Xenogeneic glycans and BHV immunogenicity

Animal tissue contains carbohydrate structures not expressed in humans. The major xenogeneic glycan is terminal galactose-α1,3-galactose-β1,4-N-acetylglucosamine (α-Gal). The α-Gal trisaccharide is expressed on glycoproteins and glycolipids of all mammalian species except humans and Old World primates. This trisaccharide is synthesized by the enzyme α1,3 galactosyltransferase (Gal transferase) in the Golgi apparatus. Gal transferase catalyses the transfer of a galactose from UDP-galactose to galactose-β1,4-N-acetylglucosamine with an α1,3 linkage. A similar α1,3 linkage of galactose is also found in the B blood group antigen, but this antigen is formed by the action of a distinct B-transferase and not Gal transferase. The Gal transferase is encoded by GGTA-1 gene. Pig tissues have high levels of α-Gal epitopes with an estimated 10^7 epitopes on pig endothelial cells and 10^{11} epitopes/mg of porcine ligament tissue (Stone et al. 2007). Cows make similarly high levels of α-Gal. The α-Gal antigen is widely expressed in all major porcine organs and on many secreted mammalian glycoproteins including thyroglobulin, fibrinogen and immunoglobin molecules (Thall and Galili 1990). A-Gal is also expressed in matrix proteins such as laminin (Arumugham et al. 1986), bovine collagen

(Langeveld et al. 1991) and heparin sulphate proteoglycans (Fujiwara et al. 1993;Maruyama et al. 2000).

Humans do not synthesize the α-Gal glycan because of mutations in the GGTA-1 gene (Joziasse et al. 1989;Larsen et al. 1990). As a consequence humans, apes and Old World monkeys which do not produce α-Gal oligosaccharide, now produce high levels of anti-Gal antibodies. These antibodies are not present at birth but develop over the first year of life presumably in response to stimulation by gastrointestinal microflora (Galili et al. 1988a). Human anti-Gal antibody is present in all isotypes, (IgM, IgG, IgA, IgE) and is highly abundant making up approximately 1% of circulating IgG immunoglobulins (Galili et al. 1993). Individual anti-Gal antibody levels can vary widely and the affinity of anti-Gal antibody for the α-Gal epitope is reduced on average 6-fold in elderly populations (70 - 96 years) (Wang et al. 1995). Anti-Gal antibodies are cytotoxic and form a first line of defence against infectious organisms, including xenogeneic enveloped viruses, bacteria and protozoa, which were found to express α-Gal antigen (Galili 2013).

1.8 Anti-Gal antibody and animal tissues

Xenotransplantation seeks to ameliorate the chronic shortage of organs for transplantation by developing animal organs (pig) which can be used for human transplantation. When pig organs are transplanted into non-human primates however they are rapidly rejected by a complement mediated process, called hyperacute rejection (HAR). This rejection is caused by naturally occurring anti-

Gal antibodies which bind to α-Gal epitopes present on porcine vascular endothelial cells (EC). Anti-Gal antibody binding activates the complement cascade resulting in EC death, a loss of vascular patency, intravascular haemorrhage and thrombosis with organ rejection within minutes to hours of transplantation. If HAR is blocked, then porcine xenotransplantation leads to a strong induction of anti-Gal antibodies (McCurry et al. 1997) resulting in acute vascular rejection (AVR) characterized by a progressive deposition of IgG, IgM, edema, diffuse thrombosis, ischemic injury and cellular necrosis. Although these studies utilize live animal tissues, and the detailed mechanism of graft rejection may not be applicable to fixed bioprosthetic tissues, these studies demonstrate the clear pathogenic potential of preformed human anti-Gal antibody even in the absence of an induced antibody response.

To eliminate anti-Gal mediated xenograft rejection, xenotransplantation researchers have used nuclear cloning technology (Wilmut et al. 1997) and homologous recombination in somatic cells to produce pigs with a targeted mutation in the GGTA-1 gene (GTKO pigs) (Lai et al. 2002;Nottle et al. 2007;Phelps et al. 2003). By numerous criteria - anti-Gal antibody and lectin staining of tissue and cells, α-Gal-specific western blots of cell proteins, flow cytometry of GTKO pig cells (Nottle et al. 2007), biochemical analysis of GTKO glycolipid tissue extracts (Diswall et al. 2010) and pig-to-primate xenotransplantation (Kuwaki et al. 2005) - GTKO pig tissue is free of the α-Gal trisaccharide. Indeed GTKO pigs have now lost tolerance to α-Gal antigen and like humans spontaneously make anti-Gal antibody (Fang et al. 2012). Use of

GTKO organs in xenotransplantation has not eliminated xenograft rejection but has highlighted the role of non-Gal antigens in xenograft rejection (Byrne and McGregor 2012). The most significant non-Gal antigens identified in xenotransplantation for BHVs are the minor xenogeneic glycans N-glycocylneuraminic acid (Neu5Gc), a modified sialic acid not produced in humans and the SDa blood group like glycan produced by porcine beta-1,4 N-acetylgalactosaminyltransferase 2, (B4GALNT2) glycosyltransferase. Both of these carbohydrate antigens are immunogenic in humans although their impact in xenotransplantation is less than the effect of anti-Gal antibody (Park et al. 2012).

1.9 Bovine and porcine BHVs express α-Gal antigen

There is strong evidence that commercial BHVs, despite fixation and processing, express the α-Gal antigen. Patients implanted with BHV show a significant increase in anti-Gal IgM antibodies after heart valve surgery whereas patients treated with MHVs or undergoing coronary artery bypass graft surgery show no similar increase. In adult patients the induced anti-Gal IgM antibody response was increased by approximately 45% (Konakci et al. 2005). Paediatric patients (median age 132 months, range: 14-330 months) show a much stronger induction of anti-Gal antibody one week after BHV implantation exhibiting up to 7-fold increase in IgM and a sustained 32-fold increase in IgG (Park et al. 2010).

In addition to these clinical observations our group directly compared the immunogenicity of commercially prepared WT and GTKO BHVs implanted in the mitral position in non-human primates. The recipients that received WT valves showed a sustained significantly increased level of α-Gal-specific immune stimulation over the first post implant year which was not observed in the GTKO valve recipients (McGregor et al. 2013).

Commercial bioprosthetic heart valves show positive staining for the α-Gal antigen using α-Gal-specific lectin (GSIB-4) or anti-Gal monoclonal antibodies. Accurate staining for α-Gal antigen can however be difficult unless one appreciates the ubiquity of this antigen in animal tissues. For example, animal sera, typically used to block non-specific binding to tissue sections, are rich in α-Gal antigen, and therefore they are inappropriate blocking agents. Likewise the lectin *Griffonia simplicifolia* lectin I isolectin B4 (GSIB-4) binds to α-Gal oligosaccharide but has an absolute requirement for calcium for α-Gal-specific binding. Commonly used calcium-free phosphate buffered saline is thus not suitable. Accounting for these technical issues it is evident that commercial BHVs clearly stain with both GSIB-4 (Kasimir et al. 2005;Konakci et al. 2005;McGregor et al. 2011;Naso et al. 2011) and anti-Gal antibodies (Naso et al. 2013a). In the best controlled staining studies, using competition with free α-Gal trisaccharide to block GSIB-4 binding and GTKO porcine tissues as negative controls, specific GSIB-4 binding is evident in valvular endothelial cells and throughout the matrix of the valve leaflet in wild type (WT), α-Gal positive [GT(+/+)], pig heart valves (McGregor et al. 2011). Glutaraldehyde fixed

commercial devices show a similar GSIB-4 staining pattern indicating that the α-Gal antigen remains after fixation (McGregor et al. 2011) and is still present even after anti-calcification treatment (Lila et al. 2010). In addition to GSIB-4 staining a monoclonal anti-Gal IgM antibody, M86 (Galili et al. 1998) has been used for staining α-Gal on commercial BHVs. Together these findings indicate that despite fixation and anticalcification treatment the α-Gal epitope remains present at high levels in BHVs and remains immunogenic.

The pathogenicity of human anti-Gal antibody in xenotransplantation, the universal presence of anti-Gal antibody in humans and the abundance of α-Gal on commercial BHVs suggest that anti-Gal antibody may mediate an antibody induced BHV immune injury, as suggested by Human and Zilla (Human & Zilla 2001), even in the absence of an induced antibody response.

1.10 Effects of anti-Gal antibodies on calcification

To determine if human anti-Gal antibody can promote calcification of fixed bioprosthetic tissue we previously compared calcification of WT and GTKO fixed porcine pericardium in the presence and absence of anti-Gal antibody in both a rat and rabbit subcutaneous implant model. We recently have shown that naturally occurring preformed human anti-Gal antibody enhances calcification of α-Gal-positive but not α-Gal-free tissue in both rat and rabbit subcutaneous implant models. Fixed pericardium disks from WT pigs implanted subcutaneously into juvenile rats or rabbits had significantly higher levels of calcium after 3 weeks, if pre-incubated with human anti-Gal antibody (111 ± 8.4

μg/mg) compared to non-labelled WT pericardium (74 ± 9.6 μg/mg). This anti-Gal mediated effect was not present when GTKO pericardium was pre-incubated with anti-Gal antibody. Indeed calcification of GTKO pericardium was generally lower than WT tissue both in the presence or absence of anti-Gal antibody (55 ± 11.8 μg/mg and 51 ±9.1 μg/mg, respectively). Labelled with anti-Gal antibody WT pericardium had significantly higher calcification (111 ± 8.4 μg/mg) compared to antibody labelled GTKO pericardium (55 ± 11.8 μg/mg) (McGregor et al. 2011). The same effect of anti-Gal antibody was present when fixed tissues were further treated with formaldehyde, ethanol and Tween 80 (FET) to reduce the lipid content and minimize calcification. FET treatment reduced levels of calcification in WT pericardium from 155.7 ± 7.1 μg/mg to 4.6 ± 4.2 μg/mg. Pre-incubation with anti-Gal antibody increased calcification of FET treated WT pericardium to 43.8 ± 8.5 μg/mg. Calcification of FET treated GTKO pericardium (0.35 ± 0.1 μg/mg) was significantly lower than in FET treated WT pericardium (4.6 ± 4.2 μg/mg). In the presence of anti-Gal antibody, FET treated WT pericardium calcified significantly more than FET treated GTKO pericardium (43.8 ± 8.5 versus 5.7 ± 2.9 μg/mg) (Lila et al. 2010). These experiments showed that anti-Gal antibody accelerates calcification in glutaraldehyde fixed WT tissue and suggest that this inflammatory response can be avoided by using α-Gal-free, GTKO tissue (McGregor et al. 2011).

1.10.1Studies in GTKO mice

GTKO mice do not make the α-Gal antigen and spontaneously produce low levels of anti-Gal IgM. With immunization these mice also produce anti-Gal IgG

(Gock et al. 2000). GTKO mice would naturally appear to be an ideal model for studying anti-Gal induced tissue calcification and some studies have been reported (Kim et al. 2015a;Kim et al. 2015b;Lee et al. 2012;Lim et al. 2013). When glutaraldehyde fixed bovine pericardium is implanted in GTKO or WT mice, tissue calcification after two months was reportedly higher in GTKO recipients compared to WT mice. This is consistent with an anti-Gal mediated tissue calcification, however, compared to rabbit and rat subcutaneous implant results, where calcification levels can reach 50 – 150 μg/mg, the calcium levels in the explanted material from GTKO mice were not very high (0.77 μg/mg of tissue compared to 0.12 μg/mg in fixed but not implanted tissue) (Lee et al. 2012). If the GTKO mice are immunized with rabbit RBCs, to induce a strong anti-Gal IgG response, the level of calcification after three months in the immunized mice (1.5 ± 0.4 μg/mg) was significantly higher than in WT mice (0.3 ± 0.1 μg/mg), but not different from naïve GTKO mice (1.1 ± 0.2 μg/mg) (Lim et al. 2013). It is difficult to know if this increase was due to higher anti-Gal antibody levels or an additional month of subcutaneous exposure. Calcification of glutaraldehyde fixed primate pericardium (free of the α-Gal antigen) and α-Gal-positive bovine pericardium has also been compared in GTKO mice. In this instance calcification of primate pericardium (3.9 μg/mg) was significantly lower than bovine pericardium (9.2 μg/mg) (Kim et al. 2015b). A fourth study compared calcification and immune response of fixed pericardium and valves of porcine and bovine origin implanted for 3 months. The IgM response in GTKO mice was significantly higher at 30 days post implantation and the IgG response remained elevated until 60 days post implantation compared to those in WT

mice. All types of implants calcified significantly more in GTKO than in WT mice (Kim et al. 2015a). These studies reported a consistent elevated calcification of α-Gal-positive tissues in GTKO recipients compared to WT recipients, but the overall level of calcification is very low compared to other models.

1.11 Assays to measure α-Gal antigen on animal cells

Galili used a classic radioimmune assay (RIA) and serial dilutions of radiolabelled GSIB-4 lectin to estimate the number of α-Gal epitopes on rabbit red blood cells (RBC). Melibiose was used as a glycan specific inhibitor of GSIB-4 to control for nonspecific lectin binding. After incubation the cells were washed by centrifugation and Scatchard analysis of free and bound lectin was used to estimate approximately 150,000 α-Gal epitopes per rabbit erythrocyte (Galili et al. 1987). This assay was initially conducted at 37 ^{o}C, where lectin binding might not be stable and there was some concern that the washing procedure might strip cells of bound lectin. The analysis was repeated incubating serial dilutions of radio-labelled GSIB-4 at 4^{o}C, for 1 hour with various cell types and the cells were separated from unbound lectin by banding in a Ficoll-Hypaque gradient. This study estimated 10x10^{6} α-Gal epitopes on porcine aortic endothelial cells and 1.2x10^{6} epitopes on mouse SP2/0 cells (Galili et al. 1988b). A second estimate of α-Gal levels on rabbit RBCs was not reported, so the impact of the change in incubation temperature and cell isolation is not obvious.

Galili later developed an anti-Gal monoclonal antibody (M86) and used it to create an inhibition assay to measure α-Gal epitopes on cells (Galili et al. 1998).

In this assay variable numbers of cells were incubated with a standard concentration of M86 overnight, at 4^{o}C, in an effort to attain equilibrium binding. The cells were then removed by centrifugation and the level of free M86 was measured by binding to a BSA-Gal conjugate in an ELISA microtiter plate. The higher the level of α-Gal expression on cells, the more they bind M86 leaving less M86 in the supernatant for the Gal ELISA. This creates an apparent inhibition of the Gal ELISA compared to M86 not incubated with cells. Galili created an inhibition profile for each cell type and used the half maximal inhibitory concentration (IC50) derived from these profiles as an estimate antigen density. The mouse myeloma SP2/0 cells (estimated to have 1.2x10^{6} α-Gal epitopes by the earlier GSIB-4 RIA analysis) were used as a reference standard. Rabbit RBC, which showed approximately 2-fold greater inhibition in the Gal inhibition ELISA compared to the SP2/0 standards were estimated to have 2x10^{6} α-Gal epitopes/ rRBC. This is more then 10-fold higher than the original estimate determined by the RIA method.

Galili and another group (Naso et al. 2011) have used the SP2/0 estimate of 1.2x10^{6} epitopes per cells as a standard multiplier for calculating α-Gal expression on other cells and tissues. This is unusual since GSIB-4 and M86 have distinctly different valency (4 vs. 10 respectively), affinity and the original RIA assay, performed at 4 ^{o}C for 1 hour, was not likely to be at equilibrium.

The practice of using this extrapolation to report epitope numbers is evident in the literature, but for the reasons above is not likely to be accurate.

1.12 Summary and aims

The presence of α-Gal antigen on commercial BHVs, the universal presence of anti-Gal antibody in patients, the continued immunogenicity of the α-Gal antigen, despite fixation and the strong induction of anti-Gal antibody in young patients after BHV implantation and the anti-Gal dependent calcification of fixed α-Gal-positive porcine pericardium suggest that anti-Gal antibody binding to α-Gal on BHVs may initiate an antibody dependent inflammation, which leads to BHV degeneration. This mechanism may significantly contribute to age-dependent SVD. The α-Gal-dependent immune injury can be eliminated if α-Gal is removed from the BHV using enzymatic removal of α-Gal with α-galactosidase (Stone et al. 2007) or using tissue from GTKO pigs. The development of new low antigen BHVs lacking the α-Gal carbohydrate may significantly enhance BHV durability in young patients. Development of this low antigen valve requires assays to monitor α-Gal levels in bioprosthetic material.

Hypothesis

My hypothesis is that antibody binding to BHVs increases their calcification and degeneration by augmenting an inflammatory reaction. Natural anti-Gal antibody, present in recipient patients, binds to the major xenoantigen α-Gal expressed on BHVs and is likely to play a crucial dominant role in this process.

Aims of the project

1) Quantification of α-Gal on fixed animal tissues.

The first aim of my project was to develop an assay that would allow reliable quantification of α-Gal on fixed bioprosthetic materials. I investigated two different approaches - a biochemical enzymatic cycling assay to detect α-Gal released by α-galactosidase and an inhibition ELISA assay using α-Gal specific lectin GSIB-4 and anti-Gal monoclonal IgM antibody M86.

2) Measuring the effects of anti-calcification processing on α-Gal levels in bioprosthetic tissues.

In order to reduce the calcification of commercial BHVs, they are processed with detergents and other chemical compounds, which may also affect the α-Gal content of the devices. The second aim of my project was to use the inhibition ELISA developed in “aim 1” to measure α-Gal levels on tissue processed with anti-calcification treatments that are applied for production of commercial BHVs, as well as in various commercial BHVs. This analysis defined α-Gal levels associated with different processing and can be used to relate the clinical performance of those devices to their α-Gal content.

3) Investigation of the effects of anti-Gal antibody binding on fixed tissue calcification *in vivo.*

The final aim of my project was to determine using an *in vivo* model whether anti-Gal antibody binding increases calcification of fixed BHV tissue depending on its α-Gal content. This aim was investigated using fixed WT and GTKO pig

pericardium implanted subcutaneously in GTKO mice. GTKO mice lack α1,3GT enzyme (GGTA-1 gene) and therefore do not express α-Gal, but make anti-Gal antibody. These experiments compared the effects of anti-Gal antibody on calcification of WT and GTKO BHV tissues in a host animal (GTKO mice) which makes anti-Gal antibody.

2 Materials and Methods

All chemicals unless noted were purchased from Sigma-Aldrich, UK.

2.1 Introduction to Methodology

Glutaraldehyde fixed pig pericardium is currently used in clinical BHVs (Medtronic, CoreValve) and was used in these studies as a model bioprosthetic tissue.

Antigen levels on cells are commonly measured by flow cytometry where quantitative estimates of antigen levels are made on a per cell basis. Tissue, consisting of a mixture of cell types and a collection of extracellular matrix components is more complex and not readily assessed by flow cytometry. Therefore, additional methods are needed to measure α-Gal on fixed animal tissue. Two different approaches were examined.

The first, detailed in section 2.2, estimates tissue α-Gal levels by detecting the amount of galactose released from the tissue after treating with α-galactosidase. In this approach the liberated galactose was quantified by reacting with galactose dehydrogenase to produce NADH which was quantified with a sensitive colorimetric enzymatic cycling system. The second approach, detailed in section 2.5, was developing an α-Gal inhibition ELISA assay (GIE) using the α-Gal-specific lectin GSIB-4 or a commercially available mouse anti-Gal monoclonal IgM antibody M86. The GIE assay was very effective and was the main analytical method used to quantify α-Gal levels on pig pericardium.

Throughout this research glutaraldehyde fixed porcine pericardium was used as a model bioprosthetic tissue. The fixation method is detailed in section 2.10. Also in that section are described the anticalcification extraction methods. These extraction processes model the commercial process commonly used for clinical BHVs. Our interest was to determine, using the GIE, if the anticalcification effect of these extraction methods eliminates α-Gal. Subcutaneous implantation of fixed pericardium in GTKO mice (2.12.3) is the method used to investigate the role of anti-Gal antibody to promote tissue calcification. Subcutaneous implantation in rodents or rabbits is a standard method used to assess the propensity of tissue to calcify, but in this instance we use the GTKO mouse line which spontaneously makes anti-Gal antibody. The remaining methods are standard procedures used to detect anti-Gal antibody (α-Gal ELISA section 2.6), genotype GTKO mice (PCR genotyping section 2.11), characterize anti-Gal reagents and the sensitivity of the GIE (flow cytometry section 2.7) and detect tissue calcification (section 2.13).

2.2 Enzymatic detection of α-Gal antigen

Enzymatic detection of α-linked galactose was adopted from commercial methods to detect lactose (Essig and Kleyn 1983;Huber et al. 1975). The assay was based on the following strategy. Coffee bean α-galactosidase, specifically cleaves galactose in α 1,3 glycosidic bond, was used to release galactose from α-Gal containing tissue (Luo et al. 1999). Galactose was subsequently reacted with galactose dehydrogenase (GH) and nicotinamide adenine dinucleotide (NAD), to yield a stoichiometric production of reduced NAD (NADH) and D-

galactono-1,4-lactone (**Figure 2.1**). The initial detection method was to monitor production of NADH by measuring its absorbance at 340 nm using a NanoDrop 2000 spectrophotometer (ThermoScientific, UK).

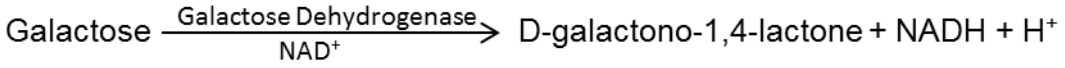

Figure 2.1 Reaction of galactose with galactose dehydrogenase in the presence of NAD^+ forms NADH and D-galactono-1.4-lactone.

To calibrate this detection method galactose solutions from 0.039 mM to 10 mM were incubated in 200 µl reactions with 5 µg/ml β-galactose dehydrogenase from *Pseudomonas fluorescens* (Sigma-Aldrich, UK) in a reaction buffer containing 1 mM NAD, 20 mM trisaminomethane (Tris) and 150 mM NaCl, pH 8.6, at 25 ^{o}C for 1 hour.

For enhanced detection of NADH a commercially available NAD^+/NADH colorimetric assay (CycLex, MBL, UK) was used. The CycLex system, based on enzymatic cycling, is an amplifier which couples the reactions of alcohol dehydrogenase (ADH) and diapharase, to continuously cycle the conversion of NADH into NAD and back (**Figure 2.2**). Linked to this is the NADH dependent formation of a coloured, water soluble formazan terazolium salt (WST-1), which is measured by absorbance at 450nm. The enzymatic amplification process starts by addition of NADH or NAD and results in a proportionate formation of WST-1-formazan.

Elimination of NAD and NADH

Because the CycLex enzymatic cycling system is activated by the addition of either NADH or NAD, these components, must be eliminated from the tissue (present at low levels). The high levels of NAD during the GH reaction (**Figure 2.1**) must also be eliminated prior to the cycling reaction. NAD and NADH were depleted as described in (LOWRY et al. 1961). NAD was eliminated using 0.05 M NaOH, pH 10 and heating at 60 ^{o}C in thermoblock (Analog Heatblock, VWR) for 1 hour. After alkali heat treatment the samples were left to cool to room temperature (RT) and were neutralized by addition of HCl to 0.05 N and put on ice for 5 minutes (min). NADH was eliminated with 0.05 M HCl, pH 4, at 60 ^{o}C, for 1 hour. Prior to cycling enzyme reaction samples were centrifuged at 14,000 rpm (Microfuge 16 Centrifuge, Beckman Coulter, UK) for 5 min to remove the precipitating salts and supernatants were transferred into a 96-well microplate (Nunc, UK). To 25 µl of each sample 75 µl of cycling enzyme reaction mix was added with the final reaction mix containing 6% ethanol, 100 mM Tris pH 8.6, 59 µg/ml ADH, 100 µM WST-1, 100 µg/ml diaphorase. Samples were left to react in the dark at RT for 1 hour. The amount of formazan was measured by absorbance at 450 nm using a microplate reader (BioTek, ELx808) and Gen5 1.11 software. A standard curve of serially diluted NADH (15.6 nM – 1000 nM) was measured in parallel.

The overall strategy for this enzymatic detection of α-Gal antigen is depicted in (**Figure 2.2**).

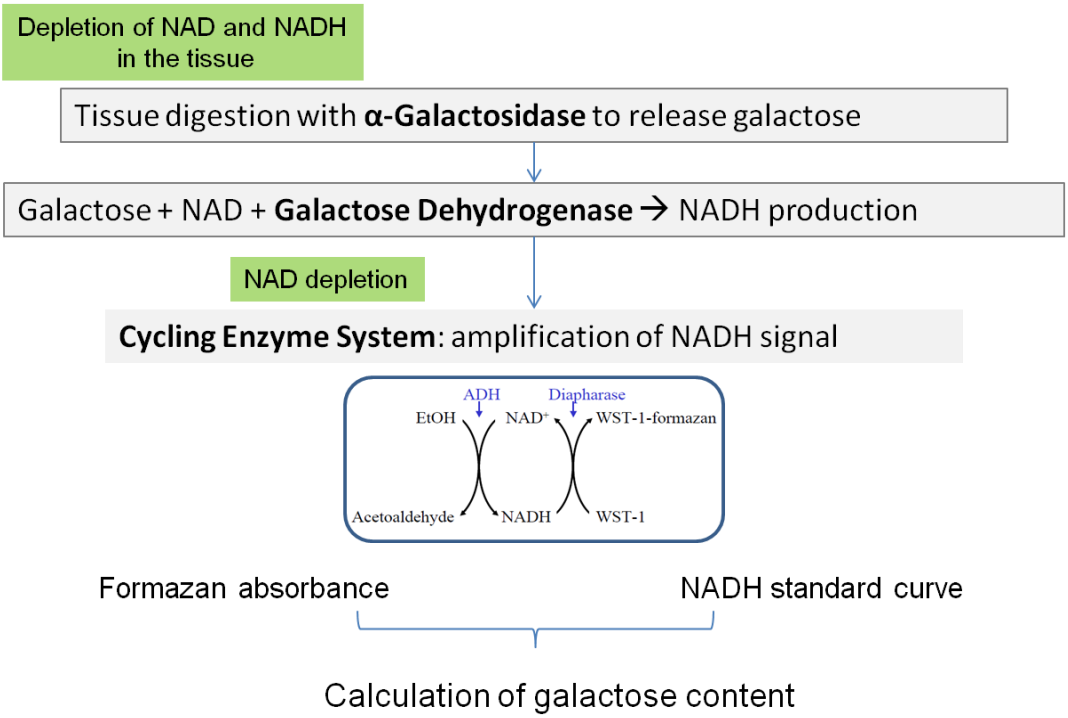

Figure 2.2 Enzymatic detection of galactose. NAD and NADH in the tissue were depleted by acidification at pH 4, or alkalisation at pH 10, respectively, with heating at 60 ^{o}C. Tissue was digested with α-galactosidase to release galactose. Galactose was reacted with galactose dehydrogenase to produce stoichiometric amount of NADH. NAD from this reaction was depleted by addition of NaOH until pH=10 and heating at 60 ^{o}C. Samples were neutralized with HCl and subsequently mixed with the cycling enzyme system reaction mix. A coloured WST-1 formazan was produced and measured at 450 nm. NADH standards were used to calibrate galactose content.

2.3 Cell culture

Primary α-Gal positive porcine aortic endothelial cells (PAECs) and a transformed α-Gal-free (GTKO) PAEC cell line (15502) with a disruption of the GGTA-1 galactosyltransferase gene (Azimzadeh et al. 2014) were used. Cells were cultured in endothelial cell basal medium-2 (EBM-2) supplemented as indicated by the manufacturer with 10 ml fetal bovine serum (FBS), 0.5 ml human recombinant vascular endothelial growth factor (VEGF), 0.5 ml ascorbic acid, 0.2 ml hydrocortisone, 0.5 ml gentamycin sulphate (GA-1000), 2 ml

recombinant human fibroblast growth factor (rhFGF-B), 0.5 ml recombinant human epidermal growth factor (rhEGF), 0.5 ml recombinant long R insulin-like growth factor 1 (R^3-IGF-1) and 0.5 ml heparin (Lonza, UK). Cells were cultured in 75 cm^2 polystyrene flasks (Corning, The Netherlands) in a 37^oC, 5% CO_2 and 95% humidified incubator. Cells were expanded when they reached 70-80% confluency by washing with phosphate-buffered saline (PBS) [155.17 mM sodium chloride (NaCl), 1.06 mM potassium phosphate monobasic (KH_2PO_4), 2.97 mM sodium phosphate dibasic (Na_2HPO_4-$7H_2O$)], pH 7.4 (Gibco, UK), followed by a trypsin digest (TrypLE Express, Gibco) at 37 ^oC, for 1 - 2 minutes, to detach the cells from the plate. Cells were resuspended in 10 ml media by repeated pipetting and transferred to a 50 ml centrifuge tube. To determine the cell number an aliquot of cells was mixed 1:1 with trypan blue solution (Sigma-Aldrich, UK) and the number of live cells, which exclude the trypan blue dye, were counted in a haemocytometer. For continued cell growth the cells were split 1:3 and fed with new culture media at 2 day intervals. Primary PAECs were not cultured beyond the 6th passage.

2.4 Production and purification of anti-Gal hybridoma antibody

Anti-Gal IgG-secreting hybridomas GT5 (Xu et al. 2003) were cultured in protein-free medium RPMI 1640 + GlutaMAX –I (Gibco) in a humidified 5% CO_2 incubator at 37 ^oC. Approximately 1 litre of exhausted hybridoma supernatant was produced using 3-layer multi-flasks (TripleFlasks, Nunc, UK). Supernatants were collected and equal volume of filtered (0.2 μm vacuum filtration system, VWR, UK) saturated ammonium sulphate was added drop

wise at 4^{o}C under constant stirring. The mixture was kept at 4 ^{o}C overnight to precipitate. The precipitated proteins were centrifuged at 18,000 rpm in a Sorvall centrifuge, at 4 ^{o}C for 30 min and re-suspended in approximately 1.5 ml sterile PBS. Samples were dialysed (SnakeSkin pleated dialysis tubing, Thermo Scientific, UK) against PBS at 4^{o}C under constant stirring for 4 hours after which the PBS was replaced and dialysis continued at 4 ^{o}C overnight. The purity of the precipitated anti-Gal antibody was measured by sodium dodecyl sulfate polyacrylamide gel electrophoresis (SDS-PAGE) and the protein concentration was determined by absorbance at 280 nm using a Nanodrop spectrophotometer.

2.5 A-Gal Inhibition ELISA (GIE)

An α-Gal-specific inhibition enzyme linked immunosorbent assay (ELISA) was used to quantify the amount of α-Gal present in fixed α-Gal-positive and GTKO pig cells and pericardium. This assay which was adapted from the method developed by Galili (Galili et al. 1998) consisted of two stages. In the first stage α-Gal containing oligosaccharides, tissues or cells were incubated with an anti-Gal reagent. For our analysis we tested three reagents, biotinylated *Griffonia simplicifolia* lectin I isolectiin B4 (GSIB-4) (Vector laboratories, UK) and anti-Gal IgM hybridomas M86 (Enzo life sciences, UK) and anti-Gal IgG hybridoma GT5 (Xu et al. 2003). During this incubation a portion of the anti-Gal reagent is complexed with α-Gal antigen. In the second stage a Gal ELISA was used to measure the level of free α-Gal binding reagent. The apparent inhibition due to binding of the anti-Gal reagent and α-Gal

antigen, compared to the anti-Gal reagent alone was used to estimate the amount of α-Gal in the sample.

Stage 1: Gal Inhibition

PAECs (0.5 up to $7.5x10^6$ cells), glutaraldehyde fixed (0.6%) 3 mm diameter disks (4 or 8 disks per sample) of porcine pericardium, or monomeric α-Gal trisaccharide (30 µM – 7500 µM) were incubated at 4 ^oC, overnight or for two days, with either 150 µl of a 1:10 dilution of M86 supernatant, or biotinylated GSIB-4 (0.125 µg/ml) in microcentrifuge tubes (Elkay, UK). The M86 and GSIB-4 were diluted in 1% bovine serum albumin (BSA) in 50 mM Tris, 150 mM NaCl, 10 mM $CaCl_2$, 10 mM $MgSO_4$, pH 7.4. After primary incubation tissue or cells were removed by centrifugation at 1500 rpm, at 4 ^oC, for 10 min in a refrigerated centrifuge (Microfuge 22R Centrifuge, Beckman Coulter, UK). Supernatants were transferred into clean microcentrifuge tubes and were further centrifuged at 13,500 rpm at 4 ^oC for 30 min. The final supernatants were tested by Gal ELISA. For each experiment a minimum of 3 samples (cells or pericardium) were tested for each condition and at least 3 independent replicate experiments were performed.

Stage 2: Gal ELISA

Microtiter plates (Nunc, Thermo Scientific, UK) were coated with 50 µl of BSA-Gal (10 µg/ml, Vector Laboratories, UK) in carbonate buffer (15 mM Na_2CO_3, 35 mM $NaHCO_3$ and 2 mM NaN_3, pH 9.6), at 4 ^oC, overnight. Coating solutions were aspirated and the plate was blocked with 200 µl of 1% BSA in 50 mM Tris, 150 mM NaCl, 10 mM $CaCl_2$, 10 mM $MgSO_4$ and 0.1% Tween 20, pH 7.4, at RT for 1 hour.

Samples (50 µl) were incubated in duplicate at 4 ^{o}C for 90 minutes after which the plate was washed 5 times with 0.1% Tween 20 PBS in an ELx50 microplate washer (BioTek, UK). For detection of biotin conjugated GSIB-4 50 ul of ExtrAvidin-Peroxidase (Sigma-Aldrich) 1:1000 was added to each well and incubated at RT for 1 hour. For detection of M86 (IgM) or GT5 (IgG) the plates were incubated with a biotin conjugated goat anti-mouse IgM (Sigma, UK) or IgG (Sigma, UK), diluted 1:1000 or 1:5000 respectively, at RT for 1 hour, washed and then incubated with ExtrAvidin-Peroxidase as previously described. After incubation with ExtrAvidin-Peroxidase the plates were washed 5 times and anti-Gal binding was visualised by addition of TMB (3,3',5, 5'-tetramethylbenzidine liquid substrate, T4444, Sigma) in darkness at RT for 2 min. The reaction was stopped by addition of 0.5 M sulfuric acid (100 µl/ well) and the plate absorbance was read at 450 nm in an ELx808 microplate reader (BioTex, UK).

The α-Gal content was estimated by the Gal Inhibition ELISA (GIE) by comparing anti-Gal reactivity after primary incubation with cells or tissues to Gal reactivity of the reagent alone. This was expressed as the percentage of inhibition calculated by the following equation:

Equation A

% Inhibition = ((OD reagent – OD sample) / OD reagent**)** x 100

"OD reagent" was the optical density measured with the anti-Gal reagent alone. "OD sample" was the optical density measured after incubation with α-Gal trisaccharide, cells or pericardium disks.

To compare GIE results in assays using GSIB-4 (GIE_{GSIB4}) and M86 (GIE_{M86}) the GIE was performed with increasing amounts of free monomeric α-Gal trisaccharide (tri-α-Gal). The tri-α-Gal oligosaccharide is galactose-α1,3–galactose-β1,4-GlcNAc with a hexanoic acid spacer, containing five methylene groups and a carboxylic acid (Byrne et al. 2002). The inhibition curves were fitted as four parameter logistic curves using SigmaPlot software and the 50% inhibition level (IC50) was calculated. This reference analysis allowed us to correlate the number of cells, or amount of tissue which produced an equivalent amount of inhibition compared to tri-α-Gal. A flow diagram of the process is presented in (**Figure 2.3**).

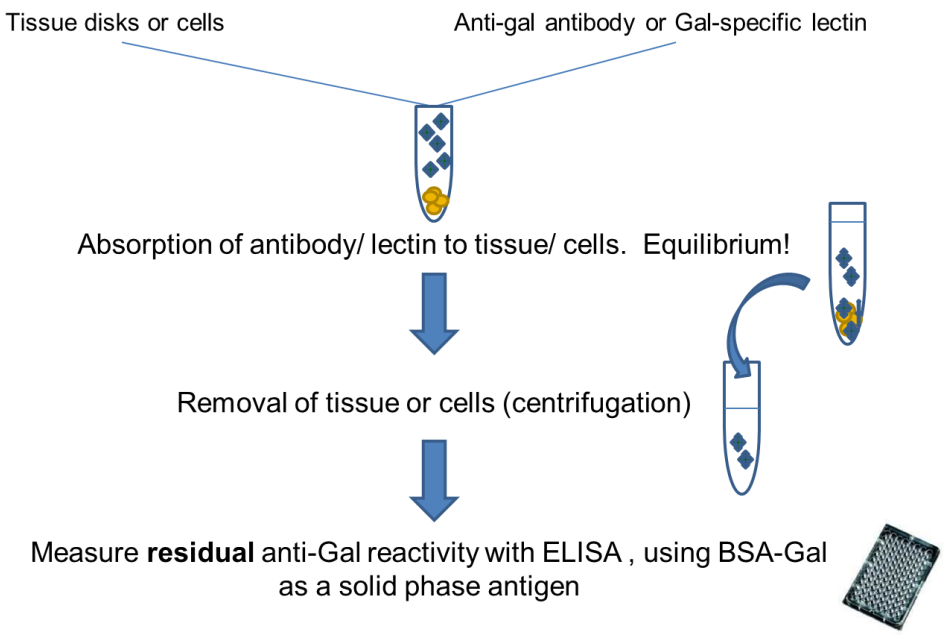

Figure 2.3 α-Gal Inhibition ELISA (GIE) for quantification of α-Gal on tissue or cells. Fixed pig pericardium disks (3 mm) or cells were incubated with anti-Gal reagent at 4 ^{o}C until equilibrium was reached. Disks or cells were removed by centrifugation and the remaining free anti-Gal reactivity in the supernatants was measured by Gal ELISA using BSA-Gal as a solid phase antigen.

2.6 Detection of mouse anti-Gal IgM and IgG

Microtiter plates were coated as described in paragraph 2.5 with BSA-Gal using 50 µl of (10 – 30) µg/ml BSA-Gal in carbonate buffer. Mouse serum dilutions were made in 1% BSA, PBS, containing 0.1% Tween 20. For anti-Gal IgMs dilutions of 1:8 to 1:128 generally covered the linear range of the assay. Background reactivity for anti-Gal IgM was defined by binding to BSA coated wells. For the primary incubation 50 µl of each dilution was tested in duplicates for binding to BSA-Gal and one well for biding to BSA.

To detect mouse anti-Gal IgG a serial titration (dilutions 1:16 to 1:4096) was performed to determine the dilutions within the linear range of the assay. Mouse IgG often showed a high background so an additional negative control, other than binding to BSA, was used to define Gal specific reactivity. In addition to the standard serum dilutions a parallel dilution series was prepared using 1% BSA, PBS, 0.1% Tween 20 containing 10 mM tri-α-Gal monomer to specifically block anti-Gal reactivity. Mouse anti-Gal specific IgG reactivity was calculated by the equation:

Equation B

Mouse anti-Gal IgG = $(OD_{BSA\text{-}Gal}) – (OD_{BSA\text{-}Gal + tri\text{-}\alpha\text{-}Gal})$

The mouse Gal ELISA plates were incubated at 4 ^{o}C for 90 minutes with the primary serum dilutions, washed in a microplate washer 5 times in PBS, 0.1% Tween 20, re-blocked for 30 minutes with 200 µl per well of 1%BSA, PBS, 0.1% Tween 20 at RT and antibody binding detected using 50 µl of HRP-conjugated goat anti-mouse IgG (Pierce, Thermo Scientific, UK), or IgM (Life Technologies,

UK) each at 1:2000 dilution. Secondary antibodies were incubated for 60 minutes at room temperature after which the plates were washed and incubated with 100 µl of pre-warmed TMB at room temperature for 4 - 5 minutes in darkness. The reaction was stopped with addition of 100 µl per well of 0.5 M sulfuric acid. Data was collected by reading the plate in a plate reader at 450 nm.

All ELISA plates contained a dilution series of GT5 (IgG) or M86 (IgM) as internal standards to normalize for day to day and plate to plate variation. The serum optical density data, for a minimum of 4 serum dilutions, was used to calculate a serum anti-Gal titre based on the serum dilution required to attain an OD of 1.0 (IgG) and 0.5 (IgM). This titre was expressed after normalizing to the dilution of GT5 or M86, required to attain an OD of 1.0 or 0.5, according to the equation:

Equation C

Serum IgM titre = titre anti-Gal $IgM_{(0.5)}$ / titre $M86_{(0.5)}$

Serum IgG titre = titre anti-Gal $IgG_{(1.0)}$ / titre $GT5_{(1.0)}$

2.7 Flow Cytometry

Binding of anti-Gal IgG (GT5 hybridoma), IgM (M86 hybridoma) or lectin GSIB-4 to α-Gal-positive and GTKO PAECs was determined by flow cytometry analysis (fluorescence-activated cell sorting: FACS) using a FACS Calibur (Becton Dickinson, UK). PAECs ($2x10^5$ per assay tube) were resuspended in FACS buffer (1% BSA in PBS) and incubated with GT5, M86 supernatant, or

GSIB-4 (5 µg/ml) diluted in D-PBS (Gibco, UK), on ice for 60 min. The cells were washed in 3 ml of PBS by centrifugation and resuspended in 100 µl of phycoerythrin (PE)-conjugated goat anti-mouse IgG (Invitrogen, UK), fluorescein isothiocyanate (FITC)-conjugated rat anti-mouse IgM (BD Pharmigen, UK), or PE-conjugated streptavidin (Anaspec, Cambridge) respectively and incubated in darkness, on ice, for 45 min. Cells were subsequently washed and resuspended in 500 µl 1% paraformaldehyde PBS prior to analysis.

2.8 Alpha-galactosidase digestion of cells

Primary α-Gal positive PAECs and the α-Gal-free 15502 cell line were cultured as described in 2.3. Cells were harvested and rinsed in PBS and transferred in microcentrifuge tubes at 1.5 x 10^6 cells/sample (100 µl). Cells were incubated with Green coffee bean alpha-galactosidase (Sigma-Aldrich, UK) in a phosphate-citrate saline buffer (0.2 M dibasic sodium phosphate, 0.1 M citric acid, 0.15 M sodium chloride, pH= 6) at concentrations (2 – 10) units/ml, at room temperature, for 1 hour. Cells were washed twice by centrifugation using PBS to remove the enzyme and subsequently used for GIE as described in (2.5), or stained for FACS analysis (2.7).

2.9 Alpha-galactosidase digestion of fixed pig pericardium and valves

Glutaraldehyde fixed porcine pericardium or heart valve leaflets (8 disks per sample) were incubated with green coffee bean α-galactosidase (2–10 units/ml)

in phosphate-citrate saline buffer (consistency described in 2.8) at RT, overnight. Samples were washed in PBS and used in the $GIE_{GSIB4.}$

2.10 Anticalcification treatments of glutaraldehyde fixed porcine tissue

Glutaraldehyde fixation: Porcine pericardium was freed from adherent fat, rinsed three times in big volumes of PBS and placed in 0.6% glutaraldehyde in 20 mM HEPES, 130 mM $MgCl_2$-$6H_2O$, 150 mM NaCl for 24 hours, at RT. Then it was placed in 0.2% glutaraldehyde and kept at 4^oC.

Different anticalcification treatments used in the production of commercial BHVs were used to treat glutaraldehyde fixed porcine tissue to determine their impact on α-Gal levels. Before each treatment pericardium was rinsed in PBS.

Glycine is used to cap free aldehyde groups that remain after glutaraldehyde fixation. The protocol was performed as described in (Lee et al. 2012):

Glutaraldehyde fixed porcine tissues were incubated in 0.2 M glycine in PBS, pH 7.4, at 37 ^oC, for 2 days. The tissues were subsequently rinsed twice in PBS (30 min each) and incubated with 0.1 M sodium borohydride ($NaBH_4$) at room temperature, overnight. After $NaHB_4$ reduction the disks were washed twice in PBS (30 min each wash) and stored in PBS with 0.05% NaN_3, 4 ^oC.

Ethanol is used to extract phospholipids. The protocol was applied as in describe in (Vyavahare et al. 1997):

Glutaraldehyde fixed tissues were placed in 80% ethanol prepared in 50 mM HEPES buffer, pH 7.4, at room temperature, for 24 hrs. Subsequently the

tissue was rinsed in 0.9% NaCl at room temperature, for 24 hrs and stored in PBS with 0.05% NaN_3, 4 ^oC.

FET treatment consists of treating the tissue with formaldehyde, ethanol and Tween 80 to remove phospholipids (Shen et al. 2001):

Glutaraldehyde fixed porcine pericardium or valve leaflets were placed in a buffer containing 4% formaldehyde, in 20 mM HEPES, 13 mM $MgCl_2$-$6H_2O$, 22% ethanol and 1.2% Tween 80 at 37 ^oC, for 6 hrs. Subsequently tissue was extensively rinsed in PBS and finally stored in PBS- NaN_3 0.05%, 4 ^oC.

SDS is a detergent used to extract phospholipids from the tissue:

Glutaraldehyde fixed porcine pericardium or valve leaflets were placed in 1% SDS in 6 mM HEPES buffer, pH 7.4, at room temperature, for 8 hrs. The SDS buffer was replaced with fresh and left at RT, overnight. The tissue was extensively rinsed in PBS and finally stored in PBS- NaN_3 0.05%, 4 ^oC.

Prior to the inhibition assay tissue was blocked in 1% BSA-DPBS containing 0.1% Tween 20 and 0.05% NaN_3 for GSIB-4 staining or in 1% BSA-PBS containing 0.1% Tween 20 and 0.05% NaN_3 for M86 staining, overnight, 4 ^oC.

2.11 Genotyping of mice

2.11.1 DNA extraction

Balb/c mice (Line 9260, C-Ggta-1^{tm1}, Taconic Labs, Germantown New York, USA) with a mutation in the α-galactosytransferase gene GGTA-1 (GTKO mice) were genotyped by polymerase chain reaction (PCR). Frozen ear biopsies in eppendorf tubes were digested with 200 µl of proteinase K lysis buffer [5 mM ethylenediaminetetraacetic acid (EDTA), 200 mM NaCl, 0.2% sodium dodecyl

sulfate (SDS), 100 mM Tris-HCl (pH 8.5) and 1/100 volume of a 10 mg/ml proteinase K stock solution] in a heat block at 55 ^{o}C, with occasional vortexing and left overnight. Proteinase K digests were inactivated by incubation at 80 ^{o}C for 15 minutes then extracted with an equal volume of phenol - chrloroform (1:1) by vigorous vortexing for 1 min. Samples were centrifuged at 14,000 rpm for 5 min and the upper aqueous phase containing the DNA was collected, carefully avoiding the protein interface, and transferred to clean tubes. The phenol-chloroform extraction was repeated once more and the DNA was precipitated by addition of 300 µl isopropanol. The DNA was pelleted by centrifugation at 14,000 rpm for 10 min. The supernatant was discarded by inverting the tubes and 700 µl of 70% ethanol was added to wash out residual salts. The DNA was centrifuged at 14,000 rpm for 5 min, the supernatant was discarded by inversion and the pellet was dissolved overnight in 50 µl of distilled water (dH_2O).

2.11.2 DNA Quantitation by spectrophotometry

DNA dilutions (1:5) were prepared in distilled water (dH_2O) and the absorbance of 2 µl samples were measured using a NanoDrop spectrophotometer at 260 and 280 nm. Distilled water was used as a blank.

2.11.3 PCR reactions

Three primers were used to identify the neomycin disrupted GGTA-1 gene, mGTKOFwd (5'-GCACCTGAACCCTCTACATTCCTTAC-3'), mGTKORv (5'-AGGTTGAGAATGTGAGTAGGCGTTCC-3') and pgkNeo (5'-ACTTGTGTAGCGCCAAGTGC-3'), (Eurofins Genomics, Ebersberg, Germany). The mGTKOFwd primer binds to GGTA-1 exon 9 upstream of the PGK-neo

insertion site and the mGTKORv primer anneals to GGTA-1 exon 9 downstream of the PGK-neo insertion site. In the absence of a PGK-neo insert these primers amplify a 358 bp product. When exon 9 is disrupted by a PGK-neo insert this primer combination does not produce a PCR product because the length of the product is too long (~ 1600 bp) for the extension time (30 seconds). The pgkNeo primer is a reverse primer which anneals to the 5' portion of the PGK-neo insert. This primer with mGTKOFwd primer produce a 235 bp PCR product only when there is a PGK-neo insertion in exon 9 of GGTA-1 (**Figure 2.4**).

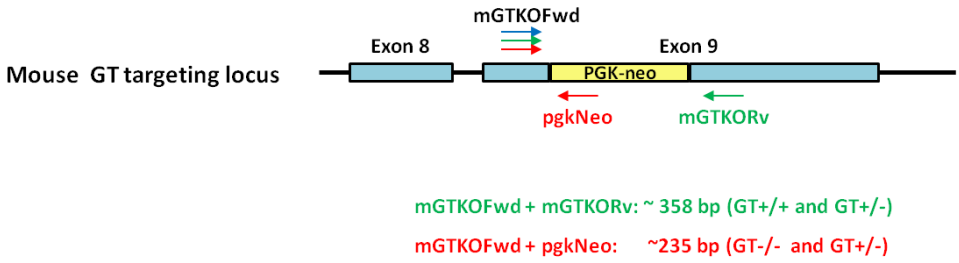

Figure 2.4 Targeting of GGTA-1 locus (GT transferase gene) in mice.

Each PCR reaction was prepared using 200 ng of mouse genomic DNA, all three primers and GoTaq G2 Green Master Mix, (Promega, Madison WI, USA) according to the following table using an automated Mastercycler personal (Eppendorf by Thermo Fisher Scientific):

PCR reaction	
	(µl)
Primer GTKO Fw	1 (25 µM)
Primer GTKO Rv	1 (20 µM)
Primer GTKO Neo	1 (25 µM)
Distilled Water	12
DNA	10 (200 ng)
2x Green GoTaq buffer	25

The PCR cycling program consisted of an initial denaturation at 95 ^{o}C for 2 min, followed by 30 cycles of denaturation at 95 ^{o}C for 30 seconds, annealing at 60 ^{o}C for 30 seconds, elongation at 72 ^{o}C for 30 seconds. After the last cycle there was an extended elongation at 72 ^{o}C for 5 minutes followed by a cooling to 6 ^{o}C.

2.11.4DNA gel electrophoresis

The PCR products were analysed by electrophoresis in a 2% agarose gel using TBE buffer (89 mM Tris, 89 mM Boric acid, 2 mM EDTA) containing 10 µg/mL of ethidium bromide. PCR products were loaded into a submerged well along with control samples representing WT, HET and GTKO mice and DNA molecular weight markers, DNA 100 bp ladder (Promega, Madison WI, USA). All samples were mixed with loading buffer (10x buffer was 30% glycerol and 0.2% orange G in water) prior to loading on the gel. The gel was electrophoresed at 75 volts until the dye front reached 4 cm from the end of the gel. DNA bands separated in the gel were viewed and recorded under ultraviolet light using the BioDoc-It^{TM} Imaging System Benchtop 3UV Transilluminator (UVP, Analytik Jena, Germany).

2.12 Animal experiments

2.12.1 Ethical approval and Home Office licence

Tissue calcification is a multifactorial process. This study focuses on the contribution of an immune reaction to this process and therefore animal experiments were required to study the systemic effect of anti-Gal antibody and α-Gal interaction.

Ethical approval for the animal experiments was received from the Home Office (United Kingdom), [Project Licence (PPL) Number: 70/7825] in accordance with the Animals (Scientific Procedures) Act 1986. I received my personal licence (PIL) (Number: I2C8F8704) after completing Modular Courses (modules 1 – 4) for Home Office Licence Applicants provided by the Royal Veterinary College.

Animal housing and experiments took place at the Cruciform UCL Biological Services Unit and were planned and performed according to the 3Rs principles. Throughout the experiments, care was taken to ensure the wellbeing of the animals.

2.12.2 Establishment of mice colony

Heterozygous GTKO line 9260 C-Ggta1^{tm1} mice were imported from Taconic Farms, Germantown, NY, USA and re-derived at the UCL Institute of Child Health Transgenic Services unit. The offspring were screened and found heterozygous for the α-galactosyltransfarase gene as expected. Re-derived mice were transferred to the Cruciform Animal facility where they were

maintained. Re-derived heterozygous individuals were crossed to produce homozygous GGTA-1 knockout offspring which were kept to establish a double knockout (GTKO) breeding colony for our experiments.

2.12.3Subcutaneous implantation

Forty-day-old Balb/c GTKO mice (male and female) received subcutaneous implants of sterile glutaraldehyde fixed pig pericardium disks. Disks (6.0 mm) were cut from sheets of glutaraldehyde-fixed WT (expressing the α-Gal antigen) or GTKO pig pericardium using a punch biopsy (World Precision Instruments,Inc., Sarasota, USA), rinsed in sterile PBS and blocked in sterile 1%BSA- PBS. Some of the disks were labelled with M86 supernatant diluted 1:10 in a mixture of anti-Gal IgG GT5/GT6 (1:1) supernatants, at 4^{o}C, for 1 hour, rinsed in sterile saline and kept on ice until transferred to the animal unit for implantation. The antibody labelling of the disks had to be completed not earlier than 30 min prior to implantation.

Recipients were initially anaesthetized with 2.5% isoflurane in an induction chamber. Anaesthesia was maintained using a facial mask with a flow of (1.0 - 12.5) % isoflurane. The implant site on the dorsal surface was shaved and cleansed with the antiseptic “Hibitane scrub”, (Chlorhexidine Gluconate 4% w/v). Two incisions were made along the dorsal surface, one per side and a “pocket” was formed under the skin using forceps. One disk was inserted in each pocket and smoothly placed against the body musculature, making sure it was flat and not folded. The incisions were closed with 2 - 3 sutures (Mersilk, 3-

0, RB-1, 17 mm, 1/2C, round bodied). The animals were placed in a recovery chamber (37 ^{o}C) and were monitored until fully recovered from anaesthesia.

Recipient mice (N = 10) received the following types of glutaraldehyde fixed implants:

- WT pericardium,
- WT pericardium pre-incubated with a mixture of anti-Gal IgM M86 and IgG GT5/GT6 antibodies (positive control),
- GTKO pericardium
- GTKO pericardium pre-incubated with a mixture of anti-Gal IgM M86 and IgG antibodies (negative control).

Age matched mice that did not receive any implants were kept in parallel to provide control serum for each time point.

Each group was composed of approximately 10 animals with 2 implanted disks each. This sample size was selected based on a variance (estimated from a review of the literature) in mean calcification levels of ± 25% and should be sufficient to detect with 90% confidence a 20% change in the average level of calcification between samples (Anon 2013a;Anon 2013b).

2.12.4Blood sampling and implants retrieval

Implants were maintained for 60, 90, and 120 days after which the animals were euthanized by terminal anaesthesia (5% isoflurane) followed by cerebral

dislocation. The implants were recovered and blood was collected via cardiac puncture.

Blood samples were left to clot at room temperature and the serum was recovered after centrifugation at 1500 rpm for 10 min in a refrigerated centrifuge (Microfuge 22R Centrifuge, Beckman Coulter, UK). Serum was transferred to clean microcentrifuge tubes and further centrifuged at full speed (14,000 rpm for 20 min) to clarify. The final serum samples were stored at – 80 ^{o}C until analysed.

Implanted disks were removed starting with an incision behind the animal's neck and pulling the skin down until the implanted disks were exposed (**Figure 2.5**). The disks were carefully retrieved from the skin, while retaining whatever encapsulating layer. Disks were then placed in microcentrifuge tubes with cold, sterile saline and briefly kept on ice until further processed for histology and calcium analysis.

Approximately 1/8th sized samples of each disk was cut with a scalpel and placed in formalin for histological analysis. The remaining portion was cleaned of the surrounding encapsulating layer, placed in an empty microcentrifuge tube and kept at – 80 ^{o}C, until calcium determination.

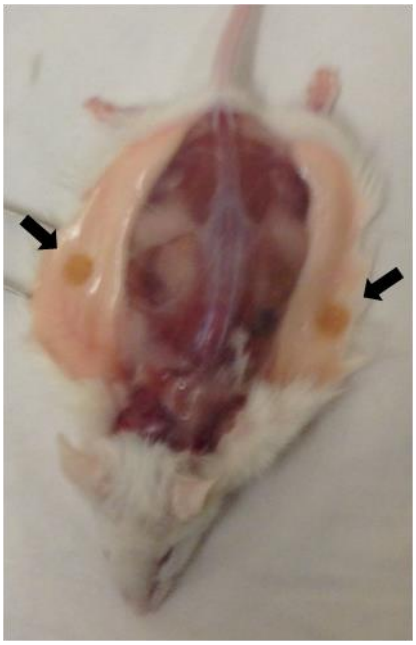

Figure 2.5 Retrieval of implanted disks. An incision behind the animal's neck was made and the skin was removed to expose the implanted disks. Arrows point at the implanted disks.

2.12.5KLH-Gal conjugation

Conjugation of α-Gal with keyhole limpet hemocyanin (KLH) to form KLH-Gal was performed using the Imject EDC carrier protein spin kit (Thermo scientific, UK) using the methods described by the manufacturer. In brief, a total of 4 mg KLH was conjugated to 24 mg of tri-α-Gal sugar in 0.1 M 2-[N-morpholino]- ethanesulfonic acid, (MES), 0.9 M NaCl, 0.02% NaN_3, pH 4.7 with 500 µg of [1-ethyl-3-(3-dimethylaminopropyl) carbodiimide hydrochloride], (EDC), in an overnight reaction. The KLH-Gal conjugate was purified from unreacted materials using a size exclusion spin column and recovered in 0.5 ml of elution buffer (8 mg/ml). Sterile water for injection was used to produce the conjugation and column elution buffers for the conjugation reaction. This

material was stored at – 20 ^{o}C until used. Prior to immunization the KLH-Gal was diluted to 2 mg/ml in sterile saline and mixed with vigorous vortexing with an equal volume of Freund's incomplete adjuvant. Animals were immunized with 0.1 ml (100 µg KLH-Gal) by intraperitoneal injection at 30 days of age.

To test the efficiency of conjugation, KLH-Gal was diluted to 10 µg/ml in carbonate buffer and coated on an ELISA plate. Lectin binding to the KLH-Gal conjugate was compared to KLH, BSA and BSA-Gal.

2.13 Calcium measurement

Calcium analysis on explanted porcine pericardium disks was done in collaboration with Professor John McArthur, Professor of Geology, UCL Earth Sciences, using inductively coupled plasma spectroscopy. Preparation of the samples for analysis was done by Dr Heide Kogelberg (UCL Institute of Cardiovascular Science, Cardiothoracic Surgery and Interventional Medicine Group).

Fixed but not implanted WT and GTKO porcine pericardium disks served as negative controls for calcium content prior to implantation. Explanted pericardial samples were cleared of any encapsulating materials and rinsed in sterile saline. The tissues were placed in weighed microcentrifuge tubes and dried at 65 ^{o}C for 20 hours. Then the microcentrifuge tube with the pericardium was weighed and the tissue dry weight was recorded. Dried pericardium was transferred to 8 ml glass vial and hydrolysed with 0.5 ml of concentrated nitric acid at 65 ^{o}C for 15 min with periodic vortexing after which 0.5 ml hydrogen

peroxide was added, mixed well and incubated at 65 ^{o}C for an additional 15 minutes. The sample was vortexed until tissue was completely dissolved. The dissolved materials were diluted with 3 ml of nanopure water, mixed well and 0.2 ml was transferred to a Sarstedt tube with 4.9 ml 1% nitric acid. Samples were then analysed in a 720 ICP-AES, axial configuration Inductively Coupled Plasma-Optical Emission spectrometer (Varian, USA).

Internal calcium standards were analysed as controls during each analysis. Calcium chloride dihydrate was dissolved in ultrapure water, hydrolysed as indicated above and diluted to produce calcium standards ranging from 0 to 5 µg/ml. These standards were run with each analysis and a blank and mid-range standard were repeated at regular intervals in each analysis to monitor and adjust for instrument drift.

2.14 Histology

Immunohistochemistry

Glutaraldehyde fixed pericardium or valve leaflets were embedded in optimal cutting temperature control compound (OCT), frozen and 8 micron sections cut with a Leica CM3050 cryostat. Sections were air dried and fixed in acetone for 10 minutes and frozen at – 80 ^{o}C until used. Tissue sections were thawed, air dried and circled with Pap Pen. The hydrophobic Pap Pen perimeter was left to air dry for 2 hours prior to staining. Slides were washed with water for 5 min in two changes to remove OCT, incubated in PBS for 10 minutes and blocked with 1% BSA in DPBS for 60 min, room temperature. Sections were incubated with GSIB4 (2 µg/ml diluted in DPBS with 1% BSA) overnight, at 4 °C, washed 3

times with PBS, 3 min each, blocked with 1% BSA in DPBS for 30 min, room temperature and incubated with streptavidin HRP (1:500) for 60 min, room temperature. The sections were washed 3 times with PBS 3 min each and stained with 3,3'- diaminobenzidine (DAB) for 5-15 min, room temperature. After staining the sections were washed extensively with water and counter stained with acid-Haematoxylin using standard techniques. Slides were subsequently dehydrated through an ethanol series (70% – 100% ethanol) and HistoClear prior to making a permanent mount in Perimount.

Immunohistochemistry staining for α-Gal with haematoxylin and eosin (H & E) counter stain was performed by our lab technician Miss Elisa Chisari.

Von Kossa and H&E staining of explanted pericardium were done by the UCL IQ Path facility, UCL Institute of Neurology.

2.15 Statistical analysis

GIE results are represented as mean values ± standard error of the mean (SEM). Comparisons of effective inhibition between different genotypes and different incubation conditions or different anticalcification treatments were analysed using student's t-test (two-tailed distribution, two-sample equal variance). P-values less than 0.05 were considered significant.

Sigmaplot software was used for curve fitting and to calculate IC50 values based on a four parameter logistic curve for the inhibition profiles of anti-Gal reagents with monomeric α-Gal trisaccharide. Excel was used for semi-log curve fitting to calculate mouse anti-Gal IgM and IgG titres.

Calcium content values and antibody titres are presented as mean values ± SEM. Comparisons between different implantation groups were analysed using t-test as described above. Linear regression and correlation analysis between calcification levels of WT implanted pericardium and anti-Gal IgM and IgG titres were performed using the corresponding Data Analysis tools in Excel. As some of the data was not normally distributed, the Spearman's rank correlation was calculated (r_s) in addition to Pearson correlation coefficient (r).

2.16 Laboratory work and summary of collaborative contributions

I performed all aspects of the laboratory work involving the enzymatic cycling reaction, hybridoma and endothelial cell culture, anti-Gal hybridoma purification, flow cytometry staining and analysis, Gal inhibition ELISAs, pig pericardium fixation and anticalcification processing, mouse serum anti-Gal antibody titration ELISAs, α-galactosidase digestion of cells or pericardium, as well as mice genotyping. Some of the mouse anti-Gal antibody ELISAs to determine the IgG titres were performed under my direction and training by Elisa Chisari.

Immunohistochemical staining for α-Gal with H&E counter stain was performed by technician Elisa Chisari. Von Kossa staining for calcium and H&E of explanted pericardium was done by the UCL IQ Path facility, UCL Institute of Neurology.

Calcium measurement on explanted pericardium was done in collaboration with Prof John McArthur, Professor of Geology, UCL Earth Sciences. Samples were prepared for calcium analysis by Dr Heide Kogelberg.

I was trained in general animal procedures, as part of getting my personal licence, by taking part in a series of required training courses (modules 1,2, 3,4) at the Royal Veterinary College. Specific training for the subcutaneous implant surgeries was from Dr Guerard Byrne. I performed all of the surgeries and Dr Byrne assisted with induction and maintaining anaesthesia during surgery. Retrieval of explants and terminal blood collection via cardiac puncture was performed by me. Due to its highly technical nature blood collection via cardiac puncture was supervised and assisted by the unit's technologists.

RESULTS

3 Enzymatic detection of galactose

We initially tried to adapt an enzymatic method used to measure lactose to detect α-linked galactose. In this approach galactose was released by digestion with α-galactosidase and the amount of galactose was measured by reacting with GH. GH in the presence of NAD produces NADH in stoichiometric amounts from galactose. NADH can be directly measured by measuring its absorbance at 340 nm. Initial tests of this reaction using galactose concentrations ranging from 39 µM to 10,000 µM showed that NADH could be detected, but the sensitivity of the method was low. Galactose concentrations of 312.5 µM or higher were required for reliable detection (**Figure 3.1A**). This was equivalent to approximately 1.8 x 10^{20} molecules of galactose.

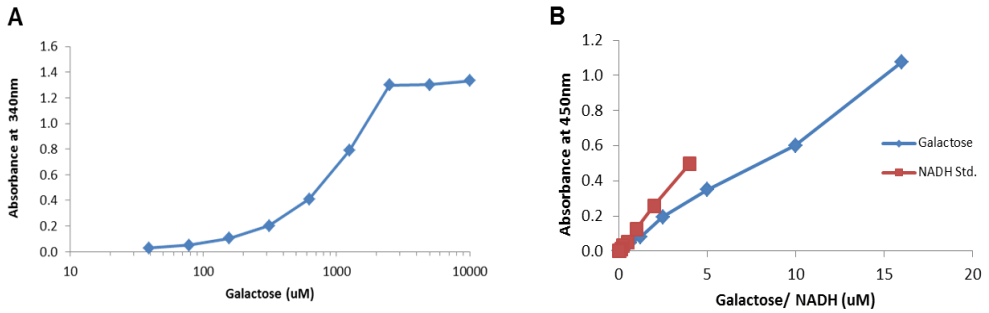

Figure 3.1 NADH production from galactose by galactose dehydrogenase. Different concentrations of galactose were incubated with galactose dehydrogenase (GH) and stoichiometric amount of NADH was produced. **A:** The NADH produced by GH was measured by spectrophotometry at 340 nm. **B:** Formazan was produced using enzymatic cycling to amplify the signal of the NADH produced by GH from galactose (blue line), or by testing NADH standard concentrations (red line).

Using conservative estimates, the amount of α-Gal derived from small samples of BHVs or pig tissue was expected to be much lower, in the order of 10^{11} α-Gal epitopes/mg porcine tissue (Stone et al. 2007). To improve the sensitivity for detecting NADH an enzymatic cycling system (CycLex, MBL) was used. This enzymatic cycling system has the potential to detect 0.0156 µM NADH, which is equal to $9.4x10^{15}$ molecules. When the cycling system was coupled with the GH reaction, the lower limit of detection was approximately 1 µM galactose ($6.022x10^{17}$ molecules) (**Figure 3.1B**).

Although the GH reaction and the enzymatic cycling system reactions were coupled successfully, they did not provide a satisfactory level of sensitivity. A very large amount of tissue or cells would still be required to detect galactose within that range of sensitivity, as $6.022x10^{17}$ molecules galactose corresponded to 6 kgrams of pig tissue. This sensitivity would probably be further decreased by addition of another enzymatic step, that of α-galactosidase reaction, so the method was not further pursued.

4 Inhibition ELISA with different anti-Gal reagents

4.1 Development of the assay

4.1.1 Anti-Gal reagents inhibition with α-Gal

A Gal inhibition ELISA was developed to measure α-Gal on solid substrates (**Figure 2.3**). In this assay the amount of α-Gal on tissue or cells was estimated by the reduced amount of free anti-Gal reagent available to bind in a Gal ELISA. Three different anti-Gal reagents were tested - GSIB-4, which is a lectin widely used to detect α-linked galactose and mouse anti-Gal monoclonal antibodies M86 (IgM) and GT5 (IgG). Prior to the inhibition ELISA the concentration of each anti-Gal reagent which yielded approximately 70% of their maximal binding in the BSA-Gal ELISA was determined (0.125 µg/ml GSIB-4 lectin, 1:10 M86 IgM supernatant and 1µg/ml GT5 IgG) (**Figure 4.1**). These concentrations were selected for the inhibition studies, as they provide a sufficient dynamic range in which to measure depletion of free anti-Gal reagent by the test material.

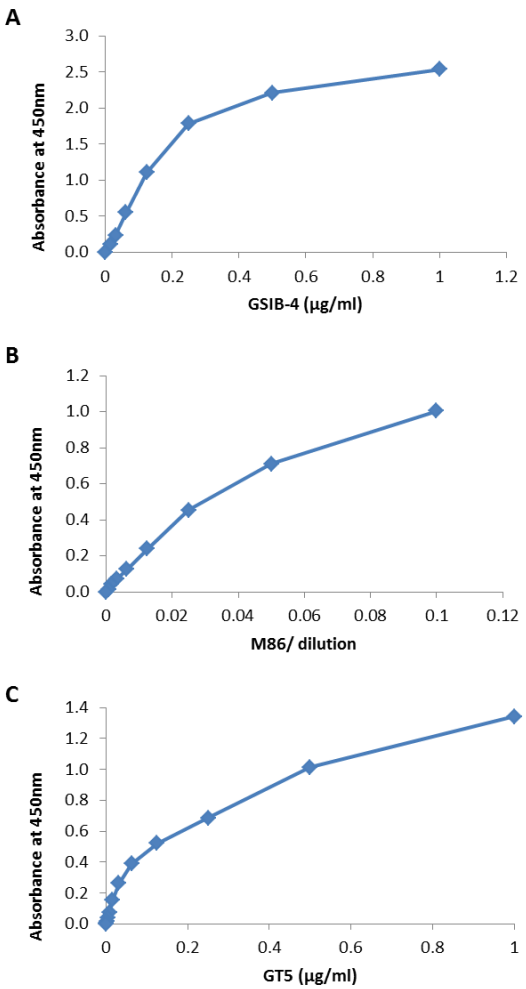

Figure 4.1 Anti-Gal reagents' binding to BSA-Gal. Serial dilutions of biotinylated GSIB-4 and anti-Gal monoclonal antibodies M86 and GT5 were tested in duplicate (50 µl/ well) in a microtiter plate coated with 10 µg/ml BSA-Gal, for 90min, at 4^{o}C. GSIB-4 (0.0039 - 1 µg/ml) binding was detected with extravidin-peroxidase (1:1000) incubated at RT for 1 hour. Detection of M86 (serial dilutions from 1:1 to 1:1280) and GT5 (0.001 – 1 µg/ml) was done using a biotin-conjugated anti-mouse IgM or IgG, respectively and then detected with extravidin-peroxidase. **A:** GSIB-4, **B:** M86 IgM, **C:** GT5 IgG.

To further characterize these reagents each was mixed at a set concentration with serial dilutions of free α-Gal trisaccharide (tri-α-Gal) at 4 ^{o}C overnight to produce an inhibition profile (**Figure 4.2**).

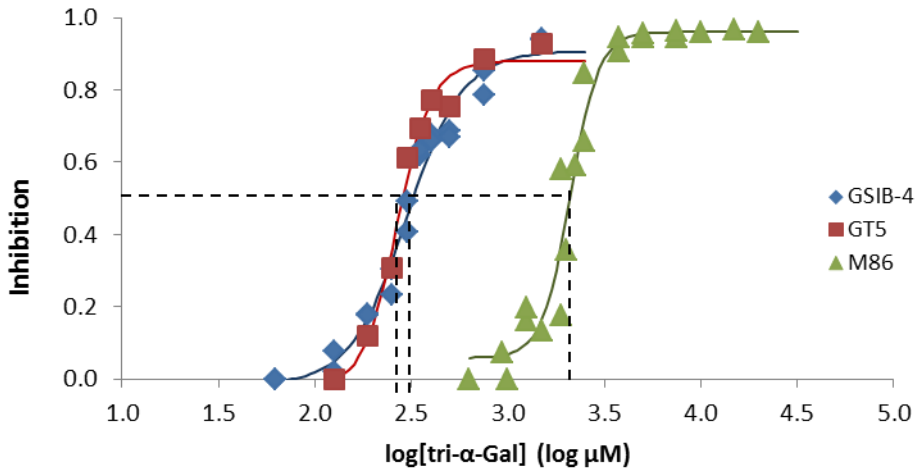

Figure 4.2 The inhibition of anti-Gal reagents by free α-Gal trisaccharide (tri-α-Gal). The graph shows the inhibition profiles of anti-Gal reagents [GSIB-4 lectin (blue), GT5 IgG (red) and M86 IgM (green)]. A constant concentration of each reagent was incubated with serial dilutions of tri-α-Gal and then tested for residual binding by ELISA using BSA-Gal as a solid phase antigen. Curves were fitted as four parameter logistic curves using the *SigmaPlot 10.0* software. The points at which the dotted lines meet the x axis represent the IC50 values for each reagent which produced 50% inhibition in the Gal ELISA. Each curve is an aggregate inhibition profile derived from several independent studies.

For each reagent a sigmoid binding curve to BSA-Gal was observed. The position of this curve on the x axis is a measure of the relative avidity of each reagent to BSA-Gal. At half maximal inhibition by free tri-α-Gal monomer an IC50 (half maximal inhibitory concentration) could be defined. The pentameric anti-Gal IgM M86 with 10 α-Gal binding sites had the highest IC50 (2089 µM). The lectin GSIB-4 with 4 α-Gal binding sites had an IC50 of 323 µM. The lowest apparent avidity was seen with anti-Gal IgG GT5 (285 µM). This indicates that nearly 6.5 times more tri-α-Gal monomer is required to inhibit M86 binding to BSA-Gal by 50% compared to GT5 or GSIB-4. The apparent avidity

for each reagent is strongly dependent on the number of binding sites, but it is also expected to be affected by the affinity of each binding site.

To confirm specific binding to α-Gal each reagent was tested for binding to Gal-positive or GTKO PAECs by flow cytometry. Binding to GTKO PAECs was used as a negative control. GSIB-4 lectin and M86 IgM bound to Gal-positive PAECs but not to GTKO cells (**Figure 4.3 A and B**). The anti-Gal GT5 IgG bound strongly to Gal-positive PAEC, but also surprisingly showed residual binding to GTKO cells (**Figure 4.3C**). Because of this background binding to GTKO PAEC GT5 was not used in additional experiments.

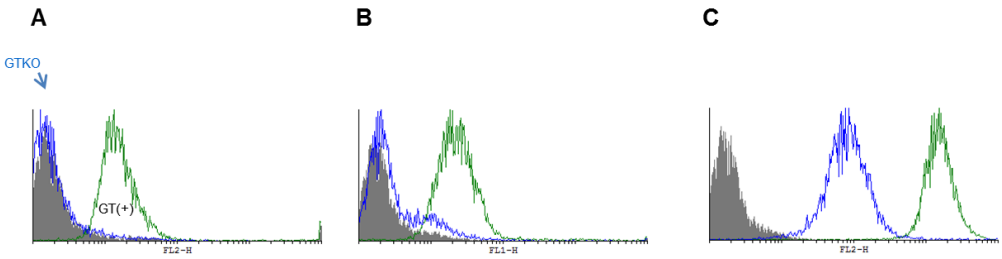

Figure 4.3 Binding of anti-Gal reagents on Gal positive and GTKO PAECs tested by flow cytometry. Cells were incubated with: **A: GSIB-4**, **B: M86** or **C: GT5**. Binding of the anti-Gal reagents was detected with PE-conjugated streptavidin (GSIB-4), FITC-conjugated rat anti-mouse IgM (M86), or PE-conjugated goat anti-mouse IgG (GT5). In each histogram, the green line represents binding to Gal-positive cells and the blue line binding to GTKO cells. The grey filled line represents a negative control where cells were stained with only the respective secondary reagent. Y axis represents counts.

4.1.2 M86 IgM binding on PAEC

M86 was incubated at 4^{o}C overnight with different numbers of Gal-positive PAECs, (0.5 – 7.5) x10^{6} cells. Under these conditions increasing numbers of

PAECs bound to proportionally higher amounts of M86, as judged by the apparent depletion of free M86 available for binding in the Gal ELISA (**Figure 4.4A**). In parallel to this cellular inhibition M86 was incubated with free tri-α-Gal under the same conditions. This resulted in an inhibition curve (**Figure 4.4B**). The inhibitory effect of tri-α-Gal against M86 binding was evident at concentrations higher than 1200 µM (log3.08) and reached approximately 100% at concentrations of approximately 3100 µM (log3.49) or higher.

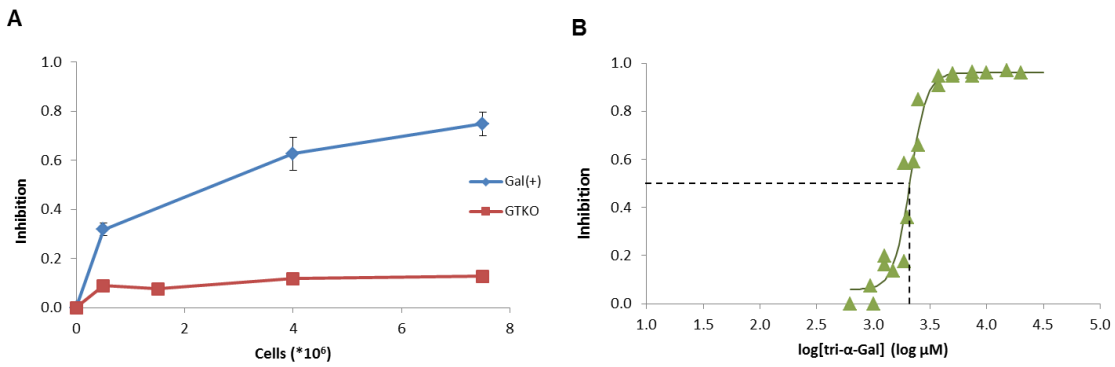

Figure 4.4 M86 IgM antibody inhibition by α-Gal. **A:** Graph shows inhibition of M86 binding to BSA-Gal ELISA by Gal-positive [Gal(+)] PAECs (blue line) or GTKO EC cell line (red). Each point for the Gal(+) PAECs shows the mean ± SEM of three independent experiments. Each sample was measured in duplicate. The GTKO cell line results are from a single experiment. **B:** Inhibition of a constant concentration of M86 by serial dilutions of free α-Gal trisaccharide (tri-α-Gal). The graph depicts the inhibition profiles for M86 from two independent experiments, each indicated by a different symbol. The point at which the dotted line meets the x axis represents the tri-α-Gal concentration which produces 50% inhibition (IC50) of M86 binding in the Gal ELISA. The curve was fitted as a four parameter logistic curve using the *SigmaPlot 10.0* software.

By comparing these curves an equivalent amount of free monomeric α-Gal which produced a specific degree of inhibition could be related to the number of cells which produced the same degree of inhibition. For cell numbers within the range of $0.5x10^6$ up to $7.5x10^6$ the equivalent amounts of α-Gal were in the

range of 1800 µM – 2600 µM (**Table 1**). For 50% inhibition of M86 by α-Gal-positive PAECs we calculated that $1.6x10^6$ PAECs are required.

Table 1 Gal(+) PAECs and equivalent concentrations of α-Gal monomer that produce the same degree of M86 inhibition in the Gal ELISA.

Gal(+) PAECs (*10^6)	% Inhibition	Equivalent α-Gal (µM)
0.5	31.8	1805.2
1.6	50.0	2089.0
4.0	62.7	2302.5
7.5	74.9	2568.7

The specificity of M86 binding was further tested in the inhibition assay by binding to GTKO PAECs under the same conditions (**Figure 4.4A**, red line). Incubation with GTKO cells did not produce appreciable inhibition of M86 binding in the Gal-ELISA. Even at high concentrations of up to $7.5x10^6$ GTKO cells M86 inhibition was only 10%, consistent with non-specific background binding to cells.

4.1.3 GSIB-4 binding on PAEC

Similar to the analysis of M86, an inhibition profile for GSIB-4 was produced. GSIB-4 bound on α-Gal-positive PAECs as determined by the increasing percentage of inhibition in the Gal ELISA (**Figure 4.5A**). A monomeric α-Gal inhibition curve for GSIB-4 lectin was done in parallel (**Figure 4.5B**) and was used to compute the equivalent amount of α-Gal monomer required to match inhibition by α-Gal-positive PAECs (**Table 2**).

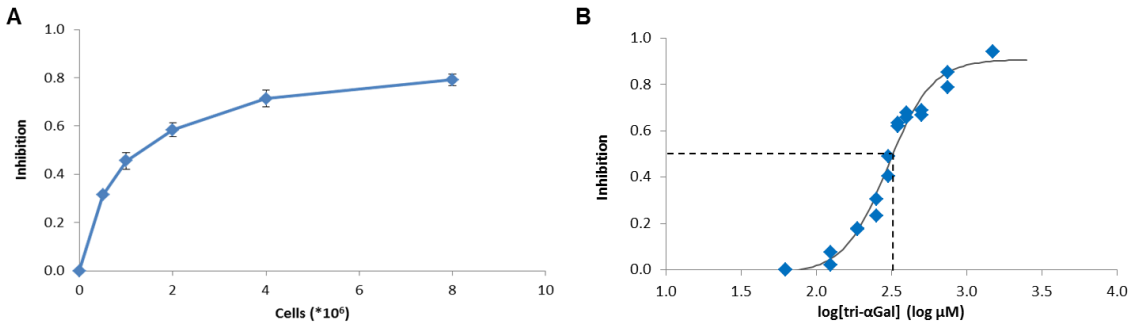

Figure 4.5 GSIB-4 lectin inhibition by α-Gal. **A:** Graph shows inhibition of GSIB-4 binding to BSA-Gal ELISA by Gal-positive PAECs. Each point shows the mean ± SEM of three independent experiments. Each sample was measured in duplicate. **B:** Inhibition of a constant concentration of GSIB-4 by serial dilutions of free α-Gal trisaccharide (tri-α-Gal). The graph depicts the inhibition profiles for GSIB-4 from two independent experiments. The point at which the dotted line meets the x axis represents the tri-α-Gal concentration which produces 50% inhibition (IC50) of GSIB-4 binding in the Gal ELISA. The curve was fitted as a four parameter logistic curve using the *SigmaPlot 10.0* software.

Inhibition of GSIB-4 by Gal-positive PAECs (0.5 – 8 $*10^6$) was equal to inhibition by 245 µM – 569 µM α-Gal monomer. We calculated an IC50 for GSIB-4 inhibition of $1.3x10^6$ cells.

Table 2 Gal(+) PAECs and equivalent concentrations of α-Gal monomer that produce the same degree of GSIB-4 inhibition in the Gal ELISA.

Gal(+) PAECs ($*10^6$)	% Inhibition	Equivalent α-Gal (µM)
0.5	31.5	245.6
1.0	45.6	302.9
1.3	50.0	322.9
2.0	58.5	367.5
4.0	71.4	465.0
8.0	79.1	569.5

Despite the 6-fold difference in apparent avidity between M86 and GSIB-4 (**Figure 4.2**) both reagents bound to Gal-positive PAEC with nearly identical IC50s and producing similar inhibition profiles (**Figure 4.6**).

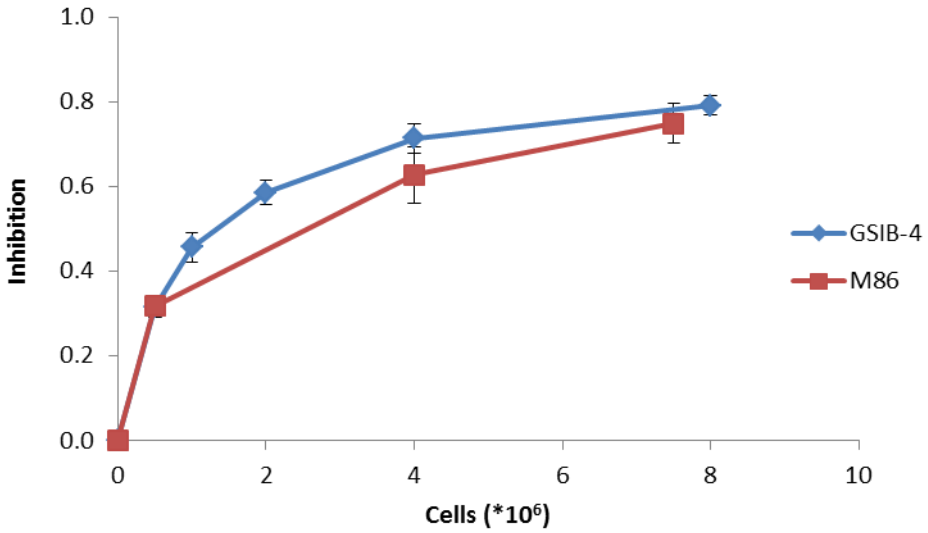

Figure 4.6 Comparison of the inhibition profiles of GSIB-4 lectin and IgM antibody M86 with Gal-positive PAECs. GSIB-4 (blue line), M86 (red line). Graph shows the mean values ± SEM of three independent experiments for each reagent.

4.1.4 GSIB-4 and fixed pig pericardium

We used glutaraldehyde (0.6%) fixed pig pericardium as a model bioprosthetic tissue. To use the inhibition assay for measuring α-Gal content of this tissue we first tested the duration of incubation. Fixed, 3mm diameter, pericardium disks (n=4) were incubated with GSIB-4 at 4^{o}C, overnight and up to 3 days (**Figure 4.7**).

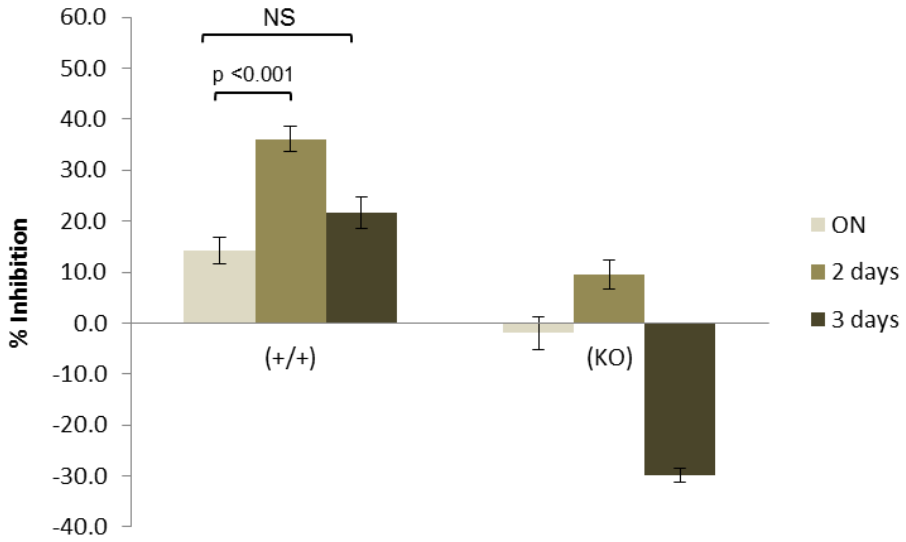

Figure 4.7 Testing the duration of incubation for GSIB-4 binding to fixed pig pericardium. The graph shows GSIB-4 inhibition by wild type (+/+) and GTKO (KO) fixed pig pericardium after overnight (ON), 2 days and 3 days incubation. All experiments were performed using four (3mm diameter) disks incubated with GSIB-4 for the indicated times. Each bar represents the mean ± SEM of a minimum of 8 independent samples. Results of student's t-test are indicated by p-values. NS: not significant.

Overnight (ON) incubation resulted in approximately 14% inhibition which increased significantly to 36% in 2-day incubation. No further increase in GSIB-4 binding occurred with longer incubation times. For ON and 2-day incubations there was little binding to GTKO pericardium. In contrast at 3-day incubation with GTKO pericardium there was an apparent increase in GSIB-4 binding in the Gal ELISA (negative inhibition) (**Figure 4.7**). This suggested that prolonged incubation does not improve lectin binding to Gal-positive tissue and may create an artefact in the Gal ELISA. When fixed heterozygous, GT(+/-), pericardium was tested in comparison to GT(+/+) and GTKO, in ON (**Figure 4.8A**) and 2-day (**Figure 4.8B**) incubations, the differences in inhibition levels produced by α-Gal-

positive and GTKO tissue were more significant after 2-day incubation (**Figure 4.8B**). We selected 2 days as the standard duration for incubation.

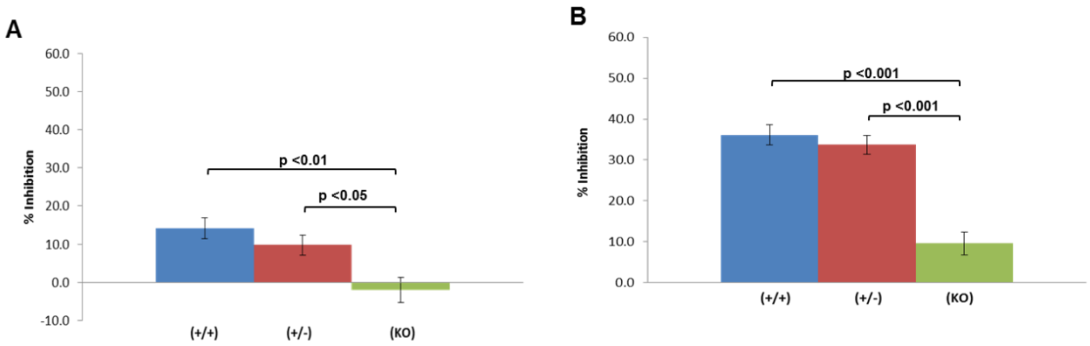

Figure 4.8 Comparing overnight (ON) and 2-day incubation for GSIB-4 lectin binding to fixed pig pericardium. Graphs depict the apparent inhibition of GSIB-4 binding in the Gal ELISA by fixed pig pericardium. Three different genotypes of pericardium were tested- Gal-positive homozygous (+/+), heterozygous (+/-) and Gal knock-out (KO). **A: Overnight** incubation. **B: 2-day** incubation. Data are expressed as mean ± SEM. A minimum of four samples (each with four, 3mm diameter, disks incubated with GSIB-4) of each genotype were used and three independent experiments were performed. Results of student's t-test are indicated by p-values.

Increasing the number of disks was expected to increase the level of inhibition. We tested whether the increase of antigen would improve the sensitivity of the assay by comparing lectin binding to Gal-positive homozygous (GT+/+), heterozygous (GT+/-) and GTKO pericardium. The number of pericardium disks used per sample was increased from 4 to 8. Increasing the amount of antigen resulted in increased GSIB-4 binding and increased inhibition in the Gal ELISA (**Figure 4.9B**). Maximal inhibition for GT(+/+) increased from 36.1 ± 8.9 % (using 4 disks) to 50.2 ± 7.2 % (using 8 disks). Background binding to GTKO tissue remained low. Under these conditions GSIB-4 binding to GT(+/-) tissue resulted in 38 ± 6.4 % inhibition. This was significantly less than GSIB-4 binding to GT(+/+) tissue. A significant difference in GSIB-4 binding between GT(+/+) and GT(+/-) tissue was not detected when 4 disks of pericardium were used (**Figure 4.9A**).

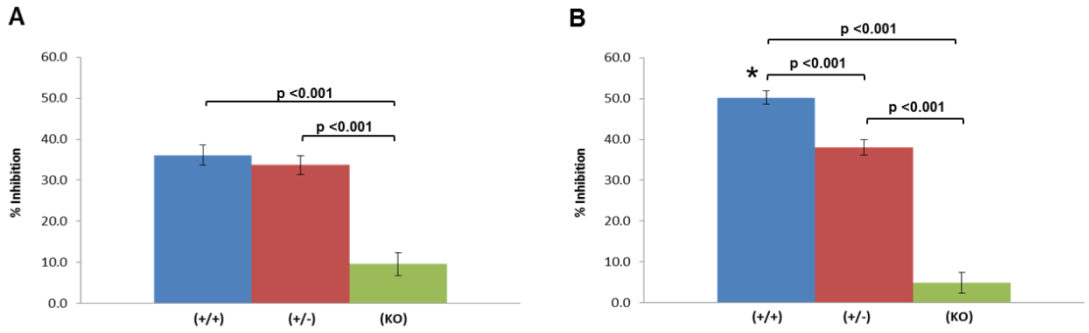

Figure 4.9 Comparing the effects of 4 versus 8 disks on GSIB-4 binding to fixed pig pericardium. Graphs depict the apparent inhibition of GSIB-4 binding in the Gal ELISA. Three different genotypes of pericardium were tested- Gal-positive homozygous (+/+), heterozygous (+/-) and Gal knock-out (KO). **A: Four** or **B: eight** disks (3mm diameter) of fixed pig pericardium per sample were incubated with GSIB-4 for 2 days. Data are presented as mean ± SEM. Minimum four samples of each genotype were used and three independent experiments were performed. Results of student's t-test are indicated by p-values. The asterisk indicates that the increase in inhibition produced by 8 (+/+) disks compared to 4 (+/+) disks was highly significant.

This suggests that 8 glutaraldehyde fixed, 3mm diameter, pericardium disks with 2 days incubation at 4^{o}C represent optimal conditions for the inhibition assay. These conditions were thus used to examine M86 binding on fixed pig pericardium.

4.1.5 M86 binding on fixed pig pericardium

M86 antibody (1:10 dilution) was incubated with 8 pericardium disks at 4^{o}C for 2 days. Under these conditions both GT(+/+) and GT(+/-) pericardium bound significantly more M86 than GTKO pericardium causing a higher apparent inhibition in the Gal-ELISA. M86 binding to GT(+/+) (25.6 ± 6.47 %) was higher than binding to GT(+/-) pericardium (18.4 ± 2.13 %). However, this did not reach significance (**Figure 4.10**).

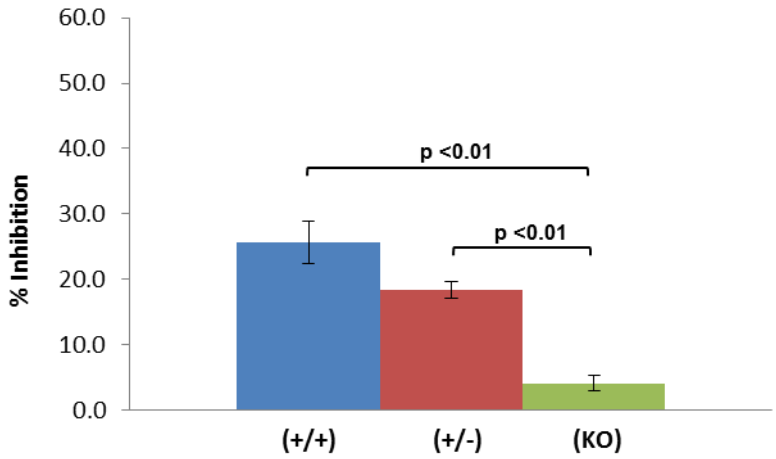

Figure 4.10 M86 inhibition by fixed pig pericardium. Graphs depict the apparent inhibition of M86 binding in the Gal ELISA by fixed pig pericardium. Three different genotypes of pericardium were tested- Gal-positive homozygous (+/+), heterozygous (+/-) and Gal knock-out (KO). Four independent samples of each genotype (each sample with eight, 3mm diameter, disks incubated with M86) were tested. Data are presented as mean ± SEM. Results of student's t-test are indicated by p-values.

GSIB-4 and M86 showed similar binding to α-Gal-positive PAECs, but showed different levels of apparent inhibition when incubated with fixed pericardium. Binding of GSIB-4 to fixed pig pericardium appeared to be more effective, as higher inhibition was produced by α-Gal-positive pericardium compared to M86 (**Figure 4.11**).

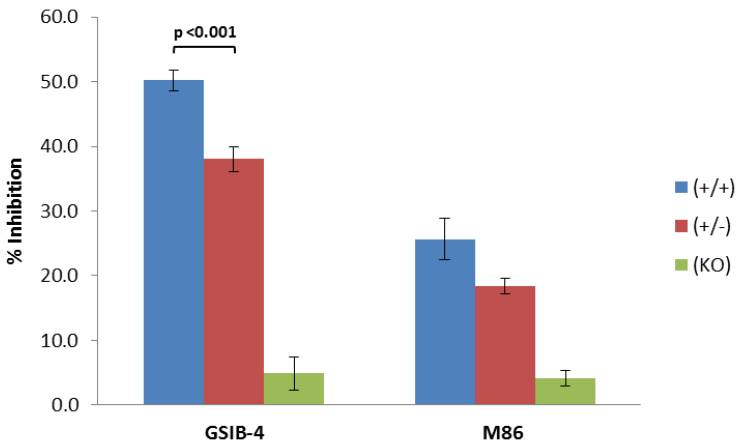

Figure 4.11 Comparison of GSIB-4 and M86 binding to fixed pig pericardium. Graphs depict the apparent inhibition of GSIB-4 and M86 binding in the Gal ELISA by fixed pig pericardium. Three different genotypes of pericardium were tested - Gal-positive homozygous (+/+), heterozygous (+/-) and Gal knock-out (KO). Bars represent averaged results of 3 independent experiments. Data are presented as mean ± SEM.

Furthermore, GSIB-4 detected a significant difference in α-Gal levels between homozygous and heterozygous α-Gal-positive pericardium (**Figure 4.11**). This suggests that despite the higher apparent avidity of M86 for BSA-Gal, GSIB-4 is more effective for measuring α-Gal in fixed pig pericardium under these conditions.

4.2 Determining inhibition ELISA's sensitivity

The aim of the following experiments was to estimate the sensitivity of the α-Gal inhibition ELISA (GIE), by measuring the smallest reduction in α-Gal content that can be reliably detected by this assay. To accomplish this I used α-galactosidase digestion to partially remove α-Gal epitopes from WT PAECs. I then used both GIE and quantitative flow cytometry to measure the changes in α-Gal expression on PAECs. By comparing these two methods I defined the

minimal reduction in α-Gal levels, as measured by flow cytometry, to identify the minimal change in α-Gal required to get reliable detection by the GIE.

WT PAECs were treated with α-galactosidase to cleave terminal α-Gal epitopes. Subsequently the cells were stained with biotin-conjugated lectin GSIB-4. Binding of GSIB-4 to PAECs was detected by streptavidin-PE or streptavidin-AlexaFluor 488. GTKO PAECs that do not express α-Gal were used as a negative control.

Digestion of PAECs with increasing concentrations of α-galactosidase resulted in progressive removal of increasing amounts of α-Gal epitopes from the cell surface. This resulted in correspondingly reduced binding of GSIB-4 (**Figure 4.12**).

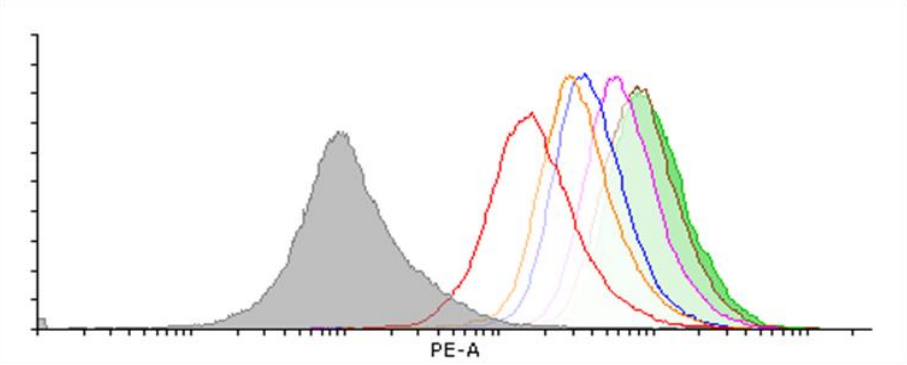

Figure 4.12 FACS histograms of WT PAECs digested with increasing concentrations of α-galactosidase. WT PAECs were treated with a range of α-galactosidse concentrations (1 – 10 units/ml). Subsequently cells were stained with GSIB-4 and streptavidin-PE. The above histogram depicts GSIB-4 binding to non-digested WT PAECs (filled green histogram), to PAECs after digestion with 1 (brown line), 2.5 (purple line), 5 (blue line), 7.5 (orange line) and with 10 units/ml (red line) α-galactosidase. The grey filled histogram represents GSIB-4 binding to GTKO PAECs. Y axis represents counts.

The results in **Figure 4.12** can be presented as a graph depicting mean fluorescence intensity (MFI) of GSIB-4 binding in relation to the α-galactosidase concentrations. This representation clearly shows that increasing levels of α-galactosidase progressively reduced the expression of α-Gal epitopes and proportionately reduced the level of GSIB-4 binding to cells (**Figure 4.13**).

Flow cytometry is an accepted standard quantitation method for determining the level of antigen expression on cells. This FACS data can be used to calculate the percentage of reduction of GSIB-4 binding compared to the MFI of non-digested PAECs using the following equation:

Equation D:

$$\%\ \text{Reduction}_{(FACS)} = \frac{(\text{MFI of non-digested cells} - \text{MFI of digested cells}) * 100}{\text{MFI of non-digested cells}}$$

In this individual experiment there was a reduction of MFI from 11,626 to 2262 at 10 units/ml of α-galactosidase representing a 80.55 % reduction of lectin binding (**Figure 4.13**).

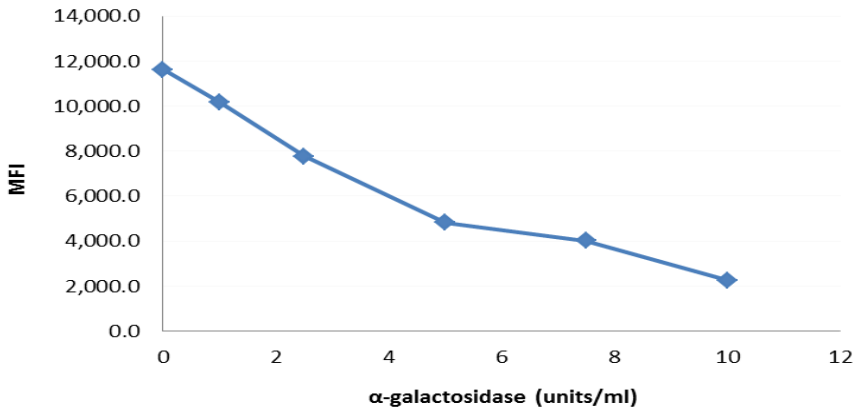

Figure 4.13 Mean fluorescence intensity (MFI) of PAECs stained with GSIB-4 after α-galactosidase treatment. The graph depicts the progressive reduction in GSIB-4 binding to WT PAECs after treatment with rising concentrations of α-galactosidase. This is a representative FACS analysis of a single digestion experiment.

A-galactosidase digestion within a range of (2-8) units/ml was used to consistently achieve moderate reduction in α-Gal epitopes. These experiments showed a consistent reduction in α-Gal level producing PAECs with reliably intermediate levels of α-Gal. A reduction of 12% to 40% of α-Gal antigen was demonstrated after digestion with a range of 2 to 8 units/ml of α-galactosidase (**Figure 4.14**).

By calculating the percentage of reduction in MFI we could monitor the loss of α-Gal antigen due to α-galactosidase digestion.

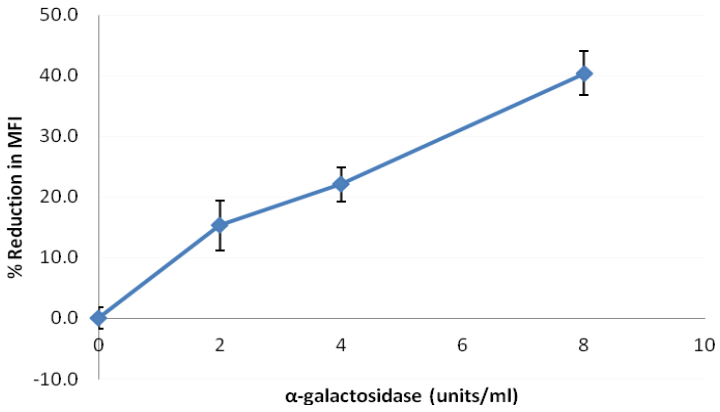

Figure 4.14 Average reduction in GSIB-4 binding to WT PAECs after α-galactosidase digestion measured by FACS. The graph shows the percentage of MFI reduction after digestion of WT PAECs with α-galactosidase. This reduction corresponds to reduction in α-Gal epitopes. Each point represents mean value from a minimum of 6 samples at each enzyme concentration. Error bars represent SEM.

To gauge the sensitivity of the GIE, WT PAECs were treated with α-galactosidase and the reduction in α-Gal antigen was measured by GIE and flow cytometry in parallel. After digestion PAECs (250,000) were stained with GSIB-4 for FACS analysis and the remaining cells ($1.25x10^6$) were used in the GIE assay. For the GIE inhibition was expressed as a percentage in comparison to the background binding of GSIB-4 to fixed GTKO PAECs as calculated by the following equation:

Equation E

$$\% \text{ Inhibition} = (OD_{GTKO} - OD_{sample}) * 100 / OD_{GTKO}$$

OD_{GTKO}: the GIE optical density measured in the presence of GTKO PAECs.

OD_{sample}: the GIE optical density measured in the presence of WT PAECs either treated or not treated with α-galactosidase.

With progressive α-galactosidase digestion the level of α-Gal antigen on PAECs was proportionately reduced. This led to a reduction of GSIB4 binding to the cells with a corresponding increase in free GSIB-4 available to bind in the α-Gal ELISA. The result was an apparent reduction in inhibition with increasing enzyme levels (**Figure 4.15**).

To compare the GIE and flow cytometry results we calculated the reduction in inhibition levels for the GIE (**Figure 4.15 B**) and compared that to the reduction in MFI for flow cytometry (**Figure 4.16**). This was expressed as a percentage of the inhibition produced by α-galactosidase digested PAECs compared to the inhibition produced by non-digested PAECs and was calculated from the following equation:

Equation F

$$\text{\% Reduction in Inhibition} = \frac{(\text{\% Inhibition of non-digested cells} - \text{\% Inhibition of digested cells}) * 100}{\text{\% Inhibition of non-digested cells}}$$

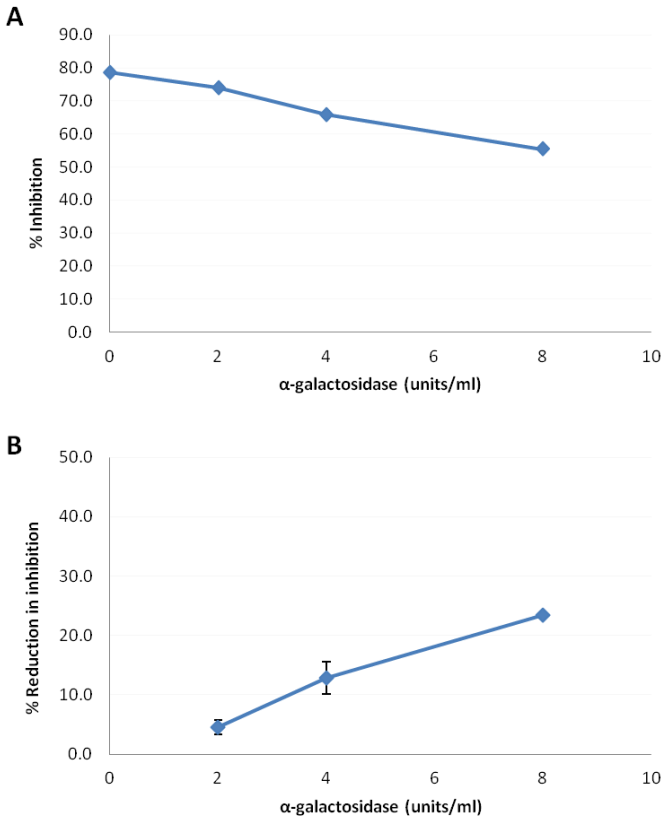

Figure 4.15 Effects of α-galactosidase digestion on the α-Gal inhibition ELISA (GIE) assay. A) The graph depicts the per cent inhibition observed in the GIE assay after α-galactosidase digestion of PAECS from a single representative experiment. Removal of α-Gal epitopes on PAECs with α-galactosidase reduced GSIB-4 binding and increased the level of free GSIB-4 available for the α-Gal ELISA. This leads to reduced inhibition in the α-Gal ELISA with increasing levels of α-galactosidase. **B**) **Reduction in inhibition after α-galactosidase digestion**. Transformation of the data in Figure 4.15A shows the apparent reduction in GIE with increasing α-galactosidase. The graph depicts the same data as presented in figure 4.15A.

By this comparison we could estimate the relative sensitivity of the GIE. The flow cytometry results showed a consistent reduction in α-Gal antigen (**Figure 4.16**) progressing from 15% to 40% reduction in GSIB-4 binding when using (2-8) units/ml α-galactosidase. In comparison the GIE appeared to be somewhat less sensitive showing only a 12% to 28% reduction across the same range of

α-galactosidase treatment. Moreover, at low α-galactosidase levels (2 – 4 units/ml) the GIE could not reliably distinguish the change in α-Gal expression.

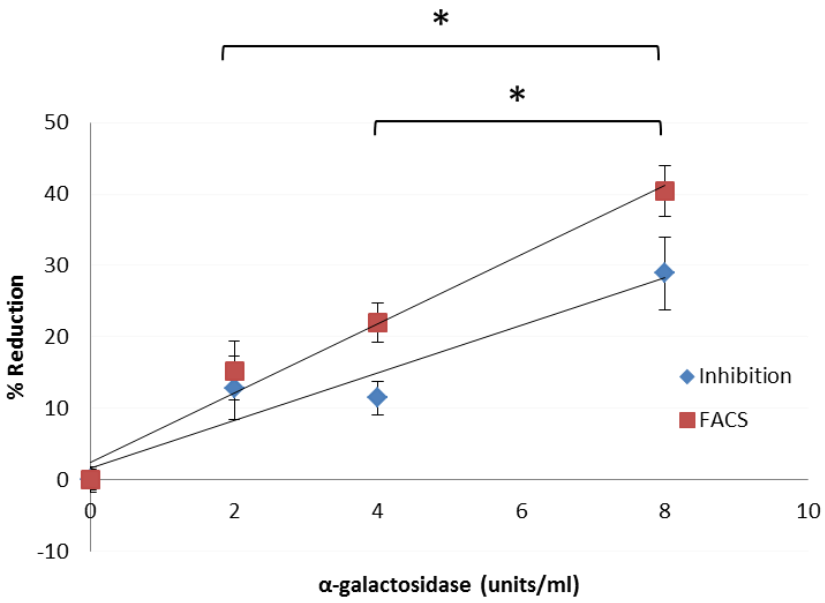

Figure 4.16 Reduction of α-Gal on PAECs after α-galactosidase digestion estimated by FACS or α-Gal inhibition ELISA. Both FACS and α-Gal inhibition ELISA showed that increasing concentrations of α-galactosidase resulted in progressive reduction in α-Gal levels from the cells surface. Each point shows the mean ± SEM from a minimum of four experiments. The differences in reduction of α-Gal levels between 8 units/ml of enzyme and 4 units/ml or 8 and 2 units/ml were significant for both methods. However none of the methods detected a significant difference in α-Gal levels between digestion with 4 and 2 units/ml. Significant differences are indicated by asterisks ($p<0.05$).

This suggests that the smallest reduction in α-Gal levels that can be detected by GIE is approximately a 20% decrease. We expect that this level of sensitivity is sufficient for the GIE to detect biologically meaningful decreases in α-Gal levels which may occur on fixed tissues after anticalcification treatments.

4.3 Summary and discussion of results

I managed to develop a robust Gal inhibition ELISA (GIE) assay for measuring α-Gal on cells and fixed tissue using two different anti-Gal reagents, lectin GSIB-4 and IgM M86. Both reagents bound to PAECs in a similar way, but GSIB-4 was more sensitive for binding to fixed pig pericardium. It detected significant differences between homozygous and heterozygous α-Gal positive tissue, while M86 could not distinguish between them. To determine the sensitivity of the GIE I used α-galactosidase digestion of PAECs to partially remove α-Gal and estimated the reduction in α-Gal levels using flow cytometry and GIE. These changes in α-Gal levels were expressed as percentage of reduction in MFI and percentage of reduction in inhibition ELISA, so that the sensitivity of the two methods could be compared. The sensitivity for the GIE assay was estimated at approximately 20% reduction in α-Gal levels, suggesting that GIE assay can be used to study the effect of anticalcification treatments to fixed tissue.

5 Effects of anticalcification processing on α-Gal levels in fixed animal tissue

Anticalcification treatments are used in industry to reduce the level of phospholipids which are thought to be sites for calcium deposition. These anticalcification processes are highly effective in the subcutaneous implant (rat and rabbit) and juvenile sheep valve implant models. While these animal models do not produce anti-Gal antibody and thus calcification is likely due to passive plasma calcium binding and crystal growth, none-the-less phospholipid extraction may also reduce the level of α-Gal antigen by removing glycolipids and this might help to reduce antibody mediated injury of BHVs. We used the GIE with GSIB-4 (GIE_{GSIB-4}) and M86 (GIE_{M86}) to assess the level of α-Gal reduction caused by various anticalcification processing methods.

Porcine pericardium or heart valve leaflets were fixed in 0.6% glutaraldehyde and then treated with glutaraldehyde capping (glycine), phospholipids extraction using either ethanol, SDS or a combination of formalin, ethanol and Tween (FET). Controls included fixed tissue treated with α-galactosidase and GTKO tissue subjected to the same capping, enzymatic or lipid extraction procedures to control for potential effects on non-specific GSIB-4 or M86 binding.

5.1 GIE $_{GSIB-4}$ assessment of α-Gal levels after anticalcification of porcine pericardium

WT porcine pericardium causes an apparent GIE_{GSIB-4} inhibition (50.27 ± 2.00 %) which was significantly higher than the non-specific inhibition by GTKO pericardium (20.5 ± 0.87 %). Overall, the anticalcification treatments had little effect on α-Gal levels in WT pericardium. GIE_{GSIB-4} inhibition for anticalcification treatments ranged from 36% to 57%, comparable to those of untreated WT tissue (**Figure 5.1A**). Extraction with SDS was the only treatment to significantly reduce α-Gal levels, lowering GIE_{GSIB-4} inhibition to 36.67 ± 3.37 %. This represents a moderate (27.05%) reduction of α-Gal antigen by SDS extraction. In contrast, α-galactosidase treatment effectively stripped α-Gal antigen from the pericardium with GIE_{GSIB-4} inhibition levels of 17.33 ± 2.20 %, similar to non-specific GTKO inhibition (**Figure 5.1A**).

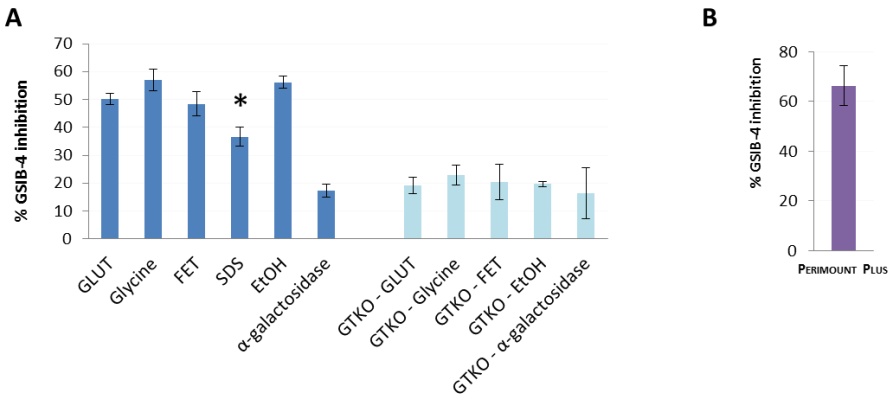

Figure 5.1 GIE $_{GSIB-4}$ estimates of α-Gal antigen on fixed porcine pericardium after processing with anticalcification treatments. **A)** WT pericardium (blue) was fixed with glutaraldehyde (GLUT) and subsequently processed with glycine for glutaraldehyde quenching, with formaldehyde–ethanol–Tween 80 (FET), sodium dodecyl sulfate (SDS) or ethanol (EtOH) to extract phospholipids. GLUT fixed pericardium was also treated with α-galactosidase to remove α-Gal epitopes. GTKO pericardium (light blue) was similarly treated to account for non-specific lectin absorption. Each bar represents the mean of a minimum of six test samples for WT pericardium and 2 samples for GTKO pericardium. The asterisk indicates the significantly ($p<0.05$) lower α-Gal levels in SDS treated tissue compared to the GLUT fixed tissue (control tissue). **B)** α-Gal antigen levels in a commercial pericardial valve, Carpentier-Edwards PERIMOUNT Plus 6900P (purple). Error bars represent standard error of the mean (SEM).

We also examined the level of α-Gal antigen present on a commercial Carpentier-Edwards PERIMOUNT Plus 6900P bovine pericardial mitral valve (Edwards Lifesciences, CA, USA). This valve was treated with the company's XenoLogiX^{TM} tissue processing which is reported to eliminate up to 90% of phospholipids and is similar to the FET treatment we have used. The PERIMOUNT Plus 6900P valve retains a high level of α-Gal antigen as evident by the high GIE_{GSIB-4} inhibition (66.27 ± 7.90 %) (**Figure 5.1B**).

5.2 GIE $_{M86}$ assessment of α-Gal levels after anticalcification of porcine pericardium

Anticalcification treatments may alter the surface of the tissue and affect presentation and accessibility of various antigens. The α-Gal-specific reagents GSIB-4 and anti-Gal IgM M86 are very different molecules with different sizes that have been widely used to detect α-Gal antigen. Due to their different structure and size they may have differential access to α-Gal epitopes. Therefore we also used a GIE_{M86} assay to estimate any changes in α-Gal levels on anticalcification processed tissue. Using both reagents helped to provide a more complete evaluation of anticalcification treatments.

A-Gal antigen levels after anticalcification processing were also measured using the GIE_{M86} inhibition ELISA. Consistent with previous results, glycine capping and the anticalcification treatments (FET, SDS, EtOH) alone or in combination had little effect on α-Gal levels as measured by the GIE_{M86} (**Figure 5.2**). Extraction of pericardium with SDS treatment again produced a significant reduction in α-Gal levels (22.08 ± 5.97%) compared to glutaraldehyde fixed pericardium. This was a 39.68% reduction compared to glutaraldehyde treated tissue. A-Gal antigen levels, while reduced by SDS treated tissue remained significantly higher than the GTKO background (6.61 ± 0.68 %). Tissues treated with α-galactosidase regardless of subsequent processing showed significantly reduced α-Gal levels with an average GIE $_{M86}$ inhibition level of 9.79 ± 0.59 % (**Figure 5.2A**) comparable to α-Gal-free GTKO pericardium which ranged from 5.52% to 10.11% dependently on the anticalcification treatments.

The PERIMOUNT Plus 6900P bovine pericardial valve showed high levels of α-Gal antigen with GIE $_{M86}$ inhibition of 50.77 ± 5.82% (**Figure 5.2B**).

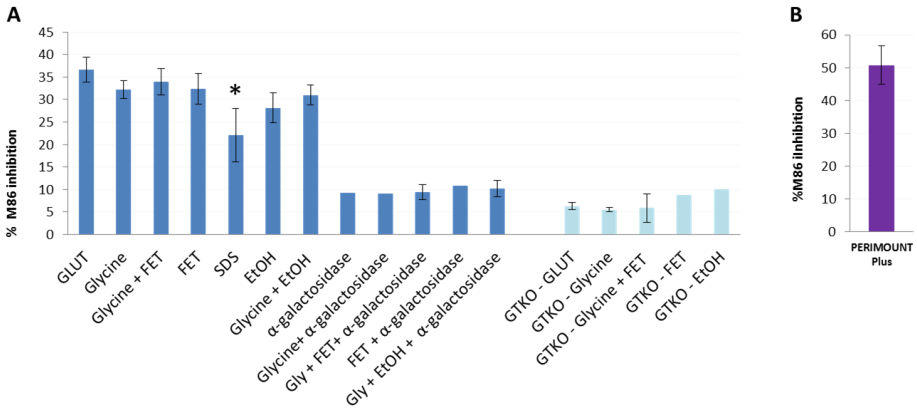

Figure 5.2 GIE M86 estimates of α-Gal antigen on fixed porcine pericardium after anticalcification treatments. A) WT pericardium (blue) was fixed with glutaraldehyde (GLUT) and subsequently processed with glycine for glutaraldehyde quenching, with formaldehyde–ethanol–Tween 80 (FET), sodium dodecyl sulfate (SDS) or ethanol (EtOH) to extract phospholipids. GLUT fixed pericardium was also treated with α-galactosidase to remove α-Gal epitopes. Combinations of these treatments were applied as well. GTKO pericardium (light blue) was similarly treated to account for non-specific M86 absorption. Each bar represents a minimum of three samples. Bars without error bars represent single samples. The asterisk indicates the significantly ($p<0.05$) lower α-Gal levels in SDS treated tissue compared to the GLUT fixed tissue. B**)** α-Gal antigen levels in a Carpentier-Edwards PERIMOUNT Plus 6900P bovine pericardial valve (purple). Error bars represent standard error of the mean (SEM).

5.3 Assessment of α-Gal levels after anticalcification of porcine heart valves

Heart valve leaflets consist of a three-layered structure which is more complex than pericardium and may be differently affected by anticalcification treatments. We used the GIE $_{GSIB-4}$ and GIE $_{M86}$ assays to measure α-Gal levels in glutaraldehyde fixed pulmonary and aortic porcine heart valves after additional processing.

The WT aortic and pulmonary valve leaflets did not differ in their α-Gal content as measured by either the GIE $_{(GSIB-4)}$ assay (62.33 ± 5.83 % and 64.23 ± 4.66 %, respectively) or the GIE $_{(M86)}$ assay (41.86 ± 3.34 and 43.28 ± 2.75, respectively). None of the anticalcification treatments, including SDS extraction, significantly reduced α-Gal in valve leaflets (**Figure 5.3A** and **5.3B**). The only consistent reduction of α-Gal levels was due to α-galactosidase digestion alone or in combination with additional processing.

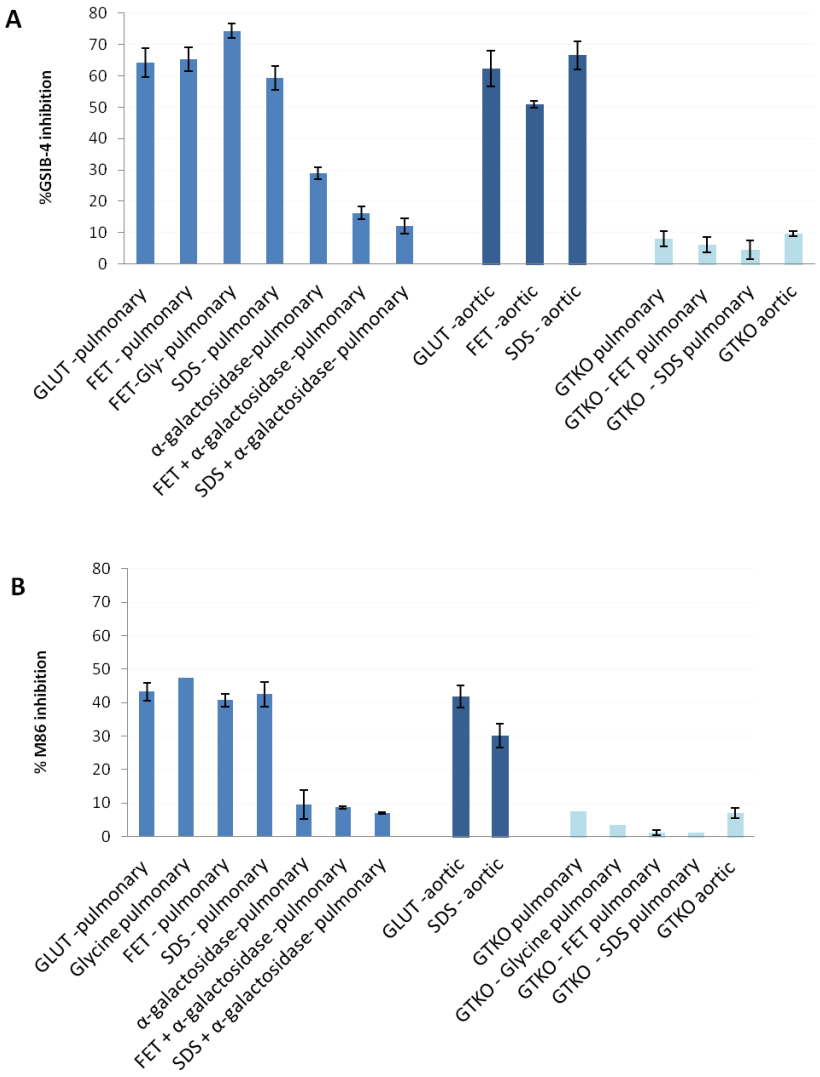

Figure 5.3 A) GIE (GSIB-4) and B) GIE (M86) estimates of α-Gal antigen on fixed porcine heart valves after processing with anticalcification treatments. WT pulmonary (blue) and aortic (dark blue) leaflets were fixed with glutaraldehyde (GLUT) and subsequently processed with glycine for glutaraldehyde quenching, or with formaldehyde–ethanol–Tween 80 (FET), sodium dodecyl sulfate (SDS) or ethanol (EtOH) to extract phospholipids. Alpha-galactosidase was used to remove α-Gal epitopes. Treatments were applied alone or in combinations. GTKO leaflets (light blue) were treated to account for non-specific lectin or M86 absorption. Each bar is the mean GIE $_{(GSIB-4)}$ or GIE $_{(M86)}$ inhibition from a minimum of three samples. Bars without error bars represent single samples. Error bars represent standard error of the mean (SEM).

5.3.1 Normalization of GIE inhibition results by tissue weight

In previous GIE assays the amount of tissue was standardized by using an equal number of disks produced from a 3 mm punch biopsy. When screening heart valves leaflets it was evident that there was a significant variation in tissue thickness. In some assays we therefore normalized the GIE inhibition results by the weight of the disks to account for this variation. After the GIE assay was completed sample disks were dried in an incubator at 65 ^{o}C for a minimum of two days and then weighed using an analytical balance.

The weights of pericardium (N=42) and valve leaflets (N=41) samples (each sample consisting of 8 disks) were within a range of 2.84 ± 0.08 mg and 3.97 ± 0.17 mg, respectively. WT aortic leaflet samples weighed significantly more than WT pulmonary leaflets. Pericardium sample weights varied less (**Figure 5.4**). We therefore normalized GIE inhibition data from valves by their corresponding weight.

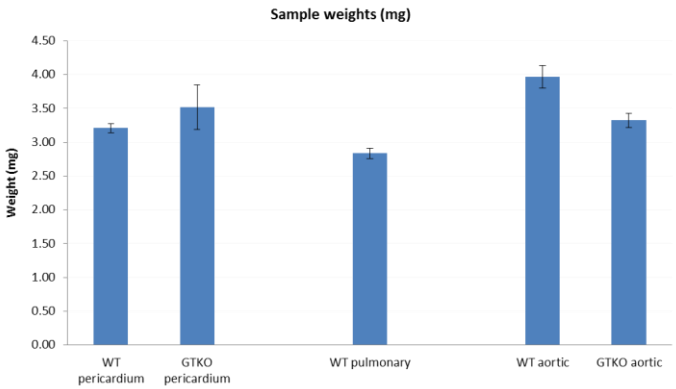

Figure 5.4 Weights of pericardium and valve leaflets samples. Disks (8 disks per sample) were dried and then their weights were determined. The mean weight of aortic leaflets was significantly higher than pulmonary leaflets.

When the GIE $_{GSIB-4}$ and GIE $_{M86}$ inhibition data was normalized by weight of tissue none of the anticalcification treatments appeared to reduce α-Gal levels on valve leaflets (**Figure 5.5A**). Only α-galactosidase digestion reduced α-Gal as indicated by the GIE $_{M86}$ assay (**Figure 5.5B**). No GIE $_{GSIB-4}$ normalized by weight data was available for α-galactosidase.

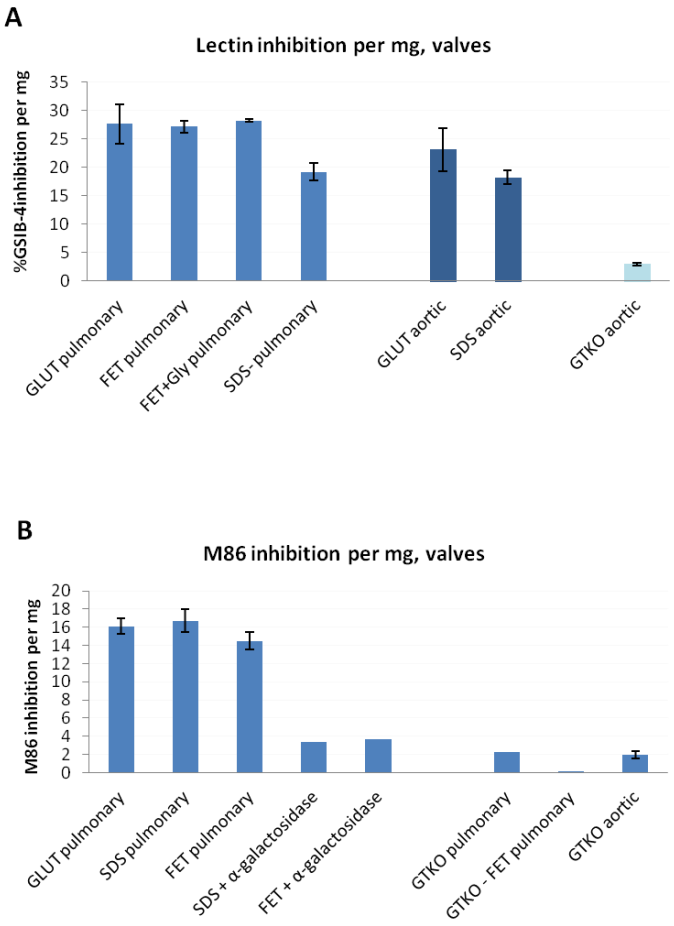

Figure 5.5 Normalization of A) GIE GSIB-4 and B) GIE M86 inhibition data by weight for valve leaflet samples. WT pulmonary (blue) and aortic (dark blue) leaflets were fixed with glutaraldehyde (GLUT) and subsequently processed with glycine for glutaraldehyde quenching, or with formaldehyde–ethanol–Tween 80 (FET), sodium dodecyl sulfate (SDS). Alpha-galactosidase was used to remove α-Gal epitopes. Treatments were applied alone or in combinations. GTKO leaflets (light blue) were treated to account for non-specific lectin or M86 absorption. After GIE assay was completed the dry weight of samples was determined and used to normalize the inhibition data. Each bar is the mean GIE $_{(GSIB-4)}$ or GIE $_{(M86)}$ inhibition normalized by sample weight from a minimum of three samples. Bars without error bars represent single samples. Error bars represent standard error of the mean (SEM).

5.4 Histochemical stain of BHVs

GIE estimates of α-Gal antigen levels in porcine pericardium and valves, whether measured using GSIB-4 or M86 consistently showed little change after anticalcification treatment, except in the case of SDS extraction of pericardium where there was a significant reduction in α-Gal levels observed. To confirm our GIE results histochemical stain with GSIB-4 was applied to two commercial BHVs, the Perimount Plus valve (treatment similar to FET) and a porcine aortic valve, Saint Jude Medical Epic (ethanol treatment). Both devices stained strongly for GSIB-4, particularly the Epic valve, while there was no staining when GSIB-4 had been pre-incubated with inhibitor tri-α-Gal (**Figure 5.6**).

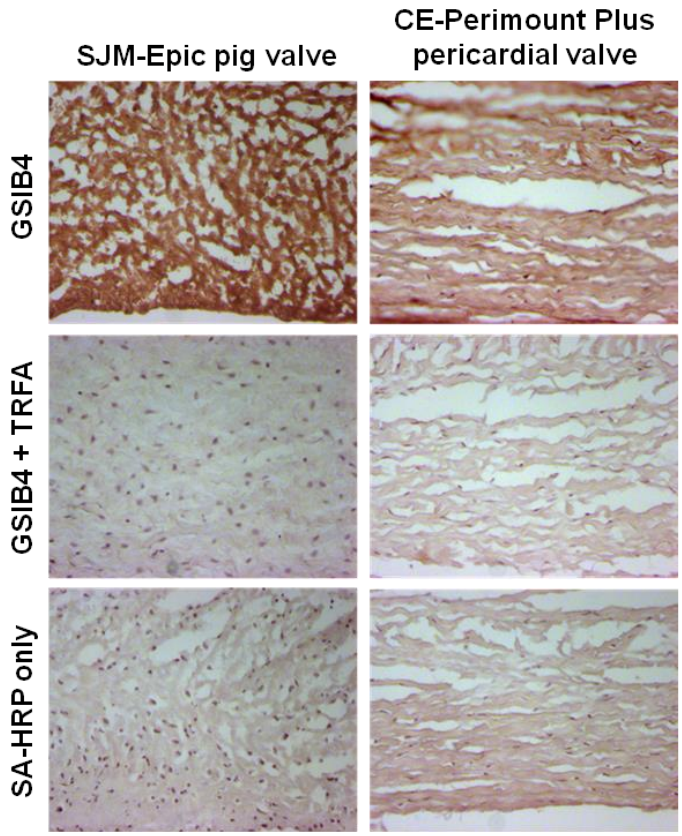

Figure 5.6 Detection of α-Gal on commercial BHVs. GSIB-4 staining was applied to sections of commercial BHVs (top panel). Controls with tri-α-Gal inhibition (middle panel) and background control with only streptavidin HRP-conjugated (bottom panel) were included. Left panel- Saint Jude Medical Epic pig valve and right panel- Carpentier-Edwards Perimount Plus pericardial valve.

Fixed pig pericardium that had been processed in the lab was also stained with GSIB-4 and confirmed the presence of α-Gal on tissue despite anticalcification treatments (**Figure 5.7**).

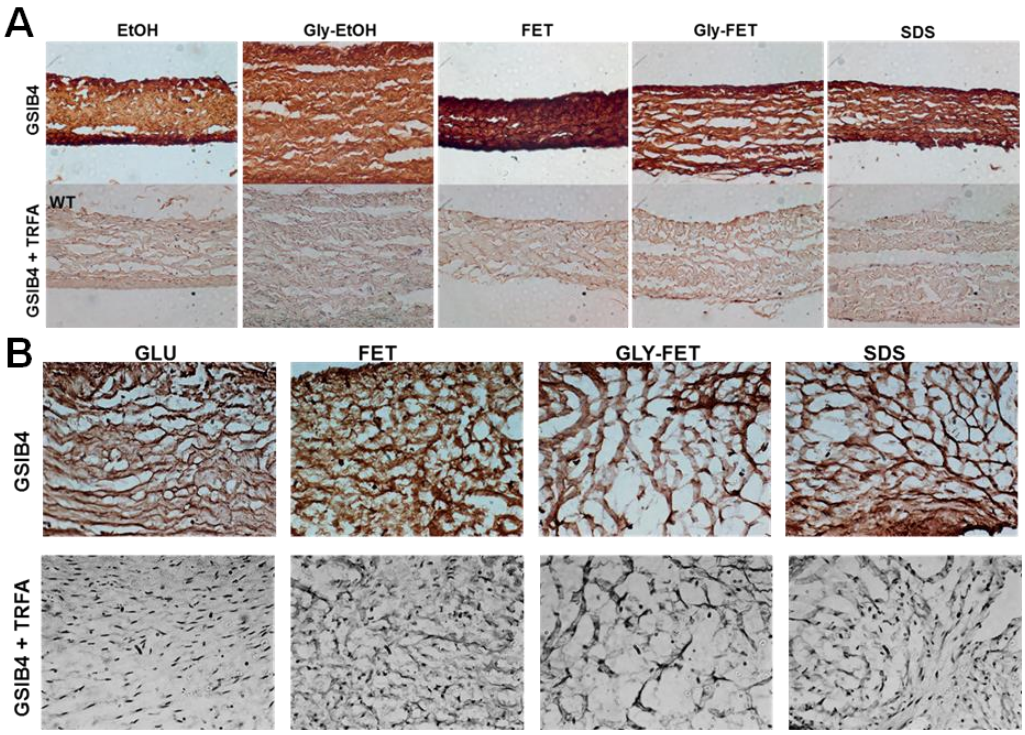

Figure 5.7 Detection of α-Gal on fixed pig pericardium after anticalcification processing. GSIB-4 staining was applied to sections of **(A) fixed pig pericardium** and **(B) fixed pig heart valves**. Tissue had previously been fixed with glutaraldehyde (GLUT) and subsequently processed with ethanol (EtOH), glycine and ethanol (Gly + EtOH), formaldehyde–ethanol–Tween 80 (FET), FET and glycine (Gly + FET), sodium dodecyl sulfate (SDS). Controls with specific inhibitor tri-α-Gal (GSIB-4 + TRFA) were included.

5.5 Summary and discussion of results

Different anticalcification treatments similar to the ones that are used in commercial BHVs were applied to glutaraldehyde fixed porcine pericardium and valve leaflets. Only SDS treatment significantly reduced α-Gal levels on pericardium, as estimated by GIE $_{GSIB-4}$ and GIE $_{M86}$. One commercial pericardial valve (Perimount Plus 6900, Edwards LifeSciences) that contains an anticalcification treatment similar to FET exhibited high inhibition levels in both GIE $_{GSIB-4}$ and GIE $_{M86}$ suggesting that it expresses high levels of α-Gal.

Normalization of GIE inhibition results by tissue weight to account for some variability in valve leaflet samples, confirmed that anticalcification processing did not eliminate α-Gal. Histochemical GSIB-4 staining on fixed porcine tissue treated in the lab and two commercial BHVs confirmed our GIE results and showed that all the tested tissues stained positive for α-Gal despite anticalcification processing.

Anticalcification treatments mainly target phospholipids, which clearly act as calcification sites and their extraction greatly limits calcification in animal models. The persistence of the α-Gal antigen after anticalcification treatment in these experimental tissues and in the commercial bovine pericardial valve may contribute to the absence of a clear improvement in commercial valve durability in younger patients treated with anticalcification processed valves. This suggests that age-dependent SVD is not primarily the result of passive phospholipid directed calcification but may be disproportionately affected by immune injury.

6 GTKO Mice

6.1 Establishment of double knock-out mice colony

Heterozygous GGTA-1 BALB/c embryos from Taconic Farms were implanted in surrogate female mice by the UCL Institute of Child Health Transgenic Services unit to re-derive GTKO mice. The offspring were genotyped and confirmed to be heterozygous for the GGTA-1 gene as expected (**Figure 6.1**).

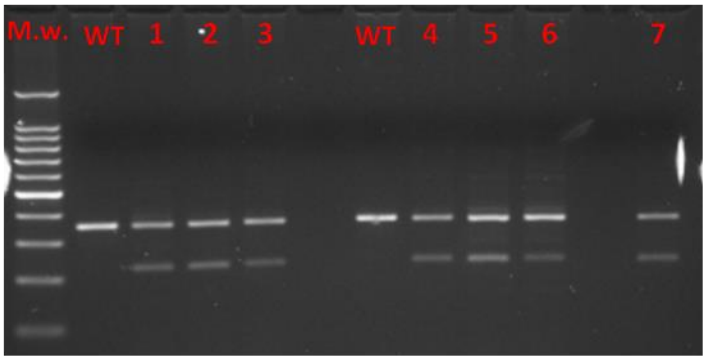

Figure 6.1 DNA electrophoresis of re-derived mice. Agarose gel (2%) analysis of PCR products amplified from genomic DNA of re-derived mice. Lane 1: 100 bp molecular weight ladder (M.w.), lanes 2 and 7: wild type mice controls (WT), lanes 3 - 5; 8 - 10 and 12: DNA samples from re-derived mice (indicated by numbers 1 – 7). WT mice show only the 358 bp product produced from the normal GGTA-1 gene. Heterozygous mice show the WT 358 bp product from one allele and a 235 bp product produced from the PGK-neo disrupted allele. All the re-derived mice were heterozygous.

Inbreeding of heterozygous mice produced offspring of all three genotypes: WT, HET and GTKO (**Figure 6.2**).

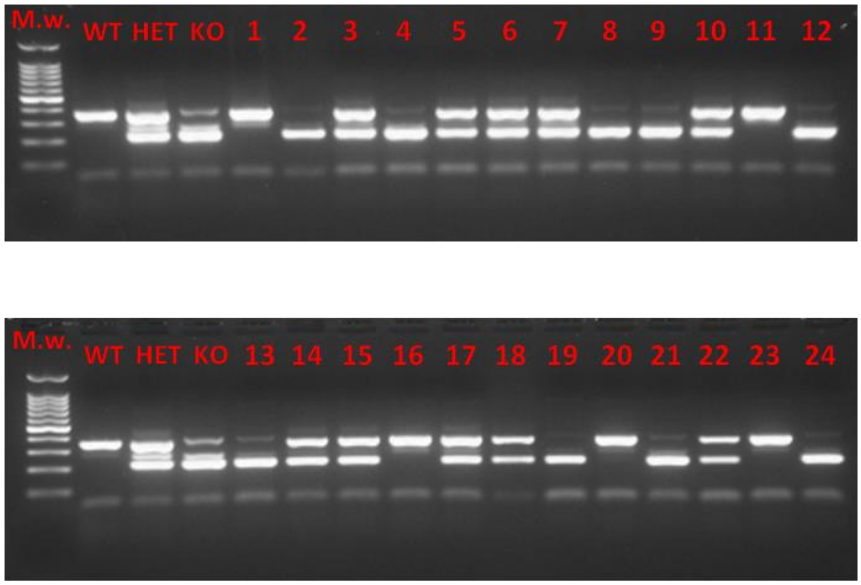

Figure 6.2 DNA screening of re-derived mice's offspring. Agarose gel (2%) analysis of PCR products amplified from genomic DNA from the offspring of re-derived mice. Lane 1: 100 bp molecular weight ladder (M.w.), lane 2: genomic WT DNA with only the 358 bp product produced from the normal GGTA-1 gene, lane 3: heterozygous GGTA-1 (+/-), (HET), control DNA with two bands corresponding to the WT 358 bp product from one allele and a 235 bp product produced from the PGK-neo disrupted allele and lane 4: GTKO control DNA with the 235 bp product produced from the PGK-neo disrupted allele. The same applies for the lower panel. DNA samples from screened mice are indicated by numbers 1-24 and were either WT, HET or GTKO.

GTKO male and females were chosen to breed and all their offspring were GTKO as confirmed by their genotyping (**Figure 6.3**).

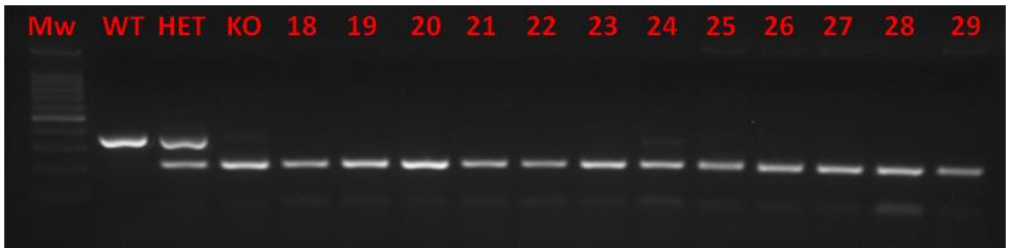

Figure 6.3. Establishment of GTKO colony by inbreeding of GTKO individuals. Agarose gel (2%) analysis of PCR products amplified from genomic DNA of offspring from GTKO mice inbreeding. Lane 1: 100 bp molecular weight ladder (M.w.), lane 2: genomic WT DNA with only the 358 bp product produced from the normal GGTA-1 gene, lane 3: heterozygous GGTA-1 (+/-), (HET), control DNA with two bands corresponding to the WT 358 bp product from one allele and a 235 bp product produced from the PGK-neo disrupted allele and lane 4: GTKO control DNA with the 235 bp product produced from the PGK-neo disrupted allele. All the screened mice (18-29) were GTKO.

Breeding couples were established to produce GTKO mice for subcutaneous implantation. Offspring of each breeding group were genotyped at least once to confirm homozygosity.

6.2 GTKO Mice: Production of anti-Gal

Serum samples were collected from GTKO mice, at 40, 70, 100, 130 and 160 days of age to measure age-dependent changes in anti-Gal antibody expression. These time points were selected because they corresponded to the duration of pericardial implantation. Age 40 days corresponds to the day of implantation and 100, 130 and 160 days correspond to 60, 90, and 120 days post implantation, respectively.

GTKO mice in the absence of immunization are known to produce mainly anti-Gal IgM antibodies and much lower levels of IgG (Chong et al. 2000;Gock, Salvaris, Murray-Segal, Mottram, Han, Pearse, Goodman, Cowan, & d'Apice 2000). We observed serum anti-Gal antibody levels increasing with age (**Figure 6.4A**). Young mice (40 days old) produced minimal levels of anti-Gal antibody. Anti-Gal IgM antibody levels substantially increased in an age-dependent way beginning at 70 days of age. Serum anti-Gal IgG levels, while detectable in some mice at 70 days, remained minimal throughout the period of study.

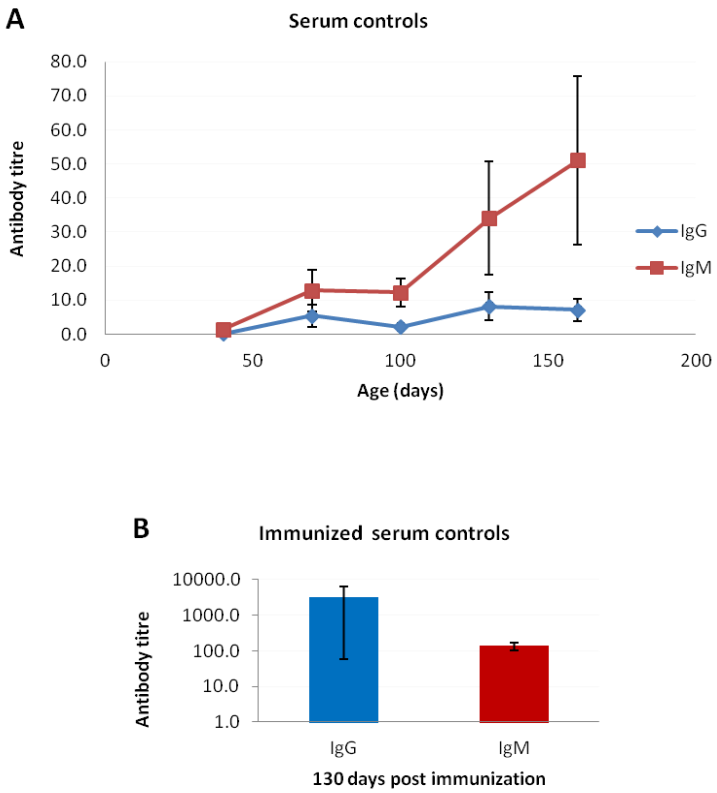

Figure 6.4 Age-dependent production of anti-Gal IgG and IgM antibodies in GTKO mice. Age matched GTKO mice that did not receive any implants served as serum control donors. **A)** Serum samples were collected at 40, 70, 100, 130 and 160 days of age. Gal ELISA analysis revealed an age-dependent increase in anti-Gal IgM levels (red line). IgG levels (blue line) remained low during the course of the study. **B)** Mice were immunized with KLH-Gal at 28 days of age. Anti-Gal IgG and IgM levels were determined 130 days later. Error bars represent SEM.

We synthesized a conjugate of keyhole limpet hemocyanin and α-Gal (KLH-Gal) to immunize GTKO mice to increase the level of anti-Gal IgG. This conjugate was preferred, compared to rabbit red blood cells which are often used for this purpose (Galili, LaTemple, & Radic 1998) because it is unlikely that KLH-Gal shares any antigens with pig pericardium, other than the α-Gal antigen. Serum anti-Gal IgG and IgM in GTKO mice 130 days after immunization with KLH-Gal showed highly elevated levels of anti-Gal IgM and

IgG (**Figure 6.4B**). Average serum titres of anti-Gal IgM increased from 50.99 ± 24.72 in age-matched unimmunized mice to 137.38 ± 34.14 in immunized mice. Likewise the average serum titres of anti-Gal IgG increase from 7.12 ± 3.23 in age matched unimmunized mice to 3283.75 ± 3225.29 in immunized mice. It is evident in the IgG response that there was a large variance in serum titre between individuals. One of the mice had a titre of 9734.29 compared to 38.23.and 78.74 in the other two mice.

6.3 Subcutaneous pericardial implantation

Fixed WT and GTKO porcine pericardium disks were implanted subcutaneously in 40 day old GTKO mice as described in 2.12.3 and implanted tissue was recovered 60, 90 and 120 days after implantation. Additionally GTKO mice were immunized with KLH-Gal by intraperitoneal injection at 30 days of age and were implanted with WT and GTKO fixed porcine pericardium disks at 40 days of age. Implantation groups are summarized in **Table 3**:

Table 3 Types of implants. WT and GTKO pericardium was implanted subcutaneously in GTKO mice according to the following table. Implants were recovered 60, 90 and 120 days after surgery in groups (WT), (KO), (WT+Ab) and (KO+Ab) and after 120 days for immunized groups (WT i) and (KO i).

Implant groups	Types of implants
WT	Fixed WT pericardium
KO	Fixed GTKO pericardium
WT + Ab	Fixed WT pericardium pre-labelled with anti-Gal antibody
KO + Ab	Fixed GTKO pericardium pre-labelled with anti-Gal antibody
WT i	Fixed WT pericardium implanted in immunized mice
KO i	Fixed GTKO pericardium implanted in immunized mice

6.3.1 Anti-Gal immune response to subcutaneous WT and GTKO implants

Implantation of α-Gal-positive fixed WT pericardium was expected to create an additional source of α-Gal-specific immune stimulation in GTKO recipients which would result in increased expression of anti-Gal antibody. Although our immunization experiments showed that GTKO mice were immunologically competent, and capable of increased expression of anti-Gal antibody when challenged, the WT pericardial implant recipients did not exhibit an obvious response (**Figure 6.5**). Serum anti-Gal IgM levels in age-matched control mice (not receiving an implant) and in mice 60, 90 and 120 days after implantation of WT pericardium were not significantly different. Recipients of α-Gal-free GTKO pericardium, as expected, did not exhibit increased levels of anti-Gal antibody after subcutaneous implantation (**Figure 6.5A**). Serum anti-Gal IgG levels in GTKO mice were lower and much more variable than IgM. There was no induced anti-Gal IgG response to WT or GTKO pericardial implantation at any duration compared to non-implanted age-matched controls (**Figure 6.5B**). Indeed for 40 of the 97 implanted mice IgG anti-Gal antibodies were undetectable (titre < 0.1).

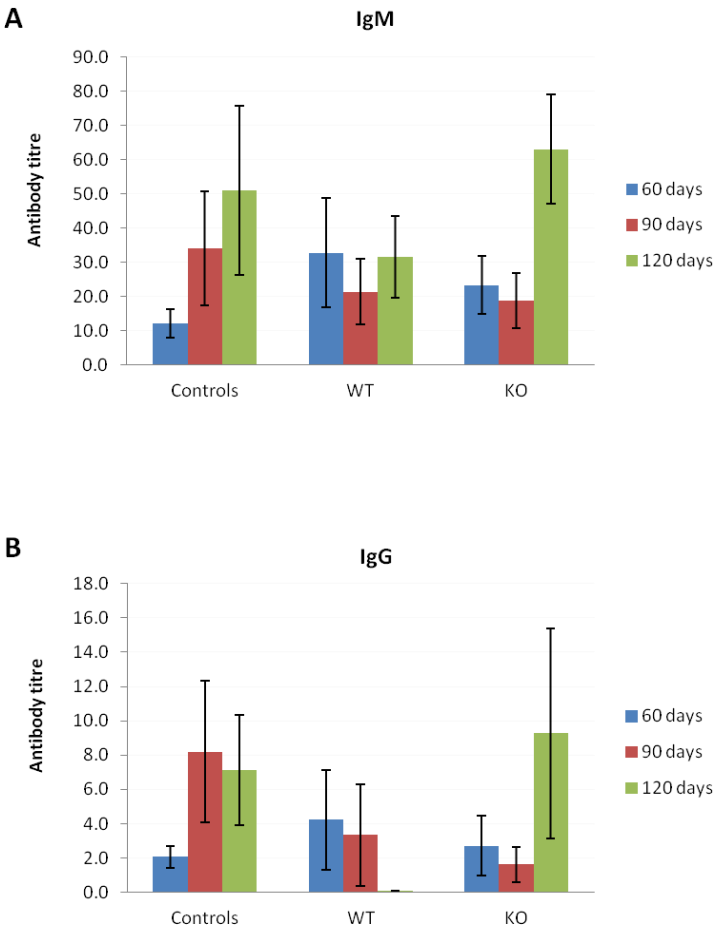

Figure 6.5 Serum anti-Gal antibody titres in GTKO mice were not significantly different after subcutaneous implantation of WT or GTKO pericardium compared to non-implanted age-matched control mice. GTKO mice were implanted subcutaneously with fixed WT or GTKO porcine pericardium and the implants were recovered after 60, 90, and 120 days. **A)** Average titre of serum anti-Gal **IgM**. **B)** Average titre of serum anti-Gal **IgG**. The results show no significant additional induction in anti-Gal IgM or IgG response in WT or GTKO implants recipients compared to age-matched animals which did not receive implants (controls). A minimum of 7 samples per group was tested. Error bars represent SEM.

6.3.2 Anti-Gal levels in immunized pericardial implant recipients

GTKO mice were immunized to raise their level of anti-Gal antibody prior to implantation of WT pericardium. This would allow us to test whether increased endogenous levels of anti-Gal antibodies would accelerate tissue calcification.

Immunization of these pericardial implant recipients increased the serum anti-Gal IgM and IgG but, as previously observed, this immune response varied wildly between individuals. Of the 13 immunized mice which received implants, 4 showed a modest induction of anti-Gal IgG (titres 33.3 - 395.5), 6 mice showed strong antibody increases (titres 1245.5 - 13,942.3) and three mice had no response, with undetectable levels of anti-Gal IgG. These serum antibody levels in immunized WT pericardial implant recipients were comparable to what was observed in animal which were only immunized (**Figure 6.6**).

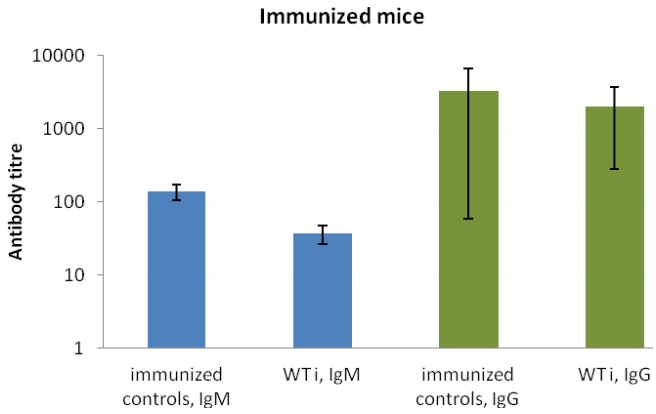

Figure 6.6 Anti-Gal IgM and IgG antibody response after WT pericardium implantation in immunized GTKO mice. GTKO mice were immunized with KLH-Gal 12 days prior to implantation that they received WT pericardial implants for 120 days. Anti-Gal serum levels were measured on the day the implants were retrieved. The graph depicts anti-Gal IgM (blue) and IgG (green) antibody levels in age-matched, immunized mice that had not received implants (immunized controls) and in immunized mice which had received WT pericardial implants (WT i). Error bars represent SEM.

These results, which take into account the progressive age-dependent increase in serum anti-Gal antibody in GTKO mice, suggest that subcutaneous

implants of WT fixed porcine pericardium did not present a chronic immune challenge to the recipients. At 60, 90 and 120 days after implantation there was little evidence of a significant induction of anti-Gal IgG, even though it is evident by KLH-Gal immunization that GTKO mice can mount an IgG response when challenged. While we would not have detected a transient early induced antibody response prior to 60 days post implant, these results suggest that the implants were effectively segregated from the immune system, such that chronic α-Gal-specific immune sensitization did not occur.

6.3.3 Calcification of pericardial implants

Previously our group had shown in rat and rabbit subcutaneous implant models that binding of human anti-Gal antibody to fixed α-Gal-positive tissue increased the level of tissue calcification. Since GTKO mice produce low levels of anti-Gal antibody in this study we pre-incubated WT fixed pericardial disks with a mixture of mouse anti-Gal IgM and IgG as a positive control to enhance tissue calcification. We also compared the calcification of WT and GTKO pericardium in the absence of exogenous anti-Gal antibody and in recipients immunized to high levels of endogenous serum anti-Gal antibody (**Table 4**).

A total of 192 pericardial disks (111 WT disks and 81 GTKO disks) were recovered between 60 to 120 days post implant for analysis of calcium content using inductively coupled plasma spectroscopy. The intrinsic calcium content for each type of pericardium, fixed WT (N=12) and GTKO (N=12) disks, prior to implantation was uniform and low showing 0.385 ± 0.101 μg/mg in WT tissue and slightly higher, 0.865 ± 0.511 μg/mg in GTKO tissue. Calcium levels in the

implanted tissue varied widely from 0.071 µg/mg to 179.456 µg/mg. The mean calcium content for WT disks was 1.73 ± 0.63 µg/mg and for GTKO disks 13.67 ± 4.24 µg/mg. A few disks (10 out of 192), particularly GTKO disks, had high calcium content (> 40 µg/mg) which increased this mean value. The vast majority of disks (159 out of 192) contained less than 2 µg/mg as is evident in the distribution of calcification for explanted pericardium (**Figure 6.7**).

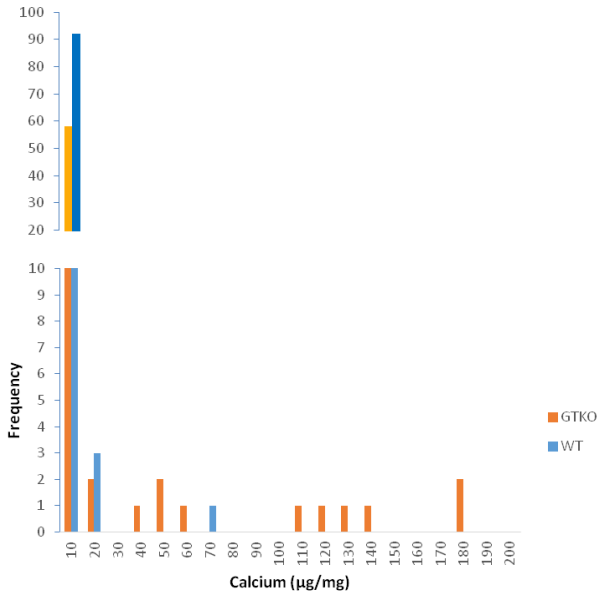

Figure 6.7 Histogram of calcification of implanted disks. The histogram depicts the frequency of calcium concentrations (y axis) that were measured in the WT (blue) and GTKO (orange) pericardial disks after subcutaneous implantation. Note the y axis is interrupted so that the distribution of samples with low frequency is clearly depicted. The majority of disks had calcium levels lower than 2 µg/mg.

More details about the experimental groups are listed in **Table 4**.

Table 4. Anti-Gal antibody titres and calcium content in experimental groups. The table lists mean values for anti-Gal IgM and IgG titres and calcium content for the different implantation groups of mice according to the type of implant they received and the duration of implantation.

Implant	IgM titre	IgG titre	Calcium (µg/mg)
WT, 60 days	32.77 ± 15.87	4.23 ± 2.91	0.31 ± 0.03
WT, 90 days	21.43 ± 9.68	3.34 ± 2.95	1.82 ± 1.07
WT, 120 days	31.51 ± 11.86	0.08 ± 0.04	0.88 ± 0.16
WT+Ab, 60 days	14.26 ± 3.71	1.98 ± 0.89	0.89 ± 0.58
WT+Ab, 90 days	29.49 ± 13.46	6.87 ± 4.99	6.58 ± 4.18
WT+Ab, 120 days	50.65 ± 10.41	1.65 ± 1.42	1.28 ± 0.25
KO, 60 days	23.32 ± 8.41	2.72 ± 1.75	0.45 ± 0.06
KO, 90 days	18.74 ± 8.04	1.61 ± 1.04	27.73 ± 14.91
KO,120 ays	63.00 ± 16.03	9.28 ± 6.13	41.15 ± 16.55
KO+Ab, 60 days	15.16 ± 7.70	2.36 ± 1.46	2.33 ± 1.51
KO+Ab, 120 days	590.04 ± 344.00	7.64 ± 5.54	1.25 ± 0.49
WT immunized (120 days)	37.08 ± 10.54	1991.26±1713.76	0.55 ± 0.08
KO immunized (120 days)	140.23 ± 62.18	2558.20±1133.25	6.64 ± 5.58
Non Implanted Controls (correspond to days post implant)			
0 days	1.40 ± 1.28	0.07 ± 0.04	
30 days	12.89 ± 6.17	5.44 ± 3.22	
60 days	12.22 ± 4.16	2.06 ± 0.66	
90 days	34.08 ± 16.73	8.20 ± 4.14	
120 days	50.99 ± 24.72	7.12 ± 3.23	
immunized, (120 days)	137.38 ± 34.14	3283.75±3225.29	
Not implanted WT disk			0.39 ± 0.10
Not implanted GTKO disk			0.87 ± 0.51

6.3.4 Calcification of GTKO pericardial implants

GTKO pericardium which was designed to be a negative control in these studies, showed minimal calcification 60 days after implantation but unusually high calcification at 90 and 120 days post implantation (**Figure 6.8**). There was very high variance at these time points with only a few disks containing very high levels of calcium. GTKO tissue (N=14) explanted at 90 days post implantation had an overall calcium concentration of 27.73 ± 14.91 μg/mg but this value was distorted by three samples with calcium content higher than 50 μg/mg. The remaining calcium values were in the range of (0.61 - 3.55) μg/mg, with a mean of 1.88 ± 0.29 μg/mg. GTKO pericardial explants at 120 days post implantation (N=14) had a mean calcium content of 41.15 ± 16.55 μg/mg, significantly higher than in the non-implanted control (**Figure 6.8**). However this mean was elevated by 4 disks with calcium higher than 100 μg/mg and 1 disk containing 40.38 μg/mg. The remaining calcium values at 120 days were in the range of (0.47–1.78) μg/mg, with a mean of 1.29 ± 0.23 μg/mg. Apart from the heavily calcified GTKO disks there was no significant increase in GTKO tissue calcification at any time point compared to non-implanted GTKO tissue.

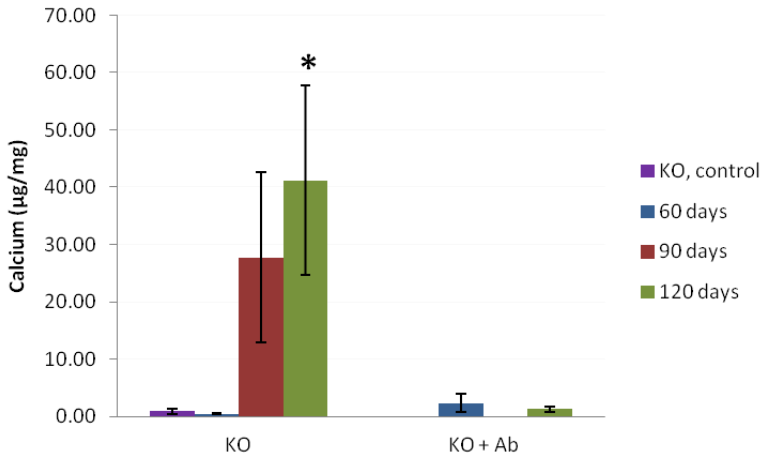

Figure 6.8 Calcification of implanted GTKO pericardium. Levels of calcium were determined using inductively coupled plasma spectroscopy on GTKO pericardium disks that were retrieved after 60, 90, 120 days of subcutaneous implantation in GTKO mice. GTKO pericardium disks that were not implanted served as reference controls for intrinsic calcification of the tissue (KO, control). GTKO pericardium implanted for 120 days had significantly ($p < 0.05$) higher levels of calcium than the control. GTKO pericardium pre-labelled with anti-Gal antibody (KO + Ab) did not calcify even after 120 days of implantation. A minimum of 12 disks per group were tested. Error bars represent SEM.

The average calcification in GTKO pericardium at 90 and 120 days post implant was much higher than calcification in GTKO tissue pre-incubated with anti-Gal antibody at the same explant times (**Figure 6.8**) and higher than the average calcification levels observed in any of the other groups (**Table 4**). GTKO pericardial disks pre-incubated with anti-Gal antibody showed low levels of calcification which was not significantly different from control GTKO disks.

We believe the high calcification of GTKO implants was an aberration clearly unrelated to the α-Gal antigen. A number of possible factors might contribute to the irregularity in calcium content. The subcutaneous implant model generally results in encapsulation of the pericardial disks. Encapsulation could be variable, even within the same animal, resulting in widely variant calcification.

Alternatively, individual inbred mice are not all identical and minor background genetic variation, for example functional single nucleotide polymorphisms (SNPs), could influence calcification. Likewise epigenetic variation among mice due to nutrition in utero could have been another factor for variation in calcification levels. Environmental factors can contribute to calcification. Many of our recipients required additional anaesthesia and re-suturing of the implant site 1 or 2 days after the initial surgery. This may have been due to self-inflicted opening of the wound or to fighting between cage-mates. The open wounds exposed the implants to air and to possible infection, both of which may have affected tissue calcification. While no obvious infections were present at explant, these early events may have variably affected tissue calcification by the time of explant. Apart from each separate factor combinations of the above might have caused the observed unusually high level of calcification in a small number of GTKO disks.

6.3.5 Serum anti-Gal antibody and WT tissue calcification

WT pericardium disks showed increased calcification at 90 days (1.82 ± 1.07 μg/mg) and 120 days (0.88 ± 0.16 μg/mg) post implantation compared to the non-implanted WT tissue (0.39 ± 0.10 μg/mg). Calcium levels after 120 days implantation were significantly higher than after 60 days implantation and than in the non-implanted WT tissue (**Figure 6.9**).

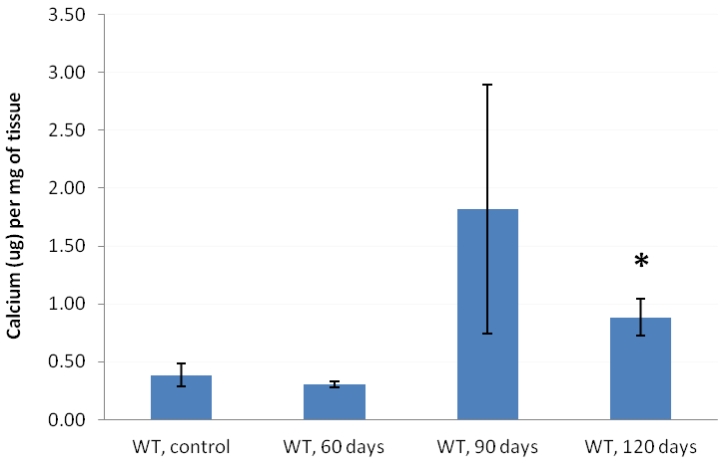

Figure 6.9 Calcification of WT pericardium. Levels of calcium were determined on WT pericardium disks retrieved after 60, 90, 120 days of subcutaneous implantation in GTKO mice. WT pericardium disks that were not implanted served as reference controls for intrinsic tissue calcium. Significantly ($p<0.05$) higher levels of tissue calcium were present at 120 days after implantation compared to the non-implanted control tissue (indicated by asterisk). A minimum of 12 disks per group were tested. Error bars represent SEM.

When WT pericardium was pre-incubated with anti-Gal antibody there was a trend to greater calcification at all explant time points. These differences were not significant (**Figure 6.10**).

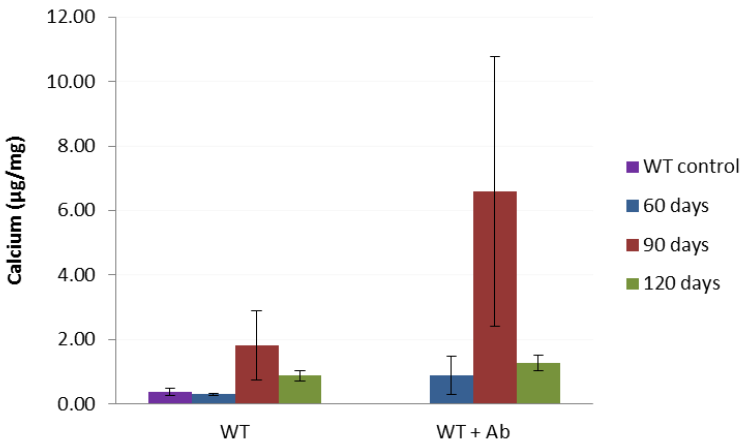

Figure 6.10 Calcification of WT pericardium implants pre-labelled with anti-Gal antibody. GTKO mice were implanted subcutaneously with fixed porcine pericardium for 60, 90, 120 days. Calcium levels in the explanted disks were measured using inductively coupled plasma spectroscopy. WT pericardium calcified moderately over time. The positive control, WT pericardium pre-labelled with anti-Gal antibody (WT+Ab), tended to calcify more than non-labelled pericardium (WT). There seemed to be increase in calcification after 90 days of implantation for the positive control, but it was not significant, as the variance was very high. A minimum of 15 disks per group were tested, except for the 90 days WT disks that consisted of 11 disks. "WT control" represents WT pericardium not implanted. Error bars represent SEM.

Overall there was no correlation between calcification of WT pericardium and antibody titres in the implant recipients (**Figure 6.11**). Correlation and regression analysis between tissue calcium and antibody titres showed no significant correlation. Pearson correlation coefficient (r) for IgM was equal to – 0.12 with a p value of 0.596 and r = - 0.134 for IgG with p=0.599. A Spearman's rank correlation coefficient (r_s) was also calculated, since some of the data was not normally distributed. This analysis also showed no correlation with r_s= 0.085 for IgM and -0.322 for IgG. Calcium levels in WT pericardium, for any duration of implantation, were in the range of (0.07-1.87) µg/mg with the exception of only one disk which contained 12.36 µg/mg. Even when this data point was excluded there was no correlation between calcification of implants and anti-Gal

IgM (r_s= 0.119) or IgG (r_s= - 0.307) response. It seems that the generally very low level of calcification detected in this study using GTKO mice is unrelated to anti-Gal antibody reactivity and is not analogous to the strong α-Gal-specific antibody induced calcification we previously observed in rats and rabbits.

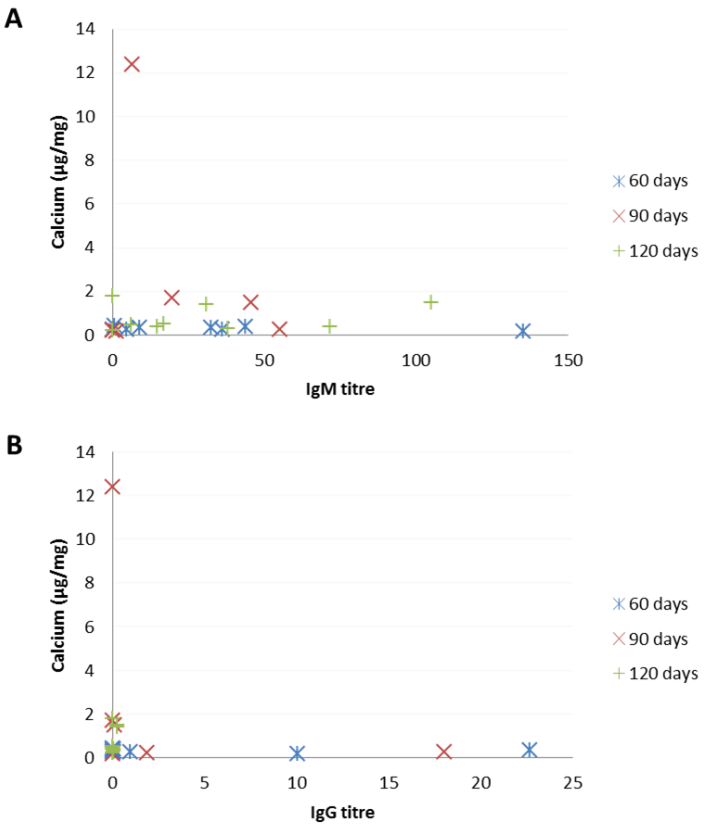

Figure 6.11 Relationship between anti-Gal antibody response data and calcification data for WT pericardium implants. GTKO mice were implanted subcutaneously with fixed porcine pericardium for 60, 90, 120 days. Calcium levels were determined in the explanted disks using inductively coupled plasma spectroscopy and anti-Gal antibody levels were estimated by Gal ELISA. There was no correlation between calcium levels and serum anti-Gal **IgM (A),** (r_s=0.085), or **IgG (B), (**r_s= - 0.322) response at any duration of implantation with most samples containing very low levels of calcium. A minimum of 15 disks per group were tested, except for the 90 days group that consisted of 11 disks.

The lack of correlation between implant calcification and levels of endogenous antibody, the absence of an induced anti-Gal immune response in WT implant recipients and the small impact of exogenous antibody incubation with the tissue prior to implant (**Figure 6.10**) suggest that the implants were isolated from the immune system, did not cause chronic α-Gal stimulation. This model may have restricted endogenous antibody from reaching the implant and did not lead to extensive tissue calcification.

6.3.6 Effect of immunization on calcification of implanted pericardium

Mice were immunized against α-Gal in order to increase serum anti-Gal antibody levels and possibly enhance the effect of anti-Gal antibody on calcification of WT pericardium. Calcification of WT implants in immunized mice was not increased compared to WT pericardium implanted in naïve mice (**Figure 6.12**).

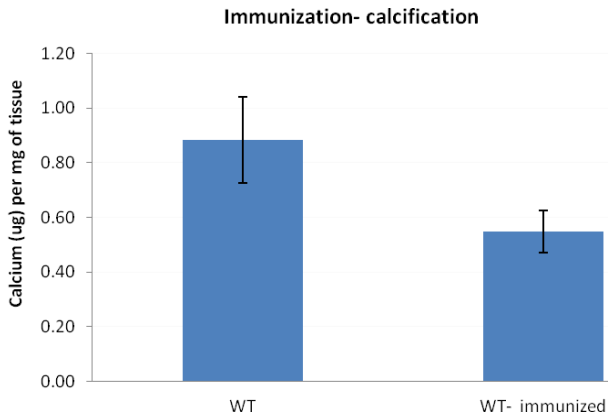

Figure 6.12 Immunization of GTKO mice did not induce calcification of WT pericardium. GTKO mice were immunized with KLH-Gal and 12 days later they were implanted subcutaneously with WT pericardium for 120 days. Calcium levels in WT implants (WT-immunized) were not enhanced compared to the calcification in non-immunized mice (WT). A minimum of 15 disks per group were tested. Error bars represent SEM.

6.3.7 Inflammatory response

Hematoxylin and eosin staining was done on some explanted disks, focusing on those with high levels of calcium (> 100 µg/mg) and on disks with low calcium levels (< 2µg/mg). Sections of this material showed a thin surface encapsulation of the pericardial disks. The encapsulating layer was cellular and likely consisted of macrophages and monocytes, although no specific staining was performed to verify cell identity. In the limited number of tissues examined we did not detect any clear association between the extent of encapsulation and tissue calcification (**Figure 6.13A**). Disks with high calcium levels (determined by inductively coupled plasma spectroscopy) were stained with Von Kossa to detect for calcium. The Von Kossa stain makes a dark granular pigmentation in the presence of calcium. There was no calcium staining in these sections

(**Figure 6.13B**). This may be due to biopsy sampling error as the explanted disks showed no macroscopic evidence (nodules or hardness) of calcification.

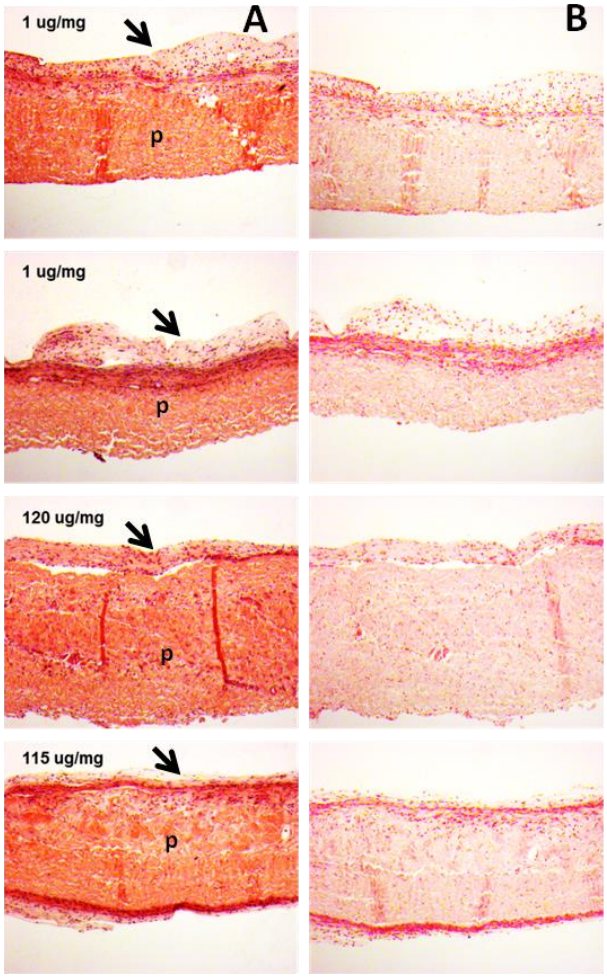

Figure 6.13 Histology results on selected pericardial explanted disks. Explanted pericardial disks with average calcification (1ug/mg) and highly calcified (120 and 115 ug/mg) disks were selected for staining. A) Hematoxylin and eosin stain. B) Von Kossa stain. There was a thin surface cellular encapsulation of the pericardial disks, most likely consisting of macrophages and monocytes (arrows). Pericardium is indicated by "p". There was no positive calcium staining.

6.4 Summary and discussion of results

GTKO mice are immunologically competent exhibiting an age-dependent increase in anti-Gal IgM levels and low levels of IgG. Immunization by KLH-Gal resulted in an induced anti-Gal IgM and IgG response, although the anti-Gal IgG titres were highly variable between individuals. Subcutaneous implants of fixed WT tissue did no induce an anti-Gal IgG or IgM response after 60, 90, 120 days beyond that accounted for by the recipient's age. This suggests that the implanted tissue was sequestered from the immune system and therefore did not act as an antigenic stimulator for the recipients.

WT and GTKO pericardium implants showed increased calcium content at 90 and 120 days post implantation compared to control non implanted disks. Most disks (159 out of 192 disks) showed relatively low levels of calcification (lower than 2 µg/mg). Only 6 out of 192 disks showed very high calcification (higher than 100 µg/mg). These exceptional disks were GTKO pericardium implanted for 90 days (2 disks) and 120 days (4 disks).

A possible explanation for the very low calcification and the lack of antibody response to WT pericardium is that the implanted disks appeared to be sequestered from the immune system. The implants in this model were largely unaffected by both exogenous and endogenous anti-Gal antibody, contrary to our experience in the subcutaneous rat model. Implantation of WT pericardium in immunized mice did not induce additional calcification compared to that in naive recipients. This suggests that circulating antibody was not getting to the graft. Exogenous antibody pre-labelling had some effect on WT pericardium,

which calcified more compared to unlabelled pericardium but the impact was small.

7 Discussion

Demand for heart valve replacement continues to increase due to ageing of global population. Emergence of improved healthcare in developing nations is likely to further increase demand for heart valve replacement. BHVs are often preferred to mechanical valves as they generally do not require anticoagulation, however their rapid degeneration in young adults and children limits their utility (Zilla et al. 2004). There has been extensive research to optimize valve design, tissue fixation and processing, but little attention has been directed to the contribution of immune mediated injury to BHV degeneration. This may be because glutaraldehyde fixation was widely believed to eliminate any BHV immunogenicity.

Relevant to immune injury is the fact that commercial BHVs express the dominant xenogeneic antigen α-Gal. Humans and Old World primates universally produce anti-Gal antibody and this carbohydrate antigen remains immunogenic in patients, especially young adults and children (Galili 1999). Patients exhibit induction of anti-Gal antibody after BHV implantation (Konakci et al. 2005;Park et al. 2010). In experimental models anti-Gal antibody is sufficient to accelerate calcification of fixed bioprosthetic tissue (Lila et al. 2010;McGregor et al. 2011). These observations suggest that antibody induced immune injury may have a significant contribution to age-dependent BHV calcification and degeneration. Antibody mediated inflammation is consistent with the histopathology of an inflammatory response present in normal BHVs recovered from LVADs prior to tissue calcification and SVD. Macrophages

mainly infiltrate the tissue, with antibodies, B and T cells also present but without accompanying severe calcification or leaflet tears of the valve. This suggests that BHVs with reduced antigenicity, lacking the dominant xenogeneic carbohydrate antigen α-Gal, will reduce this inflammatory response and possibly improve BHV durability. A durable calcification resistant BHV would be a significant contribution to cardiovascular therapy especially for younger patients, who show a disproportionately large increase in anti-Gal antibody after BHV implant surgery compared to older patients (Park et al. 2010) and patients in developing nations where anticoagulation management, required for MHVs, may be difficult.

Understanding the role of α-Gal antigen in tissue calcification and developing α-Gal-free BHVs with reduced antigenicity requires methods to measure α-Gal on solid substrates. Assays to measure α-Gal antigen on tissue can be used to understand the impact of current commercial anticalcification processing and valve durability especially in younger patients. In this project I tested two methods to assess α-Gal content of tissue and using a GTKO mouse subcutaneous implant model further tested the relationship between anti-Gal antibody, tissue α-Gal content and tissue calcification.

The α-Gal content in tissue is most frequently assessed by immunohistology or immunofluorescence staining of sections, primarily done with GSIB-4 lectin. There is some variability in the literature in reports from different groups regarding the presence of α-Gal on pig endothelial cells (Chen et al. 2000;Farivar et al. 2003) and its levels of expression in BHV tissue matrix

(Konakci et al. 2005;McGregor et al. 2011;Naso et al. 2011). This variability may result from different staining conditions, the most important of which is the requirement for calcium ions for α-Gal-dependent GSIB-4 binding. Additionally, many studies are poorly controlled and may not accurately assess background GSIB-4 staining. Our GSIB-4 staining of porcine pericardium and cardiac valves, using α-Gal inhibition and GTKO tissue as controls for non-specific background binding, shows widespread α-Gal expression on porcine valve endothelial cells and staining of extracellular matrix materials in α-Gal-positive tissues but not in GTKO tissues. We also see similar diffuse α-Gal specific staining with M86 (data not shown).

Tissue staining methods are useful to define the morphology of α-Gal expression but they are generally speaking not quantitative. I used WT (GT+/+), heterozygous (GT+/-) and α-Gal free (GTKO) porcine pericardium and heart valves to test the utility of an enzymatic assay to detect α-galactosidase liberated galactose and a α-Gal specific inhibition ELISA assay. The enzymatic detection of α-Gal was an extension of a method previously reported to characterize polymeric α-Gal conjugates (Byrne et al. 2002) which was based on commercial methods to detect lactose. This commercial method coupled β-galactosidase hydrolysis of lactose, to release galactose, with galactose dehydrogenase (GH) to produce NADH which is released in direct stoichiometric proportion to the amount of galactose (Essig & Kleyn 1983). We substituted β-galactosidase with α-galactosidase to hydrolyse the terminal alpha-linked galactose from the α-Gal antigen on tissue. In this first and simplest of iterations the spectrophotometric detection of NADH was insensitive

requiring concentration of 312 µM galactose or higher. This is equivalent to approximately 1.8 $x10^{20}$ molecules of galactose. Since previous estimates of α-Gal levels on pig tissue were in the order of 10^{11} residues per mg (Stone et al. 2007) the spectrophometric detection of NADH would require in excess of 1800 kgrams of tissue to liberate sufficient galactose for detection by this method. To improve sensitivity we tried to couple the galactose dehydrogenase reaction with a NAD/NADH coupled enzymatic cycling assay designed for measuring tissue NAD or NADH (CycLex, MBL). The CycLex NAD/NADH system is basically an amplifier which is "ignited" by the presence of NAD or NADH. This assay has the potential to detect as little as 0.0156 µM NADH corresponding to 9.4 $x10^{15}$ molecules, a 2000-fold increase in sensitivity compared to the spectrophotometer which in principle would require only (10 – 100) mg of cells or tissue. In practice however when coupled to the GH hydrolysis of galactose we could only achieve an approximately 300-fold increase in overall sensitivity. The limited sensitivity of this GH assay may have been due in part to the need to eliminate high levels of NAD required for the GH reaction prior to the CycLex reaction, a suboptimal GH reaction or an inhibition of the CycLex system's reactions by components of the GH reaction. We reasoned that the addition of an extra enzymatic step, that of α-galactosidase, and the need to scrupulously deplete NAD/NADH from tissue would inevitably further decrease the system's sensitivity, so the approach was abandoned.

As an alternative to the enzymatic detection of galactose we established a robust quantitative α-Gal-specific inhibition ELISA (GIE) method to measure α-Gal on solid substrates using two different α-Gal specific reagents, the lectin

GSIB-4 (GIE_{GSIB-4}) and anti-Gal IgM monoclonal antibody M86 (GIE_{M86}). GIE includes two sequential steps, firstly incubation of sample with anti-Gal reagent and secondly measurement of remaining anti-Gal reactivity in the supernatant by Gal ELISA. Based on their reactivity in the Gal ELISA these reagents have distinct avidity for the α-Gal antigen. The pentameric M86 exhibited high avidity for BSA-Gal with an IC50 equivalent to 2089 μM of free α-Gal trisaccharide. (**Figure 4.2**). In comparison the IC50 in the Gal ELISA for the lectin GSIB-4 was much lower (323 μM). This shows that under these conditions approximately 6.5-fold more α-Gal trisaccharide was required to block M86 binding to BSA-Gal compared to GSIB-4. The IC50 is a relative measurement of avidity, as the precise value will depend strongly on the concentration, accessibility and density of α-Gal in the ELISA assay, the method of detection in the ELISA (see "Materials and Methods") and the affinity and valency of M86 and GSIB-4 (Byrne et al. 2002). As both anti-Gal antibody (Parker et al. 1996) and lectin GSIB-4 (Goldstein et al. 1981) affinity for α-Gal is reported to be in the micromolar range, this suggests that the IC50 differences in our experiments are mainly due to differences in valency between M86, with 10 binding sites and GSIB-4 with 4 binding sites.

Despite apparent differences in overall avidity M86 and GSIB4 showed similar binding to α-Gal-positive (GT+) PAECs and similar inhibition in the GIE. For M86 we showed that approximately $1.6x10^6$ GT (+) PAECs (**Table 1**) were required to inhibit 50% of M86 binding in the GIE. A similar number of cells ($1.3x10^6$) produced 50% inhibition of GSIB-4 binding. This suggests that under these conditions both reagents react with the PAEC surface in similar fashion.

In the case of fixed porcine pericardium however, GSIB-4 appeared to bind more effectively than M86. This conclusion is based on two observations. Firstly, we consistently observed greater inhibition of GSIB-4 by fixed GT(+/+) pericardium compared to M86 (**Figure 4.11**). Secondly, the GIE_{GSIB-4}, but not GIE_{M86}, detected a significant difference in inhibition between GT(+/+) pericardium and GT(+/-) pericardium ($p<0.001$, **Figure 4.9**) suggests that GT(+/-) tissue contains lower levels of α-Gal. This is consistent with reports of reduced Gal-transferase activity in liver, lung, spleen and testis tissues of GT(+/-) pigs compared to those of GT(+/+) pigs (Park et al. 2012). Under the same conditions GIE_{M86} detected a reduced level of inhibition by GT(+/-) tissue, but this was not significantly different from GT(+/+) tissue. In these pericardial experiments, compared to the results for PAECs, the difference between these two reagents might be attributed to the smaller size of GSIB-4, 114kDa, compared to ~970kDa for M86. Smaller size may allow GSIB-4 greater access to α-Gal epitopes in the tissue matrix. One way to circumvent the accessibility issues would be mincing of the tissue (Naso et al. 2011) however, the biological significance of deeply embedded α-Gal antigen, which is only detectable after tissue disruption, is unclear. Carbohydrate binding can also be affected by the topological presentation of oligosaccharides (Bovin et al. 2012). If the presentation of α-Gal epitopes in a matrix of fixed pericardium and on the cell surface is subtly different then this might differentially affect GSIB-4 and M86 binding. Given the expense of M86 and the apparently improved sensitivity of the GIE_{GSIB-4} assay the lectin based detection of α-Gal antigens seems preferable.

Other groups have used M86 in an α-Gal inhibition ELISA to analyse α-Gal expression on tissue (Galili et al. 1998;Naso et al. 2011). These studies use a distinctly different set of conditions in their assay (both between each other and compared to ours) and report their results as the number of α-Gal epitopes per cell or epitopes per mg of tissue. We have concerns about these methods and the appropriateness of reporting the results in this format. In studies by Naso and colleagues the primary incubation of M86 with tissue is performed at 37^{o}C, for 2 hours. This high temperature, short incubation condition is not sufficient to reach equilibrium binding consistent with our observation of substantial increases in GIE inhibition between overnight and 48 hour primary incubation. It is also well known that protein and carbohydrate binding is relatively weak and is more stable at lower temperature. The non-equilibrium, high temperature conditions used by Naso render their assay relatively insensitive. This group also reports their results in terms of α-Gal epitopes per mg of wet tissue. This has the appearance of accuracy but is more likely misleading and inaccurate as the numbers are based on historical analysis by Galili (Galili et al. 1988b) using the GSIB-4 lectin under distinctly different assay conditions. In his initial study, Galili estimated the number of α-Gal epitopes on rabbit RBCs using a classic radioimmune assay format (RIA) to be 150,000 epitopes/cell (Galili et al. 1987). This analysis was performed using radiolabelled GSIB-4 with a primary incubation at 37 ^{o}C, for 1 hour. Concerned about the stability of lectin binding Galili reported a second RIA study in which the primary incubation with radiolabelled GSIB-4 was performed at 4 ^{o}C, for 1 hour. This analysis gave estimates of 10x10^{6} α-Gal epitopes/ PAEC and 1.2x10^{6} epitopes/mouse SP2/0

cell line (Galili et al. 1988b). No estimate of rabbit RBCs was reported in this study. Subsequently Galili described an M86 based GIE with primary overnight incubation at 4 ^{o}C (Galili et al. 1998). This study used the SP2/0 cell line estimate of 1.2 x 10^6 epitopes / cell (defined earlier by GSIB-4 RIA incubated at 4^{o}C for 1 hour) as a reference standard to estimate epitope density based on the M86 inhibition ELISA. This yielded estimates of 25x10^6 epitopes/ PAEC and 2x10^6 epitopes/ rabbit RBC. These values are about 2 and 13-fold higher than in previous studies (PAEC; 1x10^7/ cell estimated with lectin at 4 ^{o}C for 1 hour and rabbit RBCs of 150,000/ cell estimated with lectin at 37 ^{o}C for 1 hour). Galili correctly points out that the lower values for these cells were based on GSIB-4 binding but fails to note that the reaction conditions of the previous studies also would be expected to under estimate the epitope density. Despite this, he and subsequently Naso and colleagues, adopt the value of 1.2x10^6 epitopes per SP2/0 myeloma cells (defined by GSIB-4 at 4 ^{o}C for 1 hour) as a reference standard and multiplier for subsequent GIE studies. This practice of extrapolating from historic antigen densities based on GSIB-4 RIA assays performed under completely different assay conditions to calculate number of α-Gal epitopes based on a GIE using M86 does not seem supportable.

Naso has also used the SP2/0 benchmark of α-Gal density on cells to estimate α-Gal epitope density in BHV leaflets (Naso et al. 2011). We have shown that M86 and GSIB-4 exhibit similar inhibition profiles for binding to cells, but show differential binding to fixed pig pericardium. While the tissue in Naso's study was disrupted, it remains to be determined if a direct extrapolation about the number of α-Gal epitopes from cells to tissue is justified. In conclusion we

believe that the α-Gal inhibition ELISA, in its current form, provides a relative measurement of α-Gal epitopes as originally stated by Galili (Galili et al. 1998).

The sensitivity of the GIE was further defined by estimating the smallest detectable reduction in α-Gal levels on PAECs in comparison to quantitative flow cytometry. We used α-galactosidase digestion to partially remove α-Gal epitopes from the surface of PAECs and compared the reduction in α-Gal levels as estimated by FACS and by our GIE assay in parallel (**Figure 4.16**). FACS analysis consistently detected a minimum 12% reduction in α-Gal levels as estimated by mean fluorescence. The smallest change in α-Gal levels that could be detected by GIE $_{GSIB-4}$ was approximately a 20% reduction as estimated by FACS. This suggests that moderate reductions in α-Gal levels can be distinguished by the GIE and encouraged us to use this method to detect differences in α-Gal levels on animal tissue after anticalcification treatments.

We used a variety of anticalcification processing methods to see if they reduced the level of α-Gal antigen on fixed porcine pericardium and on porcine heart valves. These included glutaraldehyde capping, used by Carpentier-Edwards, ethanol, used by St. Jude Medical, Formalin-Ethanol-Tween extraction, used by Carpentier Edwards and extraction with SDS, used by Medtronics. None of these processes eliminated α-Gal from tissue and only SDS treatment led to a moderate reduction of α-Gal levels on pericardium. This result was consistently observed with either GIE $_{GSIB-4}$ (27% reduction) and GIE $_{M86}$ (39% reduction) assay. We also measured α-Gal levels in a PERIMOUNT

Plus BHV from Edwards LifeSciences where we found high levels of α-Gal despite being treated with a processing similar to FET. Although we had no control for fixed untreated bovine pericardium the inhibition levels of the Perimount tissue were unquestionably high and our FET studies on porcine pericardium showed no evidence of substantial α-Gal reduction suggesting that this commercial processing, like our experimental studies, did not substantially reduce α-Gal levels. Only α-galactosidase digestion resulted in very low α-Gal levels compared to untreated tissue. These GIE results were further supported by immunohistochemical staining of the pericardium after anticalcification treatment. In each case strong α-Gal-specific GSIB-4 lectin binding was detected (**Figure 5.1**). My results suggest that anticalcification processing does not eliminate α-Gal from bioprosthetic tissue. SDS treatment, the only treatment that moderately reduced anti-Gal binding to fixed tissue in our assay, is used for extraction of phospholipids in commercial BHVs, Medtronic models Hancock II and Hanckock II Ultra. The Hancock II, was first introduced in the market in 1982 and has excellent performance and durability in elderly recipients, where 20 year freedom from reoperation for aortic valve replacement is 86.8% in patients over 60, while in patients younger than 60 years of age it is 52.2% (Valfre et al. 2010). In contrast in a study on Hanckock II heart valve replacement which included younger patients the 20-year freedom from reoperation in the aortic position due to SVD was only 14.1 ± 8.7% in patients under 40 years of age, 21.5 ± 8.5% in patients aged 40-49 and 41.4 ± 8.2% in patients between 50 and 59 ($P = 0.04$) (Une et al. 2014). This age-dependent SVD suggests that although anticalcification treatments minimize calcification in

animal models, they have not resolved the problem of accelerated SVD in the young. This is consistent with the insufficient elimination of α-Gal antigen by anticalcification processing and an immune injury model of SVD.

Naso and colleagues used their inhibition ELISA to measure α-Gal on five modern bovine and two porcine commercial BHVs (Naso et al. 2013a). In this study native (unfixed) bovine and porcine pericardium or native porcine aortic leaflets were used as controls. These tissues had reported α-Gal levels of 26 x 10^{10}, 18.2 x 10^{10}, and 12 x 10^{10} epitopes/mg of wet tissue respectively. In contrast they reported a range of (0.025 - 6.62) x 10^{10} α-Gal epitopes per 10mg of wet tissue for the bovine pericardial valves and (0.05 – 5.2) x 10^{10} for the porcine valves. For the St Jude Epic valve, treated with LinxAc anticalcification, they detected 0.05 x 10^{10} α-Gal epitopes per 10mg (Naso et al. 2013b). These results suggest that anticalcification treatments significantly lower the level of α-Gal antigen on commercial devices. This conclusion however must be interpreted in light of our previous discussion concerning the sensitivity of their assay.

The importance of anti-Gal antibody in the degeneration of BHVs has not been appreciated in part because the animal models used for testing new bioprosthetic materials treatments have been performed in species that do not produce anti-Gal antibody. GTKO mice produce anti-Gal antibody and would appear to be immunologically an ideal model to study the effect of circulating anti-Gal antibody on tissue calcification. During the course of this project another group headed by Yon Jin Kim at the Sejong General Hospital in the

Republic of Korea reported on a series of comparisons of subcutaneous implantation studies in WT and GTKO mice (Kim et al. 2015a;Kim et al. 2015b;Lee et al. 2012;Lim et al. 2013). These studies are reported below.

In their initial study Lee and colleagues reported that subcutaneous implantation of WT glutaraldehyde fixed bovine pericardium significantly increased anti-Gal IgG and IgM in GTKO mice over a 2-month course of implantation and that higher levels of tissue calcification occurred in GTKO recipient mice (0.77 μg/mg) compared to WT mice (0.12 μg/mg). They concluded that WT bovine pericardium resulted in an induced antibody response in GTKO mice with a tendency to calcification (Lee C et al. 2012). In a follow up study (Lim HG et al. 2013) they extended the duration of implantation (3 months) and immunized GTKO recipient mice with rabbit RBCs to enhance antibody effect on calcification. Tissues treated with α-galactosidase to remove antigenicity were also included in the study. Anti-Gal IgG and IgM levels in both immunized and unimmunized mice were reported to have increased significantly due to implantation of fixed WT bovine pericardium and GTKO recipient mice showed higher levels of tissue calcification (1.85 ± 0.97 μg/mg) compared to WT recipient mice (0.44 ± 0.22 μg/mg). Immunization did not significantly affect tissue calcification (2.31 ± 1.02 μg/mg in naïve GTKO recipients compared to 1.85 ± 0.97 μg/mg in immunized mice). Antibody titers and calcification were lower in the groups that received treated tissue. The writers reinforced their hypothesis that immune response may cause calcification. In a third complex study including pericardium, aortic valve and aortic wall of bovine and porcine origin increased titers were reported for anti-

Gal IgM and IgG in GTKO mice (compared to WT recipients) at 30 and 60 days after implantation, respectively. Calcification of all types of implants was significantly higher in GTKO mice compared to WT mice. The authors suggested that there was more chronic immune response to the α-Gal antigen on bioprosthetic tissue in GTKO mice than in WT mice which resulted in higher calcification of the implants (Kim M-S et al. 2015). In a final report (Kim, MS et al. 2015) using 4-month subcutaneous implantation in GTKO mice they included primate pericardium in their experiments, which does not express α-Gal. Enhanced calcification was reported for the bovine pericardium (9.21 μg/mg) compared to the primate pericardium (3.86 μg/mg). Increased anti-Gal IgG response was reported in bovine pericardium recipients but not in primate implant recipients. These results reinforced the notion that an α-Gal-specific immune response to the implanted tissue enhanced calcification of the α-Gal-positive tissues, but not α-Gal-free primate tissue.

In this study I used GTKO mice recipients implanted with WT and GTKO fixed porcine pericardium for 60, 90 and 120 days. To ensure accessibility of anti-Gal antibody to the tissue, WT fixed pericardial disks were pre-incubated with a mixture of mouse anti-Gal IgM and IgG as a positive control for enhanced tissue calcification. This antibody pre-treatment was expected to induce strong calcification of WT tissue implants independent of the serum anti-Gal levels in the recipient mice. I also immunized recipients with KLH-Gal to increase endogenous serum anti-Gal antibody levels, expecting this antibody to similarly enhance calcification of WT tissue compared to unimmunized recipients.

In my study, in contrast to the studies outlined above, I did not see evidence of an induced anti-Gal immune response caused by the implanted tissue. I used a highly specific α-Gal ELISA to detect anti-Gal antibody in mouse serum. This analysis included M86 (for IgM analysis) or GT5 (for IgG analysis) reference controls to account for plate to plate and day to day variation and competition with free α-Gal trisaccharide to show specific α-Gal reactivity of mouse IgG which showed a high background to BSA. The serum anti-Gal antibody levels were also measured in age matched mice without implants to account for the age-dependent increase in anti-Gal. This analysis showed there to be an age-dependent increase in serum anti-Gal antibody in the GTKO recipients (**Figure 6.4**). When this age-dependent increase in serum anti-Gal antibody is accounted for implantation of fixed porcine WT pericardium it did not induce an appreciable anti-Gal antibody response as measured 60, 90 and 120 days after implantation. Consistent with this there was no significant difference in the serum anti-Gal antibody levels between GTKO mice with WT or GTKO implants. These results suggested that the implants did not cause chronic immune α-Gal stimulation and did not induce an α-Gal-specific antibody response. This suggests that the implants may have been rapidly sequestered from the immune system soon after implantation, thereby limiting the immune response. A possible induced response earlier than 60 days after implantation cannot be eliminated, but the lack of elevated anti-Gal levels at 60, 90 and 120 days clearly suggests that there was no chronic immune stimulation of B-cells due to the implants. Similarly, in contrast to the results of the Kim group WT

pericardium did not induce an immune response in immunized mice beyond the antibody response in immunized non implanted mice (**Figure 6.6**).

The GTKO mice were able to mount an induced anti-Gal IgM and IgG antibody response when immunized with KLH-Gal. This induced response showed a high degree of individual variability, especially for anti-Gal IgG. A second boost of KLH-Gal immunization might have raised higher, more consistent anti-Gal antibody responses, but we anticipated that implantation of WT porcine pericardium would function as an efficient secondary boost. The comparison of serum anti-Gal levels in immunized control (not implanted) and implanted mice indicate that the implant did not substantially boost the immune response, again suggesting that the implants were not accessible to the immune system at an early stage. Robust immunization against α-Gal in GTKO mice has been reported using rabbit RBCs membranes (Gock et al. 2000). This may have been a more effective immunogen than KLH-Gal, however we did not want to use rabbit RBCs due to concerns that they carry additional antigens, other than α-Gal, that might be shared with porcine pericardium.

In our study calcium levels in explanted WT and GTKO pericardial disks at all time points were higher than in the non-implanted controls (**Figure 6.8**, **Figure 6.9** and **Table 4**). Calcium levels in WT disks were significantly higher after 120 days implantation (0.88 ± 0.16 μg/mg) compared to control disks (0.39 ± 0.10 μg/mg). This level of calcification was however much lower than what we detected in previous subcutaneous rats studies where tissue calcification of 74 ± 9.6 μg/mg 3 weeks (McGregor et al. 2011) and 155.7 ± 7.1 μg/mg one month

of subcutaneous implantation (Lila et al. 2010) were observed. We also pre-labeled WT pericardium with anti-Gal antibody as a positive control for antibody induced calcification. This treatment appeared to increase calcification compared to unlabeled WT implants for all post-implant durations, but these differences were not significant. Consistent with previous studies we found that immunization did not significantly induce calcification of WT implants compared to calcification in naive mice.

Summarizing our findings in the GTKO mice model, WT pericardial implants showed increased calcification over time and even higher calcification when they were pre-labelled with anti-Gal antibody. Lack of correlation between implant calcification and levels of endogenous antibody both in naïve and immunized recipients supports the notion that the implants were isolated from the immune system early on, did not cause chronic α-Gal stimulation and endogenous serum antibody did not reach the implant. We were disappointed that a stronger antibody dependent calcification was not evident in the pre-labelled positive controls of this study but this seems to be mainly due to the mouse model where inherently lower levels of calcification occur compared to rats and the implants do not seem to induce a chronic stimulation. Consistent with this conclusion macroscopic examinations of the disks from the GTKO mice showed only minor encapsulation (**Figure 6.13**), the disks were nearly stuck to the animal's skin and when recovered were thin and soft. These findings were different compared to implants retrieved from previous studies in rats and rabbits, where the disks had a larger encapsulation reaction and there

was palpable evidence of calcification as the disks were granular, harder to the touch.

7.1 Future investigation/ studies

This project identified a reliable method to measure α-Gal levels on animal tissues and indicated that GTKO mice, while able to produce anti-Gal antibody endogenously, have a lower tendency to calcification than observed in juvenile rats or rabbits. While our group's previous results support a role of antibody in inducing calcification of fixed tissue this project's results suggest that in GTKO mice the subcutaneous implants are sequestered from the immune system, minimizing calcification and the impact of endogenous or exogenous antibody. This minimal calcification limits the utility of the GTKO mouse model. Juvenile rats have been extensively used for studying calcification of bioprosthetic materials and calcify heavily in a short period of time. It may be advantageous therefore in future experiments to produce GTKO rats, which like GTKO mice and GTKO pigs would be expected to produce anti-Gal antibody and repeat these subcutaneous implantation studies in these animals. This model with predictable rate of calcification would allow us to study the effect of circulating anti-Gal antibody on tissue calcification using shorter duration of implantation.

Valve implantation studies have traditionally been performed in the sheep model to assess valve function and tissue calcification. Standard sheep however do not make anti-Gal antibody. GTKO pigs are already used in xenotransplantation studies and could be used as valve recipients. In addition there are more anatomical and physiological similarities between pigs and

humans. Pigs have comparable coagulation and inflammatory systems to humans. Although valve implantation surgery in pigs is a very demanding procedure due to pigs aversion to cardiopulmonary bypass (Mohiuddin et al. 2015), there has been progress in optimizing anaesthesia and anticoagulation problems (Li et al. 2007). Implantation of bioprosthetic mitral valves in juvenile pigs showed that the implanted valves functioned up to 6 months and calcification, histological examination and echocardiographic data showed that this model was comparable with the sheep model (Honge et al. 2011). Substituting GTKO pigs as the recipients would allow us to study the effect of anti-Gal antibody on calcification of BHVs in a functional large animal model with a more accurate representation of the human immune system with respect to the anti-Gal antibody. Commercial porcine BHVs (for example Medtronic Mosaic, Edward Lifesciences Prima) expressing the α-Gal antigen could be implanted into GTKO and WT pigs to compare the impact of anti-Gal antibody (present only in the GTKO pig recipients) on early BHV inflammation (Konakci et al. 2005).

Xenotransplantation studies have also identified other xenogeneic carbohydrate antigens beyond α-Gal, such as Neu5Gc and SDa. These antigens are expressed on GTKO heart tissue (Park et al. 2012). It would be enlightening to incorporate in our study the role of these antigens along with α-Gal in the calcification of bioprosthetic material. Triple knock-out pigs that do not express any of these three epitopes are already available (Estrada et al. 2015), although there is as yet no information on whether they express the corresponding antibodies.

Future studies focusing on the immune response aspect of BHV degeneration will help towards development of more durable valves in young adults and children allowing them a more active way of life with fewer re-operations.

8 References

MEERA, Power Analysis, Statistical Significance, & Effect Size. 2013a.
Ref Type: Online Source

Statistical Solutions, LLC. 2013b.
Ref Type: Online Source

Albert, H.M., Bryant, L.R., & Schechter, F.G. 1977. Seven year experience with mounted porcine valves. *Ann.Surg.*, 185, (6) 717-723 available from: PM:871225

Arumugham, R.G., Hsieh, T.C., Tanzer, M.L., & Laine, R.A. 1986. Structures of the asparagine-linked sugar chains of laminin. *Biochim.Biophys.Acta*, 883, (1) 112-126 available from: PM:3730425

Azimzadeh, A.M., Byrne, G.W., Ezzelarab, M., Welty, E., Braileanu, G., Cheng, X., Robson, S.C., McGregor, C.G., Cooper, D.K., & Pierson, R.N., III 2014. Development of a consensus protocol to quantify primate anti-non-Gal xenoreactive antibodies using pig aortic endothelial cells. *Xenotransplantation.*, 21, (6) 555-566 available from: PM:25176173

BARRATT-BOYES, B.G. 1964. HOMOGRAFT AORTIC VALVE REPLACEMENT IN AORTIC INCOMPETENCE AND STENOSIS. *Thorax*, 19, 131-150 available from: PM:14128570

Bezuidenhout, D., Oosthuysen, A., Human, P., Weissenstein, C., & Zilla, P. 2009. The effects of cross-link density and chemistry on the calcification potential of diamine-extended glutaraldehyde-fixed bioprosthetic heart-valve materials. *Biotechnol.Appl.Biochem.*, 54, (3) 133-140 available from: PM:19882764

Bovin, N., Obukhova, P., Shilova, N., Rapoport, E., Popova, I., Navakouski, M., Unverzagt, C., Vuskovic, M., & Huflejt, M. 2012. Repertoire of human natural anti-glycan immunoglobulins. Do we have auto-antibodies? *Biochim.Biophys.Acta*, 1820, (9) 1373-1382 available from: PM:22365885

Bracher, M., Simionescu, D., Simionescu, A., Davies, N., Human, P., & Zilla, P. 2001. Matrix metalloproteinases and tissue valve degeneration. *J.Long.Term.Eff.Med.Implants.*, 11, (3-4) 221-230 available from: PM:11921665

Butany, J., Collins, M.J., Nair, V., Leask, R.L., Scully, H.E., Williams, W.G., & David, T.E. 2006. Morphological findings in explanted Toronto stentless porcine valves. *Cardiovasc.Pathol.*, 15, (1) 41-48 available from: PM:16414456

Byrne, G.W. & McGregor, C.G. 2012. Cardiac xenotransplantation: progress and challenges. *Curr.Opin.Organ Transplant.*, 17, (2) 148-154 available from: PM:22327911

Byrne, G.W., Schwarz, A., Fesi, J.R., Birch, P., Nepomich, A., Bakaj, I., Velardo, M.A., Jiang, C., Manzi, A., Dintzis, H., Diamond, L.E., & Logan, J.S. 2002. Evaluation of different alpha-Galactosyl glycoconjugates for use in xenotransplantation. *Bioconjug.Chem.*, 13, (3) 571-581 available from: PM:12009948

Cannegieter, S.C., Rosendaal, F.R., & Briet, E. 1994. Thromboembolic and bleeding complications in patients with mechanical heart valve prostheses. *Circulation*, 89, (2) 635-641 available from: PM:8313552

Chen, R.H., Kadner, A., Mitchell, R.N., & Adams, D.H. 2000. Fresh porcine cardiac valves are not rejected in primates. *J.Thorac.Cardiovasc.Surg.*, 119, (6) 1216-1220 available from: PM:10838541

Chen, W., Schoen, F.J., & Levy, R.J. 1994. Mechanism of efficacy of 2-amino oleic acid for inhibition of calcification of glutaraldehyde-pretreated porcine bioprosthetic heart valves. *Circulation*, 90, (1) 323-329 available from: PM:8026014

Chong, A.S., Ma, L., Yin, D., Shen, J., Blinder, L., XiuLong, X., Williams, J.W., Byrne, G., Diamond, L.E., & Logan, J.S. 2000. Non-depleting anti-CD4, but not anti-CD8, antibody induces long-term survival of xenogeneic and allogeneic hearts in alpha1,3-galactosyltransferase knockout (GT-Ko) mice. *Xenotransplantation.*, 7, (4) 275-283 available from: PM:11081762

David, T.E., Ropchan, G.C., & Butany, J.W. 1988. Aortic valve replacement with stentless porcine bioprostheses. *J.Card Surg.*, 3, (4) 501-505 available from: PM:2980054

Diswall, M., Angstrom, J., Karlsson, H., Phelps, C.J., Ayares, D., Teneberg, S., & Breimer, M.E. 2010. Structural characterization of alpha1,3-galactosyltransferase knockout pig heart and kidney glycolipids and their reactivity with human and baboon antibodies. *Xenotransplantation.*, 17, (1) 48-60 available from: PM:20149188

Essig, A.M. & Kleyn, D.H. 1983. Determination of lactose in milk: comparison of methods. *J.Assoc.Off Anal.Chem.*, 66, (6) 1514-1516 available from: PM:6689018

Estrada, J.L., Martens, G., Li, P., Adams, A., Newell, K.A., Ford, M.L., Butler, J.R., Sidner, R., Tector, M., & Tector, J. 2015. Evaluation of human and non-human primate antibody binding to pig cells lacking GGTA1/CMAH/beta4GalNT2 genes. *Xenotransplantation.*, 22, (3) 194-202 available from: PM:25728481

Fang, J., Walters, A., Hara, H., Long, C., Yeh, P., Ayares, D., Cooper, D.K., & Bianchi, J. 2012. Anti-gal antibodies in alpha1,3-galactosyltransferase gene-knockout pigs. *Xenotransplantation.*, 19, (5) 305-310 available from: PM:22970769

Farivar, R.S., Filsoufi, F., & Adams, D.H. 2003. Mechanisms of Gal(alpha)1-3Gal(beta)1-4GlcNAc-R (alphaGal) expression on porcine valve endothelial cells. *J.Thorac.Cardiovasc.Surg.*, 125, (2) 306-314 available from: PM:12579099

Fujiwara, S., Shinkai, H., Mann, K., & Timpl, R. 1993. Structure and localization of O- and N-linked oligosaccharide chains on basement membrane protein nidogen. *Matrix*, 13, (3) 215-222 available from: PM:8326911

Galili, U. 1999. Evolution of alpha 1,3galactosyltransferase and of the alpha-Gal epitope. *Subcell.Biochem.*, 32, 1-23 available from: PM:10391989

Galili, U. 2013. Anti-Gal: an abundant human natural antibody of multiple pathogeneses and clinical benefits. *Immunology*, 140, (1) 1-11 available from: PM:23578170

Galili, U., Anaraki, F., Thall, A., Hill-Black, C., & Radic, M. 1993. One percent of human circulating B lymphocytes are capable of producing the natural anti-Gal antibody. *Blood*, 82, (8) 2485-2493 available from: PM:7691263

Galili, U., Clark, M.R., Shohet, S.B., Buehler, J., & Macher, B.A. 1987. Evolutionary relationship between the natural anti-Gal antibody and the Gal alpha 1----3Gal epitope in primates. *Proc.Natl.Acad.Sci.U.S.A*, 84, (5) 1369-1373 available from: PM:2434954

Galili, U., LaTemple, D.C., & Radic, M.Z. 1998. A sensitive assay for measuring alpha-Gal epitope expression on cells by a monoclonal anti-Gal antibody. *Transplantation*, 65, (8) 1129-1132 available from: PM:9583877

Galili, U., Mandrell, R.E., Hamadeh, R.M., Shohet, S.B., & Griffiss, J.M. 1988a. Interaction between human natural anti-alpha-galactosyl immunoglobulin G and bacteria of the human flora. *Infect.Immun.*, 56, (7) 1730-1737 available from: PM:3290105

Galili, U., Shohet, S.B., Kobrin, E., Stults, C.L., & Macher, B.A. 1988b. Man, apes, and Old World monkeys differ from other mammals in the expression of alpha-galactosyl epitopes on nucleated cells. *J.Biol.Chem.*, 263, (33) 17755-17762 available from: PM:2460463

Gilbert, T.W., Sellaro, T.L., & Badylak, S.F. 2006. Decellularization of tissues and organs. *Biomaterials*, 27, (19) 3675-3683 available from: PM:16519932

Girardot, M.N., Torrianni, M., & Girardot, J.M. 1994. Effect of AOA on glutaraldehyde-fixed bioprosthetic heart valve cusps and walls: binding and calcification studies. *Int.J.Artif.Organs*, 17, (2) 76-82 available from: PM:8039944

Gock, H., Salvaris, E., Murray-Segal, L., Mottram, P., Han, W., Pearse, M.J., Goodman, D.J., Cowan, P.J., & d'Apice, A.J. 2000. Hyperacute rejection of vascularized heart transplants in BALB/c Gal knockout mice. *Xenotransplantation.*, 7, (4) 237-246 available from: PM:11081758

Goldstein, I.J., Blake, D.A., Ebisu, S., Williams, T.J., & Murphy, L.A. 1981. Carbohydrate binding studies on the Bandeiraea simplicifolia I isolectins. Lectins which are mono-, di-, tri-, and tetravalent for N-acetyl-D-galactosamine. *J.Biol.Chem.*, 256, (8) 3890-3893 available from: PM:7217062

Hamm, C.W., Arsalan, M., & Mack, M.J. 2015. The future of transcatheter aortic valve implantation. *Eur.Heart J.* available from: PM:26578195

Hogan, P., Duplock, L., Green, M., Smith, S., Gall, K.L., Frazer, I.H., & O'Brien, M.F. 1996. Human aortic valve allografts elicit a donor-specific immune response. *J.Thorac.Cardiovasc.Surg.*, 112, (5) 1260-1266 available from: PM:8911322

Honge, J.L., Funder, J.A., Pedersen, T.B., Kronborg, M.B., & Hasenkam, J.M. 2011. Degenerative processes in bioprosthetic mitral valves in juvenile pigs. *J.Cardiothorac.Surg.*, 6, 72 available from: PM:21569636

Huber, R.E., Wallenfels, K., & Kurz, G. 1975. The action of beta-galactosidase (Escherichia coli) on allolactose. *Can.J.Biochem.*, 53, (9) 1035-1038 available from: PM:241475

Human, P. & Zilla, P. 2001. Characterization of the immune response to valve bioprostheses and its role in primary tissue failure. *Ann.Thorac.Surg.*, 71, (5 Suppl) S385-S388 available from: PM:11388230

Ionescu, M.I., Mashhour, Y.A., & Wooler, G.H. 1968. Reconstructed heterograft aortic valves for human use: preparation and surgical implantation for mitral, aortic, and tricuspid replacement. *Thorax*, 23, (3) 221-229 available from: PM:5690471

Ionescu, M.I., Smith, D.R., Sutherland, T.W., & Wooler, G.H. 1972. Heart valve replacement with aortic heterografts. Follow-up study. *Ann.Thorac.Surg.*, 13, (1) 1-14 available from: PM:5061811

Ius, P., Thiene, G., Minarini, M., Valente, M., Bortolotti, U., Talenti, E., & Casarotto, D. 1996. Low-profile porcine bioprosthesis (Liotta): pathologic findings and mode of failure in the long-term. *J.Heart Valve Dis.*, 5, (3) 323-327 available from: PM:8793685

Joziasse, D.H., Shaper, J.H., Van den Eijnden, D.H., Van Tunen, A.J., & Shaper, N.L. 1989. Bovine alpha 1----3-galactosyltransferase: isolation and characterization of a cDNA clone. Identification of homologous sequences in human genomic DNA. *J.Biol.Chem.*, 264, (24) 14290-14297 available from: PM:2503516

Kasimir, M.T., Rieder, E., Seebacher, G., Wolner, E., Weigel, G., & Simon, P. 2005. Presence and elimination of the xenoantigen gal (alpha1, 3) gal in tissue-engineered heart valves. *Tissue Eng*, 11, (7-8) 1274-1280 available from: PM:16144463

KERWIN, A.J., LENKEI, S.C., & WILSON, D.R. 1962. Aortic-valve homograft in the treatment of aortic insufficiency. Report of nine cases, with one followed for six years. *N.Engl.J.Med.*, 266, 852-857 available from: PM:14455376

Khan, N.A., Butany, J., Zhou, T., Ross, H.J., & Rao, V. 2008. Pathological findings in explanted prosthetic heart valves from ventricular assist devices. *Pathology*, 40, (4) 377-384 available from: PM:18446628

Kim, M.S., Jeong, S., Lim, H.G., & Kim, Y.J. 2015a. Differences in xenoreactive immune response and patterns of calcification of porcine and bovine tissues in alpha-Gal knock-out and wild-type mouse implantation models. *Eur.J.Cardiothorac.Surg.*, 48, (3) 392-399 available from: PM:25549993

Kim, M.S., Lim, H.G., & Kim, Y.J. 2015b. Calcification of decellularized and alpha-galactosidase-treated bovine pericardial tissue in an alpha-Gal knock-out mouse implantation model: comparison with primate pericardial tissue. *Eur.J.Cardiothorac.Surg.* available from: PM:25994817

Konakci, K.Z., Bohle, B., Blumer, R., Hoetzenecker, W., Roth, G., Moser, B., Boltz-Nitulescu, G., Gorlitzer, M., Klepetko, W., Wolner, E., & Ankersmit, H.J. 2005. Alpha-Gal on bioprostheses: xenograft immune response in cardiac surgery. *Eur.J.Clin.Invest*, 35, (1) 17-23 available from: PM:15638815

Kuwaki, K., Tseng, Y.L., Dor, F.J., Shimizu, A., Houser, S.L., Sanderson, T.M., Lancos, C.J., Prabharasuth, D.D., Cheng, J., Moran, K., Hisashi, Y., Mueller, N., Yamada, K., Greenstein, J.L., Hawley, R.J., Patience, C., Awwad, M., Fishman, J.A., Robson, S.C., Schuurman, H.J., Sachs, D.H., & Cooper, D.K. 2005. Heart transplantation in baboons using alpha1,3-galactosyltransferase gene-knockout pigs as donors: initial experience. *Nat.Med.*, 11, (1) 29-31 available from: PM:15619628

Lai, L., Kolber-Simonds, D., Park, K.W., Cheong, H.T., Greenstein, J.L., Im, G.S., Samuel, M., Bonk, A., Rieke, A., Day, B.N., Murphy, C.N., Carter, D.B., Hawley, R.J., & Prather, R.S. 2002. Production of alpha-1,3-galactosyltransferase knockout pigs by nuclear transfer cloning. *Science*, 295, (5557) 1089-1092 available from: PM:11778012

Langeveld, J.P., Noelken, M.E., Hard, K., Todd, P., Vliegenthart, J.F., Rouse, J., & Hudson, B.G. 1991. Bovine glomerular basement membrane. Location and structure of the asparagine-linked oligosaccharide units and their potential role in the assembly of the 7 S collagen IV tetramer. *J.Biol.Chem.*, 266, (4) 2622-2631 available from: PM:1990011

Larsen, R.D., Rivera-Marrero, C.A., Ernst, L.K., Cummings, R.D., & Lowe, J.B. 1990. Frameshift and nonsense mutations in a human genomic sequence homologous to a murine UDP-Gal:beta-D-Gal(1,4)-D-GlcNAc alpha(1,3)-galactosyltransferase cDNA. *J.Biol.Chem.*, 265, (12) 7055-7061 available from: PM:2108966

Lee, C., Ahn, H., Kim, S.H., Choi, S.Y., & Kim, Y.J. 2012. Immune response to bovine pericardium implanted into alpha1,3-galactosyltransferase knockout mice: feasibility as an animal model for testing efficacy of anticalcification treatments of xenografts. *Eur.J.Cardiothorac.Surg.*, 42, (1) 164-172 available from: PM:22223697

Lentz, D.J., Pollock, E.M., Olsen, D.B., & Andrews, E.J. 1982. Prevention of intrinsic calcification in porcine and bovine xenograft materials. *Trans.Am.Soc.Artif.Intern.Organs*, 28, 494-497 available from: PM:7164288

Li, D., Ren, B.H., Shen, Y., Wu, H., Wang, C., Zhang, L., Zhu, J., & Jing, H. 2007. A Swine model for long-term evaluation of prosthetic heart valves. *ANZ.J.Surg.*, 77, (8) 654-658 available from: PM:17635278

Lila, N., McGregor, C.G., Carpentier, S., Rancic, J., Byrne, G.W., & Carpentier, A. 2010. Gal knockout pig pericardium: new source of material for heart valve bioprostheses. *J.Heart Lung Transplant.*, 29, (5) 538-543 available from: PM:20036160

Lim, H.G., Choi, S.Y., Yoon, E.J., Kim, S.H., & Kim, Y.J. 2013. In vivo efficacy of alpha-galactosidase as possible promise for prolonged durability of bioprosthetic heart valve using alpha1,3-galactosyltransferase knockout mouse. *Tissue Eng Part A*, 19, (21-22) 2339-2348 available from: PM:23672462

LOWRY, O.H., PASSONNEAU, J.V., & ROCK, M.K. 1961. The stability of pyridine nucleotides. *J.Biol.Chem.*, 236, 2756-2759 available from: PM:14466980

Luo, Y., Wen, J., Luo, C., Cummings, R.D., & Cooper, D.K. 1999. Pig xenogeneic antigen modification with green coffee bean alpha-galactosidase. *Xenotransplantation.*, 6, (4) 238-248 available from: PM:10704067

Mako, W.J., Shah, A., & Vesely, I. 1999. Mineralization of glutaraldehyde-fixed porcine aortic valve cusps in the subcutaneous rat model: analysis of variations in implant site and cuspal quadrants. *J.Biomed.Mater.Res.*, 45, (3) 209-213 available from: PM:10397978

Manji, R.A., Hara, H., & Cooper, D.K. 2015. Characterization of the cellular infiltrate in bioprosthetic heart valves explanted from patients with structural valve deterioration. *Xenotransplantation.*, 22, (5) 406-407 available from: PM:26315116

Manji, R.A., Menkis, A.H., Ekser, B., & Cooper, D.K. 2012. Porcine bioprosthetic heart valves: The next generation. *Am.Heart J.*, 164, (2) 177-185 available from: PM:22877802

Manji, R.A., Zhu, L.F., Nijjar, N.K., Rayner, D.C., Korbutt, G.S., Churchill, T.A., Rajotte, R.V., Koshal, A., & Ross, D.B. 2006. Glutaraldehyde-fixed bioprosthetic heart valve conduits calcify and fail from xenograft rejection. *Circulation*, 114, (4) 318-327 available from: PM:16831988

Maruyama, S., Cantu, E., III, Galili, U., D'Agati, V., Godman, G., Stern, D.M., & Andres, G. 2000. alpha-galactosyl epitopes on glycoproteins of porcine renal extracellular matrix. *Kidney Int.*, 57, (2) 655-663 available from: PM:10652044

McCurry, K.R., Parker, W., Cotterell, A.H., Weidner, B.C., Lin, S.S., Daniels, L.J., Holzknecht, Z.E., Byrne, G.W., Diamond, L.E., Logan, J.S., & Platt, J.L. 1997. Humoral responses to pig-to-baboon cardiac transplantation: implications for the pathogenesis and treatment of acute vascular rejection and for accommodation. *Hum.Immunol.*, 58, (2) 91-105 available from: PM:9475338

McGregor, C.G., Carpentier, A., Lila, N., Logan, J.S., & Byrne, G.W. 2011. Cardiac xenotransplantation technology provides materials for improved bioprosthetic heart valves. *J.Thorac.Cardiovasc.Surg.*, 141, (1) 269-275 available from: PM:21168032

McGregor, C.G., Kogelberg, H., Vlasin, M., & Byrne, G.W. 2013. Gal-knockout bioprostheses exhibit less immune stimulation compared to standard biological heart valves. *J.Heart Valve Dis.*, 22, (3) 383-390 available from: PM:24151765

Moczar, M., Houel, R., Ginat, M., Clerin, V., Wheeldon, D., & Loisance, D. 2000. Structural changes in porcine bioprosthetic valves of a left ventricular assist system in human patients. *J.Heart Valve Dis.*, 9, (1) 88-95 available from: PM:10678380

Mohiuddin, M.M., Reichart, B., Byrne, G.W., & McGregor, C.G. 2015. Current status of pig heart xenotransplantation. *Int.J.Surg.*, 23, (Pt B) 234-239 available from: PM:26318967

Nair, V., Law, K.B., Li, A.Y., Phillips, K.R., David, T.E., & Butany, J. 2012. Characterizing the inflammatory reaction in explanted Medtronic Freestyle stentless porcine aortic bioprosthesis over a 6-year period. *Cardiovasc.Pathol.*, 21, (3) 158-168 available from: PM:21816627

Naso, F., Gandaglia, A., Bottio, T., Tarzia, V., Nottle, M.B., d'Apice, A.J., Cowan, P.J., Cozzi, E., Galli, C., Lagutina, I., Lazzari, G., Iop, L., Spina, M., & Gerosa, G. 2013a. First quantification of alpha-Gal epitope in current glutaraldehyde-fixed heart valve bioprostheses. *Xenotransplantation.*, 20, (4) 252-261 available from: PM:23865597

Naso, F., Gandaglia, A., Bottio, T., Tarzia, V., Nottle, M.B., d'Apice, A.J., Cowan, P.J., Cozzi, E., Galli, C., Lagutina, I., Lazzari, G., Iop, L., Spina, M., & Gerosa, G. 2013b. First quantification of alpha-Gal epitope in current glutaraldehyde-fixed heart valve bioprostheses. *Xenotransplantation.*, 20, (4) 252-261 available from: PM:23865597

Naso, F., Gandaglia, A., Iop, L., Spina, M., & Gerosa, G. 2011. First quantitative assay of alpha-Gal in soft tissues: presence and distribution of the epitope before and after cell removal from xenogeneic heart valves. *Acta Biomater.*, 7, (4) 1728-1734 available from: PM:21118731

Nilsson, B., Korsgren, O., Lambris, J.D., & Ekdahl, K.N. 2010. Can cells and biomaterials in therapeutic medicine be shielded from innate immune recognition? *Trends Immunol.*, 31, (1) 32-38 available from: PM:19836998

Nottle, M.B., Beebe, L.F., Harrison, S.J., McIlfatrick, S.M., Ashman, R.J., O'Connell, P.J., Salvaris, E.J., Fisicaro, N., Pommey, S., Cowan, P.J., & d'Apice, A.J. 2007. Production of homozygous alpha-1,3-galactosyltransferase knockout pigs by breeding and somatic cell nuclear transfer. *Xenotransplantation.*, 14, (4) 339-344 available from: PM:17669176

Park, C.S., Park, S.S., Choi, S.Y., Yoon, S.H., Kim, W.H., & Kim, Y.J. 2010. Anti alpha-gal immune response following porcine bioprosthesis implantation in children. *J.Heart Valve Dis.*, 19, (1) 124-130 available from: PM:20329498

Park, J.Y., Park, M.R., Bui, H.T., Kwon, D.N., Kang, M.H., Oh, M., Han, J.W., Cho, S.G., Park, C., Shim, H., Kim, H.M., Kang, M.J., Park, J.K., Lee, J.W., Lee, K.K., & Kim, J.H. 2012. alpha1,3-galactosyltransferase deficiency in germ-free miniature pigs increases N-glycolylneuraminic acids as the xenoantigenic determinant in pig-human xenotransplantation. *Cell Reprogram.*, 14, (4) 353-363 available from: PM:22775484

Parker, W., Lateef, J., Everett, M.L., & Platt, J.L. 1996. Specificity of xenoreactive anti-Gal alpha 1-3Gal IgM for alpha-galactosyl ligands. *Glycobiology*, 6, (5) 499-506 available from: PM:8877370

Phelps, C.J., Koike, C., Vaught, T.D., Boone, J., Wells, K.D., Chen, S.H., Ball, S., Specht, S.M., Polejaeva, I.A., Monahan, J.A., Jobst, P.M., Sharma, S.B., Lamborn, A.E., Garst, A.S., Moore, M., Demetris, A.J., Rudert, W.A., Bottino, R., Bertera, S., Trucco, M., Starzl, T.E., Dai, Y., & Ayares, D.L. 2003. Production of Î±1,3-Galactosyltransferaseâ€“Deficient Pigs. *Science*, 299, (5605) 411-414 available from: PM:12493821

Rose, A.G. 1972. Pathology of the formalin-treated heterograft porcine aortic valve in the mitral position. *Thorax*, 27, (4) 401-409 available from: PM:4672718

Schoen, F.J. & Levy, R.J. 1999. Founder's Award, 25th Annual Meeting of the Society for Biomaterials, perspectives. Providence, RI, April 28-May 2, 1999. Tissue heart

valves: current challenges and future research perspectives. *J.Biomed.Mater.Res.*, 47, (4) 439-465 available from: PM:10497280

Schoen, F.J. & Levy, R.J. 2005. Calcification of tissue heart valve substitutes: progress toward understanding and prevention. *Ann.Thorac.Surg.*, 79, (3) 1072-1080 available from: PM:15734452

Shen, M., Kara-Mostefa, A., Chen, L., Daudon, M., Thevenin, M., Lacour, B., & Carpentier, A. 2001. Effect of ethanol and ether in the prevention of calcification of bioprostheses. *Ann.Thorac.Surg.*, 71, (5 Suppl) S413-S416 available from: PM:11388238

Siddiqui, R.F., Abraham, J.R., & Butany, J. 2009. Bioprosthetic heart valves: modes of failure. *Histopathology*, 55, (2) 135-144 available from: PM:19694820

Simionescu, D.T. 2004. Prevention of calcification in bioprosthetic heart valves: challenges and perspectives. *Expert.Opin.Biol.Ther.*, 4, (12) 1971-1985 available from: PM:15571459

Simon, P., Kasimir, M.T., Seebacher, G., Weigel, G., Ullrich, R., Salzer-Muhar, U., Rieder, E., & Wolner, E. 2003. Early failure of the tissue engineered porcine heart valve SYNERGRAFT in pediatric patients. *Eur.J.Cardiothorac.Surg.*, 23, (6) 1002-1006 available from: PM:12829079

Stein, P.D., Wang, C.H., Riddle, J.M., & Magilligan, D.J., Jr. 1988. Leukocytes, platelets, and surface microstructure of spontaneously degenerated porcine bioprosthetic valves. *J.Card Surg.*, 3, (3) 253-261 available from: PM:2980025

Stone, K.R., Abdel-Motal, U.M., Walgenbach, A.W., Turek, T.J., & Galili, U. 2007. Replacement of human anterior cruciate ligaments with pig ligaments: a model for anti-non-gal antibody response in long-term xenotransplantation. *Transplantation*, 83, (2) 211-219 available from: PM:17264818

Tam, H., Zhang, W., Feaver, K.R., Parchment, N., Sacks, M.S., & Vyavahare, N. 2015. A novel crosslinking method for improved tear resistance and biocompatibility of tissue based biomaterials. *Biomaterials*, 66, 83-91 available from: PM:26196535

Thall, A. & Galili, U. 1990. Distribution of Gal alpha 1----3Gal beta 1----4GlcNAc residues on secreted mammalian glycoproteins (thyroglobulin, fibrinogen, and immunoglobulin G) as measured by a sensitive solid-phase radioimmunoassay. *Biochemistry*, 29, (16) 3959-3965 available from: PM:2354167

Tod, T.J. & Dove, J.S. 2016. The association of bound aldehyde content with bioprosthetic tissue calcification. *J.Mater.Sci.Mater.Med.*, 27, (1) 8 available from: PM:26610931

Une, D., Ruel, M., & David, T.E. 2014. Twenty-year durability of the aortic Hancock II bioprosthesis in young patients: is it durable enough? *Eur.J.Cardiothorac.Surg.* available from: PM:24510909

Valfre, C., Ius, P., Minniti, G., Salvador, L., Bottio, T., Cesari, F., Rizzoli, G., & Gerosa, G. 2010. The fate of Hancock II porcine valve recipients 25 years after implant. *Eur.J.Cardiothorac.Surg.*, 38, (2) 141-146 available from: PM:20194029

Vesely, I. 2003. The evolution of bioprosthetic heart valve design and its impact on durability. *Cardiovasc.Pathol.*, 12, (5) 277-286 available from: PM:14507578

Vyavahare, N., Hirsch, D., Lerner, E., Baskin, J.Z., Schoen, F.J., Bianco, R., Kruth, H.S., Zand, R., & Levy, R.J. 1997. Prevention of bioprosthetic heart valve calcification by ethanol preincubation. Efficacy and mechanisms. *Circulation*, 95, (2) 479-488 available from: PM:9008467

Walley, V.M. & Keon, W.J. 1987. Patterns of failure in Ionescu-Shiley bovine pericardial bioprosthetic valves. *J.Thorac.Cardiovasc.Surg.*, 93, (6) 925-933 available from: PM:3573803

Wang, L., Anaraki, F., Henion, T.R., & Galili, U. 1995. Variations in activity of the human natural anti-Gal antibody in young and elderly populations. *J.Gerontol.A Biol.Sci.Med.Sci.*, 50, (4) M227-M233 available from: PM:7542151

Weber, P.A., Jouan, J., Matsunaga, A., Pettenazzo, E., Joudinaud, T., Thiene, G., & Duran, C.M. 2006. Evidence of mitigated calcification of the Mosaic versus Hancock Standard valve xenograft in the mitral position of young sheep. *J.Thorac.Cardiovasc.Surg.*, 132, (5) 1137-1143 available from: PM:17059935

Wilmut, I., Schnieke, A.E., McWhir, J., Kind, A.J., & Campbell, K.H. 1997. Viable offspring derived from fetal and adult mammalian cells. *Nature*, 385, (6619) 810-813 available from: PM:9039911

Xu, H., Yin, D., Naziruddin, B., Chen, L., Stark, A., Wei, Y., Lei, Y., Shen, J., Logan, J.S., Byrne, G.W., & Chong, A.S. 2003. The in vitro and in vivo effects of anti-galactose antibodies on endothelial cell activation and xenograft rejection. *J.Immunol.*, 170, (3) 1531-1539 available from: PM:12538718

Zilla, P., Bezuidenhout, D., Weissenstein, C., van der Walt, A., & Human, P. 2001. Diamine extension of glutaraldehyde crosslinks mitigates bioprosthetic aortic wall calcification in the sheep model. *J.Biomed.Mater.Res.*, 56, (1) 56-64 available from: PM:11309791

Zilla, P., Brink, J., Human, P., & Bezuidenhout, D. 2008. Prosthetic heart valves: catering for the few. *Biomaterials*, 29, (4) 385-406 available from: PM:17950840

Zilla, P., Human, P., & Bezuidenhout, D. 2004. Bioprosthetic heart valves: the need for a quantum leap. *Biotechnol.Appl.Biochem.*, 40, (Pt 1) 57-66 available from: PM:15270708